

Design of Gabion Walls: Practical Case

Tetiana Korin

Final Report Presented to the School of Technology and
Management of Polytechnic Institute of Bragança
to the Fulfilment of the Requirements for the Master Degree in
Construction Engineering

Supervised by:

Professor Manuel Teixeira Braz César

Professor from LNTU: Rotko Svitlana Volodymyrivna

Bragança

December 2022

Dimensionamento de paredes de Gabião: Caso prático

Tetiana Korin

Relatório Final Apresentada á Escola Superior de Tecnologia e
Gestão (ESTiG) do Instituto Politécnico de Bragança para o
Cumprimento de Requisitos de Mestrado em Engenharia da
Construção

Orientador:

Professor Manuel Teixeira Braz César

Professor LNTU: Rotko Svitlana Volodymyrivna

Bragança

Dezembro 2022

Acknowledgment

First of all, I would like to thank God and my parents for all their support, encouragement and unconditional love at every stage of my life, for being my support and never leaving me alone.

Special thanks to the professor Dr. Manuel Teixeira Braz César for the guidance in the development of this thesis, for his patience, willingness and teaching during my last year of study, who allowed me to acquire a complete and well-enriched preparation allowing me to develop this work. Thanks to my dean Andriichuk Oleksandr Valentynovych and co-supervisor Rotko Svitlana Volodymyrivna for their support and presence not only during my master's work, but also during the entire undergraduate course.

Subsequently, I am sincerely grateful to all the professors of the Lutsk National Technical University (LNTU) for the opportunity to study abroad, for their advice and great faith in me. Thanks to Instituto Politécnico de Bragança (IPB) for warmly welcoming me to the ranks of their students. For the support I needed when the war came to my country, they supported me in every way with words and deeds.

I also wish to express my gratitude to those who contributed directly or indirectly to the development of this graduation project.

Finally, my gratitude to the members of the jury who gave time to evaluate this work, showing care and patience.

Thank you all for giving me a home in your hearts.

Abstract

Gabion structures have been known for a long time, but now they become extremely widely used. Why have they become so popular and what are the advantages of these designs?

Perhaps the most important of the advantages is their environmental friendliness. Among a number of environmental problems of our time, one of the most influential and least controlled is the problem of carbon dioxide emissions. Our future, the future of the planet and humanity in general depends on control of this emissions. So, compared to, for example, a concrete retaining wall, a gabion wall of the same height will reduce these emissions by 80%. In addition, they can be reduced by absorption by vegetation that appears over time on the gabion structures.

Gabion structures are used to strengthen the slopes and shorelines of reservoirs, to prevent landslides, to prevent erosion, in the construction of highways, bridges, embankments etc.

Gabion structures are multifunctional - they can be considered not just as a part of the general concept or a feature of the design, but as a full-fledged basis for territory planning.

The relevance of the topic is modeling the correct approach to the design and calculation of gabion retaining walls, observing the technology of their arrangement and maintenance, understanding the possibilities of solving environmental and urban planning problems that can be avoided with using gabion structures. Thus the scope of this project is to study the gabion wall as a retaining structure in areas of possible landslides, by taking into account various factors such as stability, flexibility, environmental impact and serviceability, following the given design parameters such as overturning moment, resisting moment, sliding resistance and bearing pressure.

Nowadays, new construction methodologies have appeared, as well as design with the help of various softwares, to facilitate the implementation of the structure in practice. The main goal is to present the gabion wall as retaining structure.

Keywords: gabion, gabion construction, gabion structure, retaining wall, wire mesh.

Resumo

As estruturas de gabião são conhecidas há muito tempo, mas atualmente elas se tornaram amplamente utilizadas. Por que elas se tornaram tão populares e quais são as vantagens destas estruturas?

Talvez a mais importante das vantagens seja elas serem ambientalmente mais adequadas. De entre vários problemas ambientais de nosso tempo, um dos mais relevantes e menos controlados é o problema das emissões de dióxido de carbono. Nosso futuro, o futuro do planeta e da humanidade em geral, depende do controle dessas emissões. Assim, em comparação, por exemplo, com um muro de contenção de betão, um muro de gabião da mesma altura é capaz de reduzir tais emissões em 80%. Além disso, elas podem ser reduzidas através da absorção pela vegetação que aparece ao longo do tempo nas estruturas de gabião.

As estruturas de gabião são utilizadas para reforçar as encostas e as linhas costeiras dos reservatórios, para evitar deslizamentos de terra, para evitar a erosão, na construção de rodovias, pontes, terraplenos extensos.

As estruturas de gabião são multifuncionais - podem ser consideradas não apenas como parte do conceito geral ou uma característica do projeto, mas como uma base completa para o planejamento do território

A relevância do tópico tem modelado a abordagem correta do projeto e cálculo das paredes de contenção do gabião, observando a tecnologia de sua disposição e manutenção, compreendendo as possibilidades de solução de problemas ambientais e de planejamento urbano que podem ser evitados com o uso dessas estruturas. Assim, o escopo deste projeto é estudar a parede de gabião como uma estrutura de retenção em áreas de possíveis deslizamentos de terra, levando em conta vários fatores como estabilidade, flexibilidade, impacto ambiental e facilidade de manutenção, seguindo os parâmetros de projeto dados, tais como momento de derrube, momento de resistência, resistência ao deslizamento e pressão de suporte.

Atualmente, novas metodologias de construção surgiram, assim como o projeto com a ajuda de vários softwares, para facilitar a implementação da estrutura na prática. O principal objetivo é apresentar a parede de gabião como estrutura de retenção.

Palavras-chave: gabião, construção de gabião, estrutura de gabião, parede de contenção, malha de arame.

Index

S.No	Description	Page No.
	ACKNOWLEDGMENT	3
	ABSTRACT	4
	RESUMO	5
	INDEX.....	6
	LIST OF FIGURES	9
	LIST OF TABLES	11
	NOMENCLATURE	12
	INTRODUCTION	14
	1. STATE OF THE ART OF RETAINING WALLS.....	15
1.1	HISTORY OF GABIONS.	15
1.2	CLASSIFICATION OF GABIONS.	19
1.3	FUNCTION OF GABION STRUCTURES AND AREAS OF THEIR APPLICATION	26
1.4	PROS AND CONS OF GABION STRUCTURES.....	30
1.5	GABION RETAINING WALLS	31
1.6	DESCRIPTION AND ANALYSIS CONSTRUCTION OF THE GABION STRUCTURES. MAINTENANCE OF GABION WALLS	33
1.6.1	PREFABRICATION AND TRANSPORTATION OF GABIONS	33
1.7	SEQUENCE AND CONSTRUCTION TECHNOLOGY OF GABION GRAVITY RETAINING WALLS	34
1.7.1	TERMS.....	34
1.7.2	PREPARATION OF THE BASIS	34
1.7.3	MOUNTING OF GABIONS	35
1.7.4	INSTALLATION OF GABIONS.....	37
1.7.5	FILLING GABIONS.....	38
1.7.6	INSTALLATION OF THE GABION LID.....	41

1.7.7	ARRANGEMENT OF THE FOLLOWING ROWS / FORMATION OF THE STRUCTURE	42
1.7.8	PLACEMENT OF THE CAP	43
1.8	MAINTENANCE OF GABION WALLS	43
2.	GABION RETAINING WALL DESIGN GUIDELINES	46
2.1	GENERAL PRINCIPLES FOR THE DESIGN OF GABION RETAINING WALLS	46
2.2	TYPES AND CONFIGURATION OF GABION WALLS	47
2.3	CHARACTERISTICS OF MATERIALS	49
2.3.1	GRID SPECIFICATIONS	49
2.3.2	PROPERTIES OF MOUNTAIN ROCKS FOR FILLING OF GABIONS	51
2.3.3	FILTER MATERIAL.....	53
2.4	INITIAL DATA FOR DESIGN	55
2.4.1	MATERIALS OF ENGINEERING SEARCHES	55
2.4.2	BASIC PARAMETERS.....	55
2.4.3	DRAINAGE REQUIREMENTS	55
2.4.4	BASE WIDTH.	56
2.4.5	DEPTH OF LAYING.....	57
2.4.6	TILT ANGLE.....	57
2.4.7	DENSITY OF GABIONS.....	57
2.4.8	AMOUNT OF BACKFILL.....	58
2.5	METHODOLOGY OF CONSTRUCTION AND CALCULATION OF GRAVITY RETAINING WALLS	58
2.5.1	ULTIMATE LIMIT STATES TO CHECK ON A WALL.....	58
2.5.2	DESIGN TECHNIQUE	59
2.5.3	THE MAIN STEPS ON CALCULATION OF GABION UNDERGROUND WALLS.....	59
2.5.4	CALCULATED LOADS.....	59

2.5.5 DETERMINATION OF THE ACTIVE PRESSURE OF THE BACKFILL SOIL.....	60
2.5.6 FORCES ACTING ON THE WALL.....	60
2.5.7 EXTERNAL STABILITY OF THE GABION RETAINING WALL ..	61
2.5.8 OVERTURNING MOMENT CHECK.....	61
3. APPLICATION TO A CASE STUDY AND PARAMETRIC ANALYSIS	64
3.1 GIVEN DATA	65
3.2 MANUAL CALCULATION	66
3.3 CALCULATION USING THE "GAWAC WIN 2003" PROGRAM.....	68
3.4 CALCULATION WITH THE HELP OF THE PROGRAM "GAWAC WIN 2003"	72
4. CONCLUSION AND FUTURE WORKS	76
REFERENCES	78
ANNEX A	83
ANNEX B	123

List of Figures

1. Figure 1.1 a- use of gabions by ancient Egyptians; b- use gabions for fortifications; c-gabions at the artillery position, 1856.....	15
2. Figure 1.2 The events of the Napoleonic Wars or the defense of Sevastopol.....	16
3. Figure 1.3 The HESCO bastions.....	17
4. Figure 1.4 The instruction of installing HESCO bastions.....	18
5. Figure 1.5 Types of gabion structures: a – gabion baskets; b – gabion sacks; c – gabion mattresses.....	19
6. Figure 1.6 Gabion basket.....	20
7. Figure 1.7 Gabion mattresses.....	22
8. Figure 1.8 Gabion mattress.....	23
9. Figure 1.9 Cylindrical gabions.....	25
10. Figure 1.10 Gabion wire mesh.....	26
11. Figure 1.11 Gabions in engineering structures: a – gabion caged basket in bridge abutment; b – gabion retaining wall.....	27
12. Figure 1.12. Gabions in design: a –gabion installed as external cladding of the facade; b – elements in low-rise construction from gabion.....	27
13. Figure 1.13 Gabions In the landscape and park sculptures: b – decorative flower bed from gabion; c – bench made from gabion.....	28
14. Figure 1.14 Gabions in fence structures: a – decorative fence from gabions; b – decorative fence from gabions.....	29
15. Figure 1.15 Gabions for military purposes: a – military hesco barrier; b – welded gabion box.....	29
16. Figure 1.16 Gabions in road construction: a – gabion structures for the slopes; b – retaining walls for the road embankment.....	30
17. Figure 1.17 Examples of gabion retaining walls.....	32
18. Figure 1.18 Geometric elements of gabion basket and mattress.....	33
19. Figure 1.19 Stages of installation of the gabions.....	35
20. Figure 1.20 Unpacking and assembly process.....	36
21. Figure 1.21 Collection of parts: a - with cord; b - with C- rings.....	37
22. Figure 1.22 Gabion extract before filling.....	37
23. Figure 1.23 Filling the gabion box with stones.....	39

24. Figure 1.24 Reinforcing details.....	40
25. Figure 1.25 Filling pattern of gabion boxes.....	40
26. Figure 1.26 Gabion construction frame.....	41
27. Figure 1.27 Installation of the gabion lid.....	42
28. Figure 1.28 Tools for lacing and bracing operations.....	42
29. Figure 1.29 Gabion placement.....	43
30. Figure 1.30 Geotextile.....	44
31. Figure 2.1 Typical Cross Sections of Gabion Wall: a- with stepped; b- with batter angle; c- with offset.....	48
32. Figure 2.2 Details of mesh wire: a- mesh tipe and nominal size (D); b- selvedge, edge wire; c- polymer protective coating.....	51
33. Figure 2.3 Gabion filling with different type of stone.....	52
34. Figure 2.4 Non-woven geotextile.....	56
35. Figure 2.5 Drainage requirments. Use of non-woven geotextile in gabion retaining wall.....	56
36. Figure 2.6 Gabion wall with batter angle.....	57
37. Figure 2.7 Extent of backfill.....	58
38. Figure 2.8 Possible schemes of ultimate limit states of gabion gravity wall	58
39. Figure 2.9 Gravity wall design: a- stepped front face; b- stepped back face.....	60
40. Figure 2.10 Calculation scheme to determine wall resistance to overturning.....	63
41. Figure 3.1 Gabion retaining wall.....	65
42. Figure 3.2 Designed gabion retaining wall.....	66

List of Tables

1. Table 1.1 Standard dimensions of box gabions.....	21
2. Table 1.2 Standard dimensions of mattress gabions.....	24
3. Table 1.3 Standard dimensions of cylindrical gabions.....	25
4. Table 2.1 Density of the zinc coating of the wire	49
5. Table 2.2 Strength limit of mesh with hexagonal links of double-twisted steel wire;	49
6. Table 2.3 The diameter of the grid wires, edges, lacing.....	50
7. Table 2.4 Stone types for filling gabions.....	52
8. Table 2.5 Properties of rock to be fill in gabion.....	52
9. Table 2.6 Minimum geotextile strength of geotextile in terms of MARV under different installation.....	53
10. Table 2.7 Minimum requirement of puncture strength in different condition....	54
11. Table 2.8 Requirements for ultra violet stability.....	54
12. Table 2.9 Geotextile requirements for subsurface drainage.....	54
13. Table 3.1 Initial data for designing the gabion wall.....	65
14. Table 3.2 Parameters that were changed to compare the influence of different parameters on the design of a gabion wall.....	69
15. Table 3.3 Results of analysis of structural stability.....	70
16. Table 3.4 The analysis of changes sliding and overturning safety coefficient in the construction of the gabion wall.....	71

Nomenclature

Upper-case letters:

- P_a the total active force of the triangular pressure;
- K_a the coefficient of active soil pressure;
- H the wall height;
- B the base width;
- P_h the horizontal component of P_a ;
- M_r the resisting moment;
- M_o the overturning moment;
- SF_o the safety factor against overturning;
- SF_s the safety factor against sliding;
- W_g the weight of the gabion wall;
- W_v the sum of the vertical forces;
- P the maximum pressure under the base;
- P_b soil bearing pressure;

Lower-case letters:

- w_s the soil density;
- w_g gabion fill density;
- q distributed surcharge pressure;
- α slope angle of backfill surface;
- β acute angle of back face slope with vertical;
- δ angle of wall friction;
- φ angle of internal friction of soil;

d_a the distance of the total active force;

d_g horizontal distance to Wg ;

μ the coefficient of the sliding friction;

e eccentricity;

Introduction

Unlike reinforced concrete structures, similar structures made of gabions are advantageously distinguished by ease of installation, moreover, they can be built at any time of the year and do not require large costs. Every year, the effectiveness of gabions increases more and more. Gabion structures have gained considerable popularity due to a large number of advantages. Therefore, I chose a gabion retaining wall for research.

The relevance of the research topic consists in modeling the correct approach to the design and calculation of gabion retaining walls, observing the technology of their arrangement and maintenance, understanding the possibilities of solving environmental urban planning problems that can be avoided when using gabion structures.

The purpose of the work is to study the method of calculation and features of the design of gabion retaining walls.

The main tasks of the study:

- to determine the current trends in the use of gabion structures;
- determine the advantages and disadvantages of using gabions for the construction of retaining walls;
- to investigate the method of calculation of gabion retaining walls;
- perform the calculation of the retaining wall manually and with the help of programs;
- draw conclusions, give recommendations on the design of a gabion retaining wall.

The object of the study is the method of calculating a gabion retaining wall.

Chapter 1

1. STATE OF THE ART OF RETAINING WALLS

1.1 History of gabions.

Gabion from the Italian word ‘Gabbione’, means “big cage.”[1]

One of the oldest cases of using gabion cages was recorded approximately 7000 years ago - by the ancient Egyptians (figure 1.1a) They wove a basket with reeds or vines and filled it with stones to protect the banks of the Nile from erosion.

For the first time in the 15th century, Leonardo da Vinci used a gabion called Corbeille Leonard to build the foundation of the Castle of San Marco in Milan. The construction is so called the construction, which is made of metal mesh and filled with stone or other materials.

It follows that gabion is a volumetric mesh container, filled with stones from dense rocks. In other words, gabion structure is a gravity structure made of galvanized convoluted mesh filled with natural stones, which have a dimensional box (cylindrical) structure.

According to the established ancient "tradition", the most often novelties of certain technologies come into the life of civilians from the military sphere. Obviously gabions are no exception. Before becoming an integral element in design solutions, gabions were widely used in the Middle Ages (5th to 15th centuries) for military purposes, in particular for the construction of military bastions and fortifications, as shown in Figure 1.1b-c.

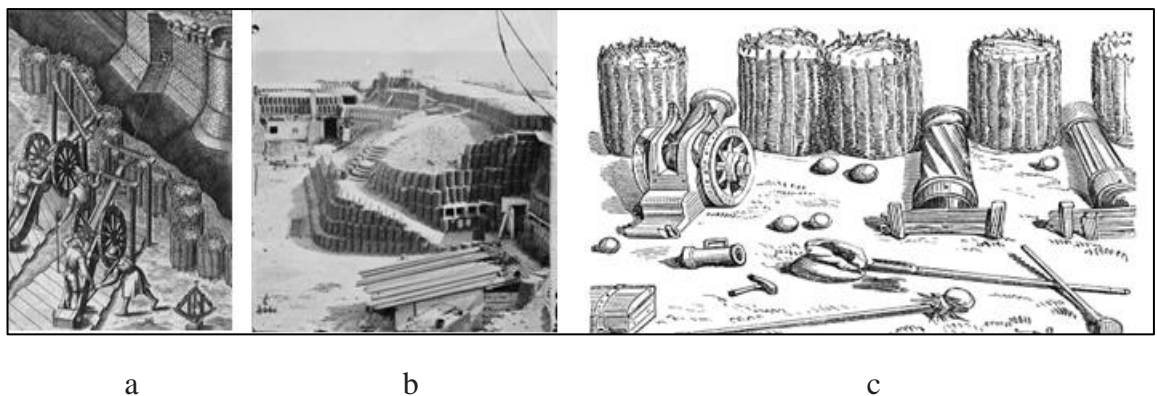


Figure 1.1 a- use of gabions by ancient Egyptians; b- use gabions for fortifications; c-gabions at the artillery position, 1856. [1]

Figure 1.2 shows the use of gabion baskets for the protection of artillerymen and infantry as defensive structures. Wicker baskets filled with rammed earth were quite effective at that time for protection against bullets, buckshot, and even kernels.

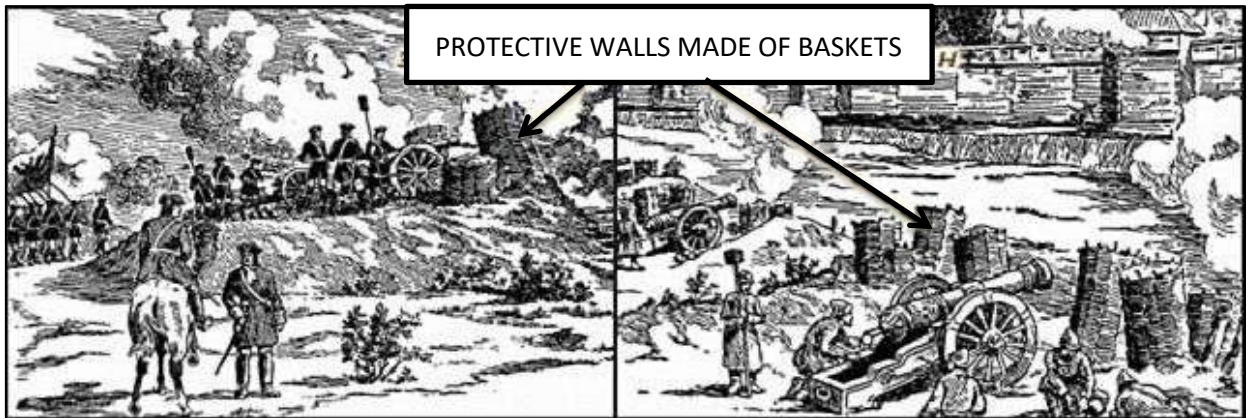


Figure 1.2 The events of the Napoleonic Wars or the defense of Sevastopol. [1]

International experience using gabion structures over a century, clearly shows the effectiveness and reliability of this structures. To this day, gabion structures are used at NATO military bases. They are made of strong steel wire mesh and are designed for quick and convenient filling using automatic bucket loaders. In addition to military purposes, gabions were often used in heavy hydraulic engineering and road construction, including for strengthening slopes, dams and for strengthening river banks.

The most common use of gabions in civil construction has been patented and refined by Gaetano Maccaferri in the late 1800s in Sacerno, Emilia Romagna/Italy. [3] The structures restrained water flows during floods and served as good dams (dykes) to protect settlements from natural disasters. Besides, gabion retaining walls were used in mountainous areas to contain rock slides and strengthen slopes along roads.

Despite the fact that gabions were invented several centuries ago, today their appeal has increased significantly. This type of construction is being rediscovered for many infrastructure and architectural projects. With the development of technical progress and science, engineers are increasingly trying to use the latest materials, technologies and trying to implement new knowledge in the field of construction.

The time of thoughtless use of natural resources and minerals is a thing of the past. In developed countries, synthetic and chemical materials are being replaced by safe and ecological natural materials every year. One of such materials with a wide range of applications is gabions.

Modern gabions are becoming more and more integrated into the environment and are more often used in landscape design, design of courtyards, greening of territories, in the construction of facades, fences, walls and elements of small architecture.

A key factor of the growing popularity of gabions is their versatility, availability, ease of manufacture and assembly technology. They allow to create a visual effect that matches its natural surroundings. By infilling cages with locally sourced materials, new spaces can easily be tied into the culture of an area and location. Smart use of filler helps reduce waste, such as reusing needless materials to create different shapes, patterns and layers that create great visual interest. [4]

A further reason for the urgent need for construction a barrier to protect against, mortars, shrapnel, small arms, grenades and other common types of weapons on the battlefield was the invasion of russian troops into Ukraine. The Ukrainian military began to use analogues of the British HESCO bastions, which were developed by the Lviv Company Plit LLC.

The HESCO was first used in a security context in the 1990s. A Hesco bastion is a type of gabion used as a military fortification.

The Figure1.3 shows the HESCO bastions that are made up of a collapsible "wall" of wire mesh with a thick synthetic fabric.

The advantage of such gabions is the ease and speed of installation, which is an important indicator for protection and reducing the number of human losses on the battlefield. [5]



Figure 1.3 The HESCO bastions [5]



Figure 1.3 The HESCO bastions [5]

Figure 1.4 shows the construction and step-by-step instructions for installing gabions of this type.

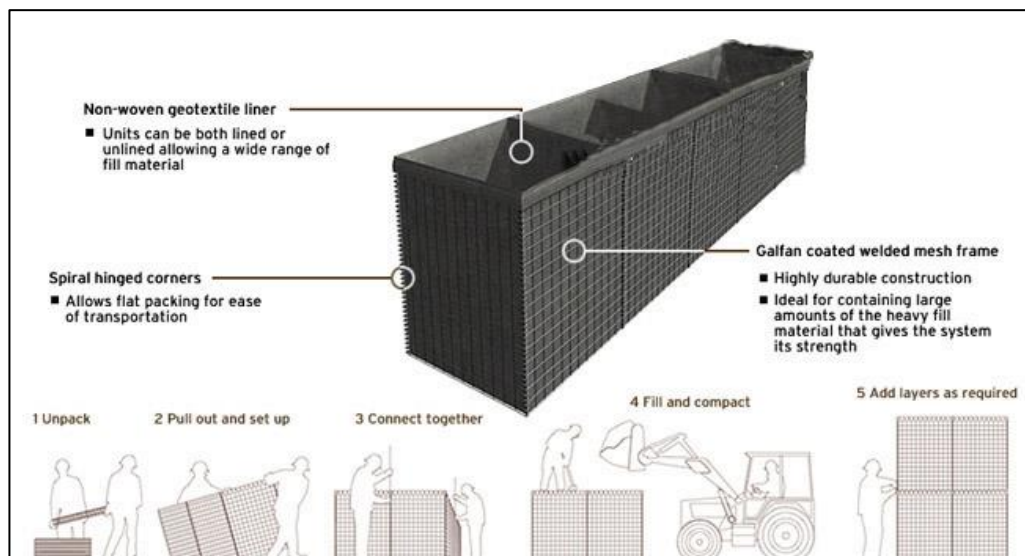


Figure 1.4 The instruction of installing HESCO bastions [5]

1.2 Classification of gabions.

Gabions are divided into different categories, depending on material of manufacture, structural features, type of mesh, functional purpose and other aspects.

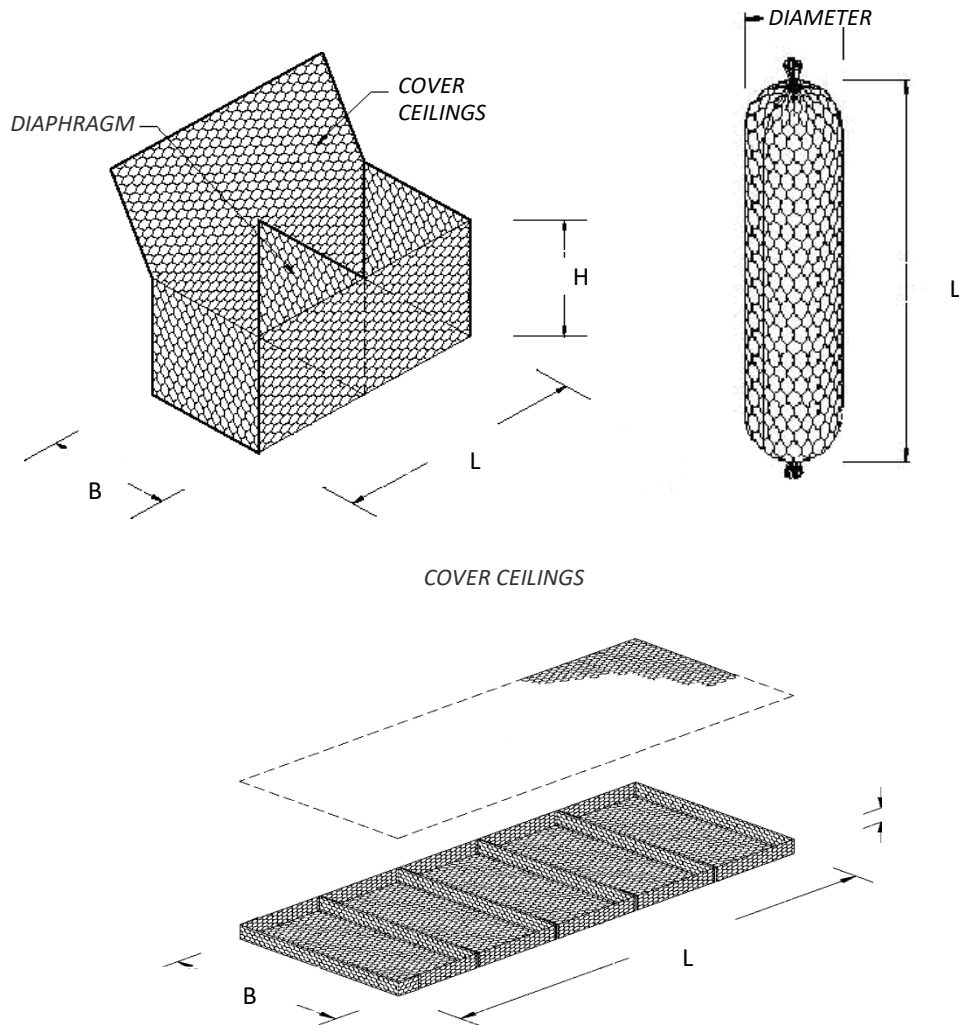


Figure 1.5 Types of gabion structures: a – gabion baskets; b – gabion sacks;
c – gabion mattresses. [13]

Accordingly, each of the gabions has its own specific name, shape and purpose. In various literary sources, there are the differences in the classification of gabion structures, so consider several types into which gabion structures are divided. [11]

According to structural features, gabions are divided to:

- Gabion baskets;
- Gabion mattresses;
- Gabion sacks.

Some sources additionally subdivide- gabion wire mesh. [11]

Figure 1.5 shows the types of each of the above-mentioned gabions.

Each of the aforementioned types is considered in more detail below. [1]

▪ Baskets-type gabion or “Jumbo” gabions are rectangular boxes made of wire mesh with hexagonal or square opening size. This type of gabion is the most common in the construction.

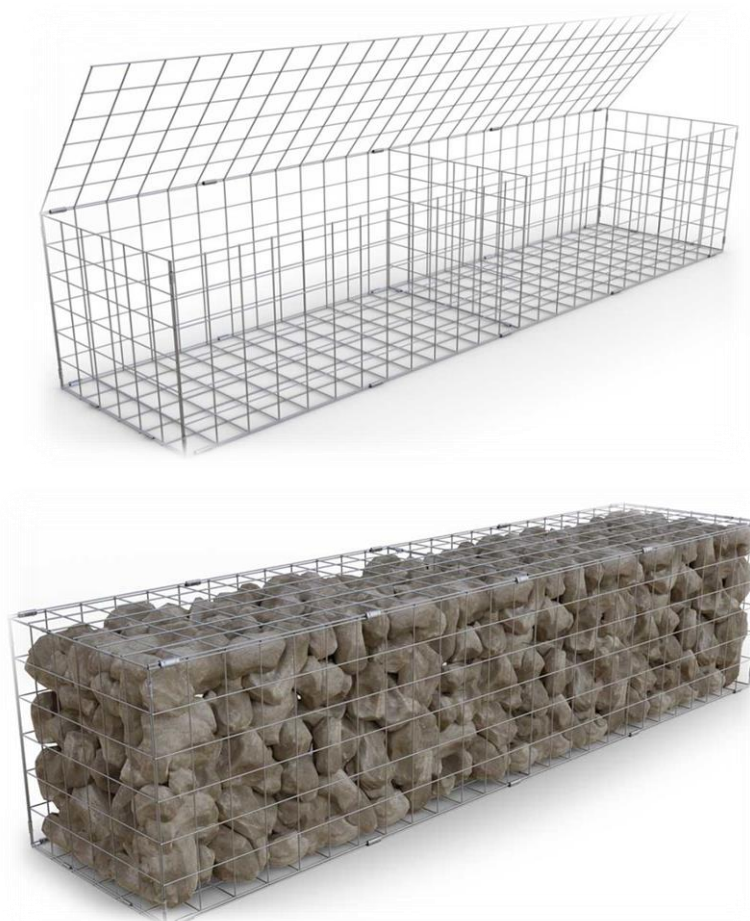


Figure 1.6 Gabion basket

Usually, the height (H) of the container is twice its width (B). Proportions of gabions: width (B): 1 m, length (L): 1.5-4 m, height (H): 0.5-1 m. If the length of the "Jumbo" gabions is larger (from 2 meters), then the structure is divided into sections, strengthened inside with the help of additional partitions (membranes), respectively they fasten the opposite walls to each other and thus strengthen the stability of the walls and increase the rigidity of the structure and evenly distribute the load. The frame of this type of construction is made from both welded mesh and twisting. As a result of connecting the containers together, an overall strong structure with clear lines and high strength characteristics is created.

Figure 1.5(a) shows the design of box-type gabions, where:

- B – the width of the gabion box panels;
- L – the length of the gabion mesh sheet;
- H – the height of gabion box panels.

Table 1.1 Standard dimensions of box gabions (table according to [12]).

Size, (m) LxBxH	Cell size, (mm)	Wire thickness, (mm) grids/edges	Wire coating
1,5x1x0,5	80x100	2,7/3,4; 3,7/4,4	Zn, PVH
2,0x1x0,5	80x100	2,7/3,4; 3,7/4,4	Zn, PVH
3,0x1x0,5	80x100	2,7/3,4; 3,7/4,4	Zn, PVH
4,0x1x0,5	80x100	2,7/3,4; 3,7/4,4	Zn, PVH
1,5x1x1,0	80x100	2,7/3,4; 3,7/4,4	Zn, PVH
2,0x1x1,0	80x100	2,7/3,4; 3,7/4,4	Zn, PVH
3,0x1x1,0	80x100	2,7/3,4; 3,7/4,4	Zn, PVH
4,0x1x1,0	80x100	2,7/3,4; 3,7/4,4	Zn, PVH

The main areas of using box-type gabions:

- construction of retaining walls;
- strengthening of roads and railways;
- strengthening of slopes and dams, banks;
- protection of pipelines;
- construction of fences, foundations, terraces, parapets, etc.;
- protection against erosion;
- production of decorative elements;
- for decorative use in landscape design.

If the structure will be located in an aggressive environment for a metal (constant contact with water), then a PVC-coated (Polyvinyl Chloride) mesh is used, which will protect the material not only from moisture, but also from chemical, mechanical, and corrosion damages. [1]

▪ Mattress gabion or "Reno", (picture 1.7) the name of this type comes from their characteristic shape, which resembles a mattress (they have a rectangular parallelepiped shape). The height (H) of these gabions is much smaller than the width (B) and length (L). They are designed in the following sizes: width (B) 2 m, length (L) 3-6 m, height (H) 0.17-0.30 m. "Reno" gabions usually have just one size of width (B) 2 meters, by analogy with a standard double bed.

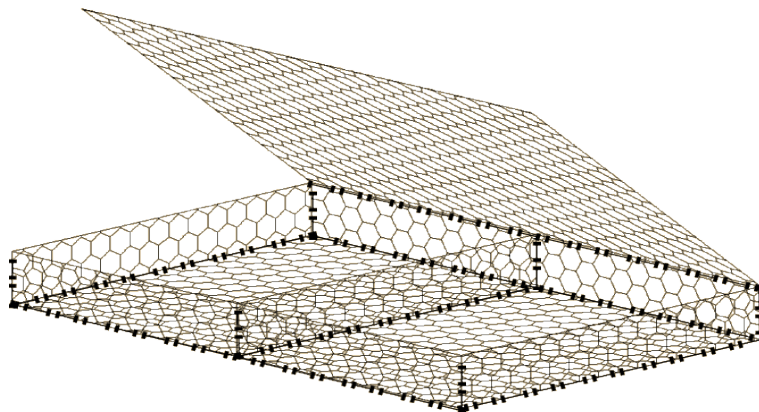


Figure 1.7 Gabion mattresses

This type of gabion can quickly adapt to small terrain irregularities, so the structure can be laid directly on the ground surface. For additional rigidity in the middle of the structure diaphragm partitions are installed every meter (figure 1.8).

Standard dimensions of mattress gabions are in the Table 1.2 Therefore, these mattresses can level the impact of water waves, thereby preventing soil erosion. Unlike "Jumbo" gabions, "Reno" mattress structures are easier to install, they have a smaller thickness and, accordingly, a smaller amount of filling materials. Usually, "Reno" mattresses are installed exclusively in a horizontal position, but there are cases when they were also installed vertically as sections of a fence. But it should be noted that this position of the structure requires additional strengthening with the help of pipes or structural channels.

This type of gabions is used to strengthen a retaining wall built from "Jumbo" boxes, as it perfectly distributes the load and strengthens the structure. [1]

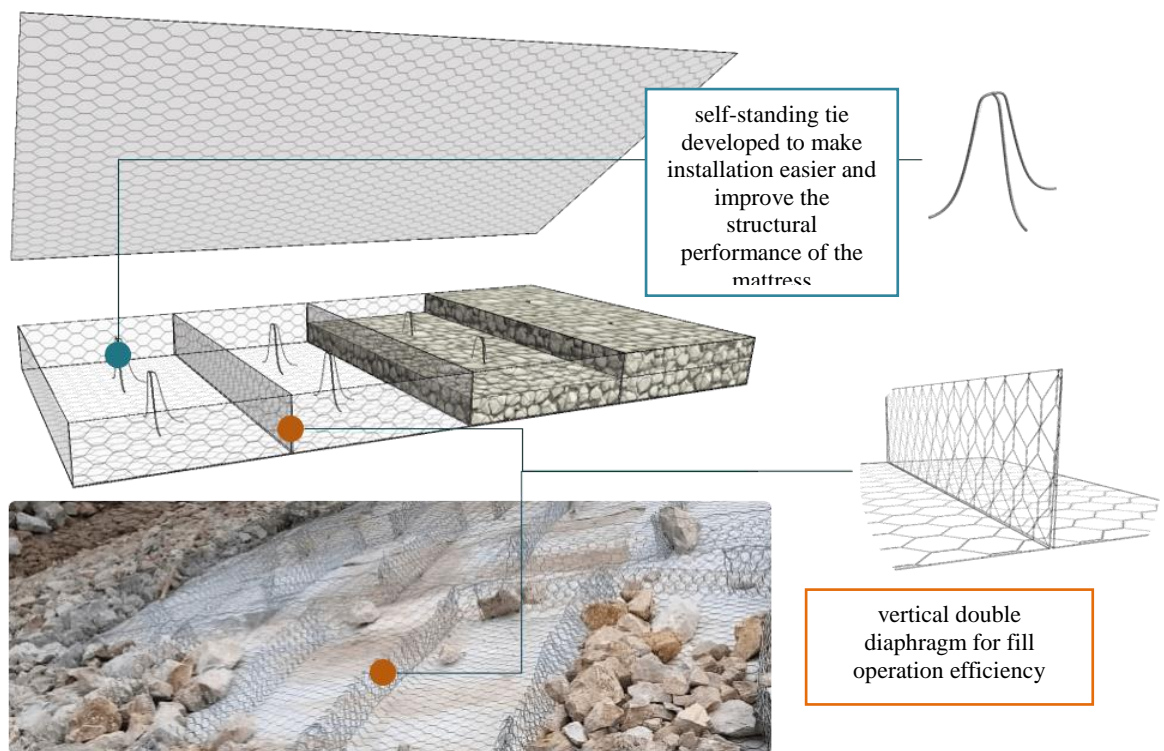


Figure 1.8 Gabion mattresses [19]

The main areas of using mattress gabions:

- lining of slopes and dams;
- strengthening of the coastline, ravines, canals.
- basis for hydrotechnical structures;
- foundation for box-type gabions;

Table 1.2 Standard dimensions of mattress gabions (table according to [12])

Size,(m) LxBxH	Cell size,(mm)	Wire thickness, (mm) grids/edges	Wire coating
3,0x2x0,23	80x100	2,7/3,4; 3,7/4,4	Zn, PVH
4,0x2x0,23	80x100	2,7/3,4; 3,7/4,4	Zn, PVH
5,0x2x0,23	80x100	2,7/3,4; 3,7/4,4	Zn, PVH
6,0x2x0,23	80x100	2,7/3,4; 3,7/4,4	Zn, PVH
3,0x2x0,30	80x100	2,7/3,4; 3,7/4,4	Zn, PVH
4,0x2x0,30	80x100	2,7/3,4; 3,7/4,4	Zn, PVH
5,0x2x0,30	80x100	2,7/3,4; 3,7/4,4	Zn, PVH
6,0x2x0,30	80x100	2,7/3,4; 3,7/4,4	Zn, PVH
3,0x2x0,50	80x100	2,7/3,4; 3,7/4,4	Zn, PVH
4,0x2x0,50	80x100	2,7/3,4; 3,7/4,4	Zn, PVH
5,0x2x0,50	80x100	2,7/3,4; 3,7/4,4	Zn, PVH
6,0x2x0,50	80x100	2,7/3,4; 3,7/4,4	Zn, PVH

▪ Unlike the first two types, cylindrical gabions (also often called bags) do not have an internal membrane have a porous structure, so they are easily and quickly placed on significant terrain irregularities and have higher flexibility. Figure 1.9 shows examples of cylindrical gabions. Gabions in the form of a cylinder have dimensions: length 2,3,4 m and diameter 65 — 95 centimeters.

The main areas of using cylindrical gabions:

- shore fortification, strengthening of slopes;
- protection of soils from possible erosion near the river and during hydraulic works in the event of a malfunction or accident;
- serve as a basis for leveling uneven terrain;
- protection against disasters;
- regulation of riverbeds (change of direction or division of the river, formation of sewage channels);
- protection of pipelines;
- creation of reliefs of different levels on the plots;
- decorative use.

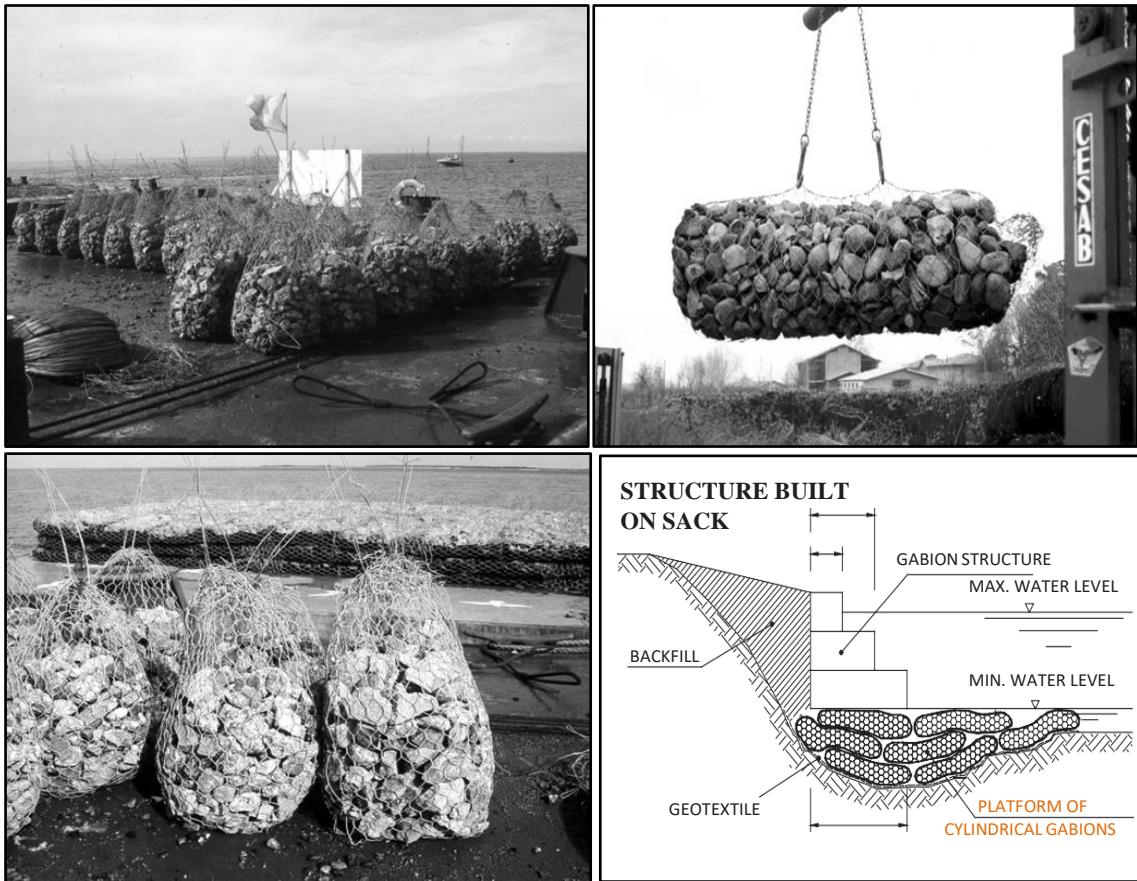


Figure 1.9 Cylindrical gabions

Table 1.3 Standard dimensions of cylindrical gabions (table according to [12]).

Size,(m) LxBxH	Cell size,(mm)	Wire thickness, (mm) grids/edges	Wire coating
2,0x0,65	80x100	2,7/3,4; 3,7/4,4	Zn, PVH
3,0x0,65	80x100	2,7/3,4; 3,7/4,4	Zn, PVH
4,0x0,65	80x100	2,7/3,4; 3,7/4,4	Zn, PVH
2,0x0,95	80x100	2,7/3,4; 3,7/4,4	Zn, PVH
3,0x0,95	80x100	2,7/3,4; 3,7/4,4	Zn, PVH
4,0x0,95	80x100	2,7/3,4; 3,7/4,4	Zn, PVH

▪ Gabion wire mesh are presented in the form of a grid, which is used to protect railways and roads from possible rock falls. Gabion wire mesh in combination with geogrid reinforcement is used to increase the strength of the soil embankment. [11]

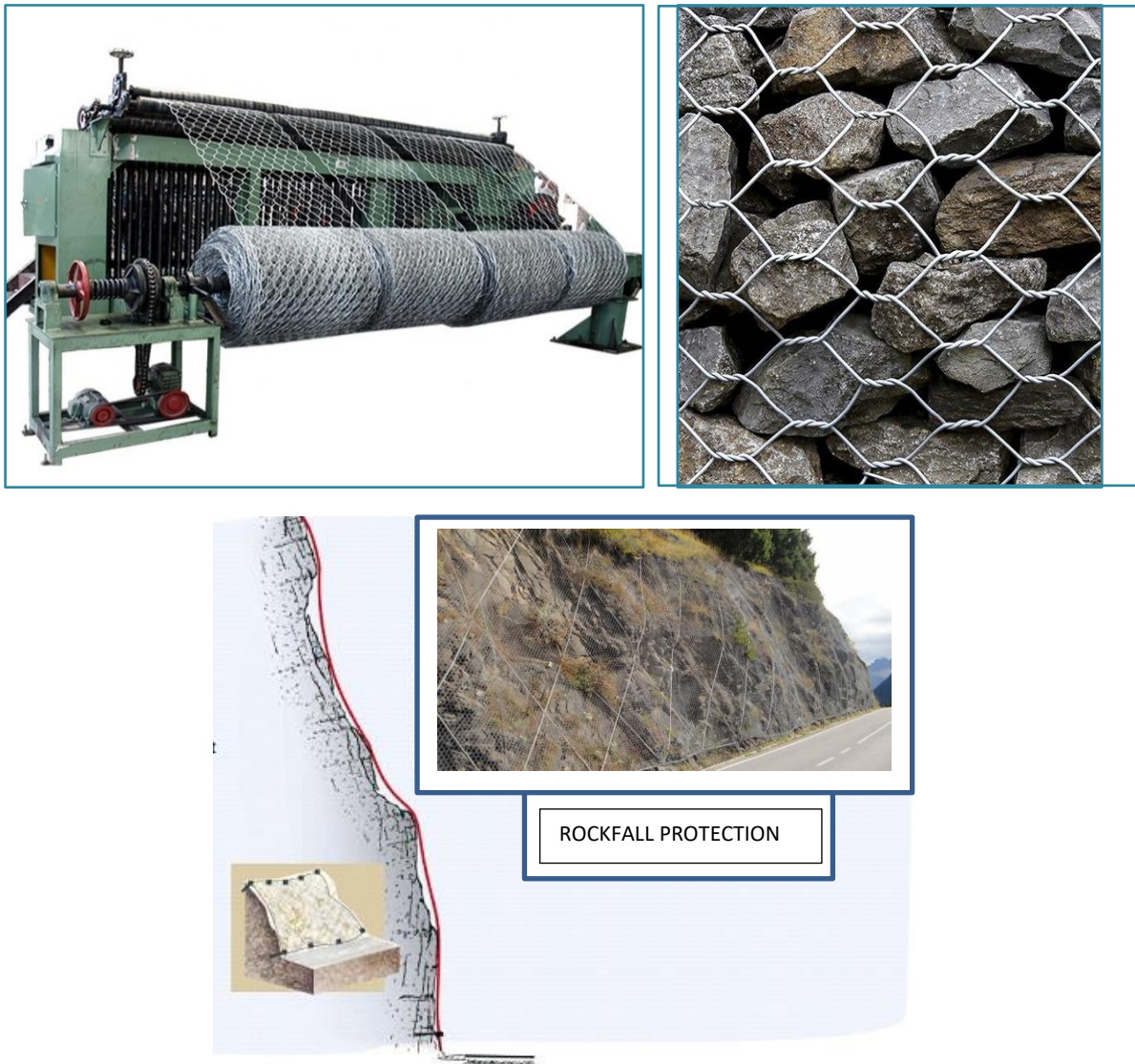


Figure 1.10 Gabion wire mesh

1.3 Function of gabion structures and areas of their application

In modern construction, gabions have acquired a wide range of applications, ranging from military purposes or road construction to decorative elements of garden and park sculptures. In European countries, they are actively used in elements of design, decor, and architectural solutions.

According to their functional purpose, gabions are divided to:

1. Gabions used on land;
2. Gabions used under water;
3. Gabions for variable water levels.

Each of the above gabions is used to prevent various damages and deformations. Having analyzed the wide possibilities of using gabion structures it is possible to determine the main areas of their application: [1,7,10,11],

- In engineering structures: retaining walls; strengthening of stability for banks and slopes; construction of dams, foundations; noise-absorbing barriers; temporary flood walls; structures for road embankment; prevention of rock slides; protection soils from erosion; protective structures for pipelines (figure 1.11);



Figure 1.11 Gabions in engineering structures: a – gabion caged basket in bridge abutment; b – gabion retaining wall. [31]

- In design: architectural cladding for walls and buildings; various decorative elements for the exterior and interior; construction of arches; construction of staircases and basement structures; installed as external cladding of the facade, used for the construction and finishing of columns, pylons and other elements in low-rise construction (figure 1.12);

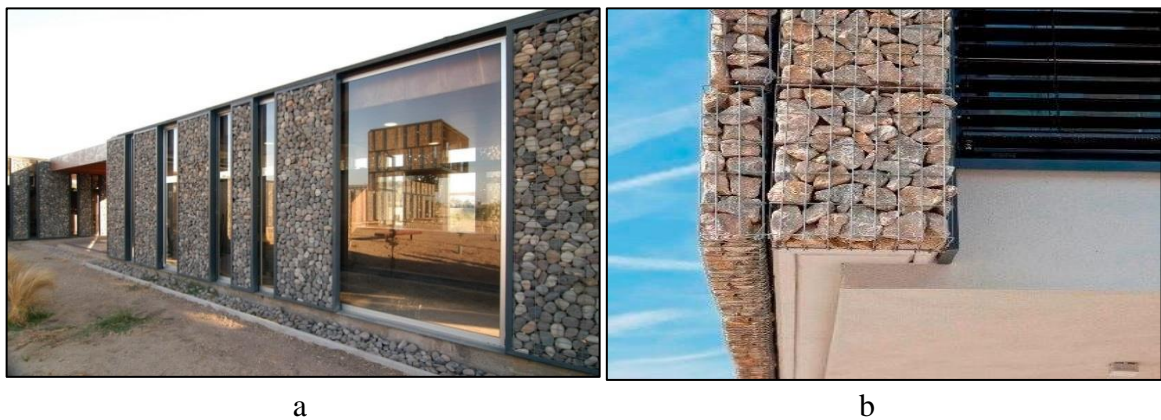


Figure 1.12. Gabions in design: a –gabion installed as external cladding of the facade; b – elements in low-rise construction from gabion.

- In the landscape and park (garden) sculptures: street furniture installed in the courtyard: tables, benches, chairs, fountains, etc.; garden paths; zoning and decoration of the courtyard; design of fences for framing lawns and flower beds, creating labyrinths and various geometric shapes; exterior decoration of outdoor stoves, grills, barbecues, swimming pools (figure 1.13);



a



b

c

Figure 1.13 Gabions In the landscape and park sculptures: b – decorative flower bed from gabion; c – bench made from gabion. [available online]

- In fence structures: construction of walls and fences, employed as a noise barrier) in the role of a temporary flood wall (figure 1.14);

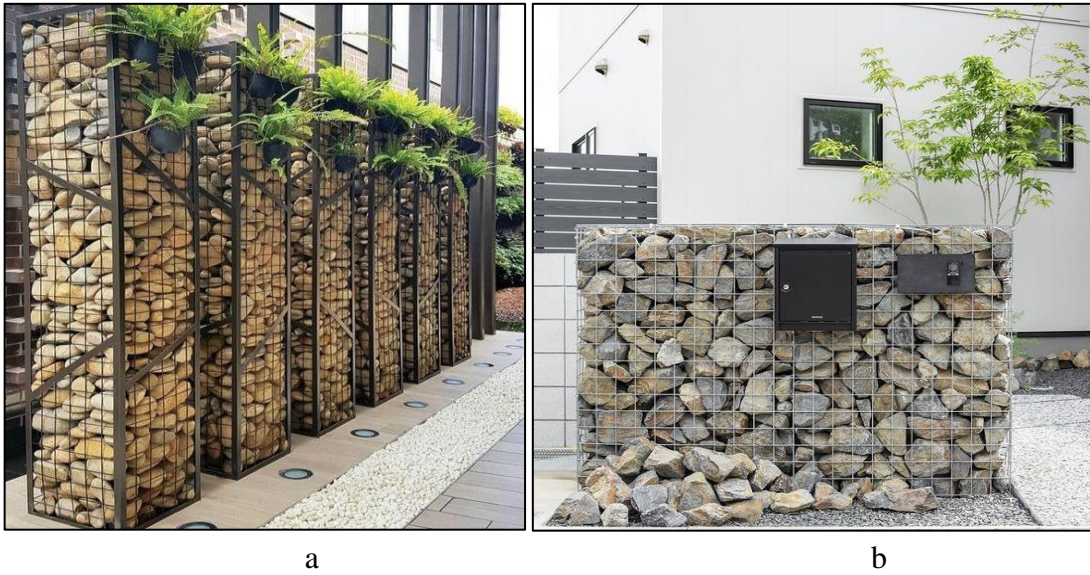


Figure 1.14 Gabions in fence structures: a – decorative fence from gabions;
b – decorative fence from gabions [available online]

- For military purposes used as fortification structures (figure 1.15);

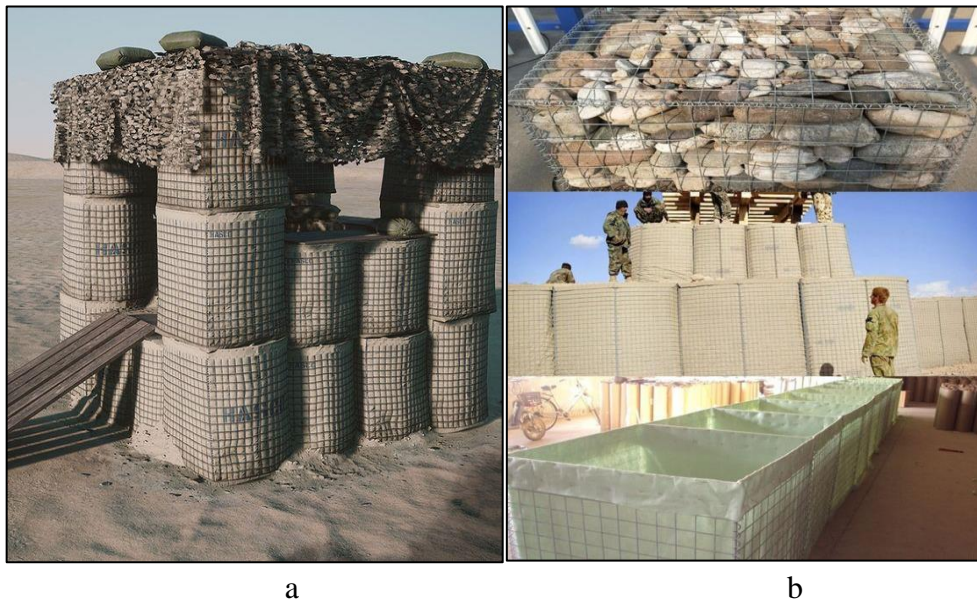


Figure 1.15 Gabions for military purposes: a – military Hesco barrier;
b – welded gabion box [available online]

- In the road construction: installation of protective structures for the slopes of the ground surface, overpasses; highway stabilization; retaining walls for the road embankment (figure 1.16);

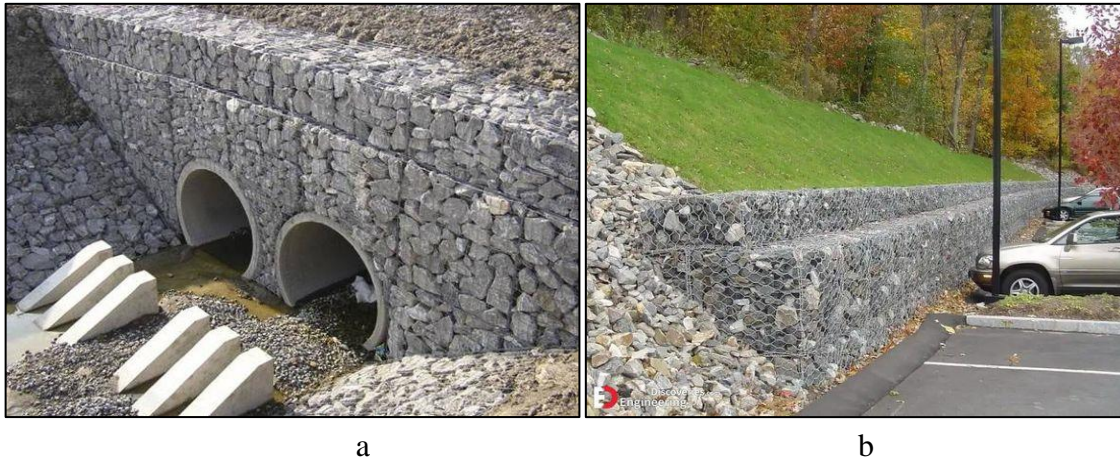


Figure 1.16 Gabions in road construction: a – gabion structures for the slopes; b – retaining walls for the road embankment [available online]

1.4 Pros and cons of gabion structures

Gabion structures have gained considerable popularity due to a large number of advantages.

- ✓ **Durability** (constructions made of other materials begin to break down over time, but not gabions. On the contrary, over the years, gabions only become stronger due to the filling of voids and the fusion of stones with each other. The product does not deteriorate due to temperature changes and does not stagger due to strong wind. In consequence of the galvanized wire, gabions are quite resistant to corrosion).
- ✓ **Flexibility** (one of the features of gabions, which allows their construction on areas with significant irregularities, in mountainous areas, in places with steep slopes and cliffs, in conditions of unstable soils. Gabions deform and settle, without losing their properties and effectiveness);
- ✓ **High permeability** (gabion is a good drainage element, so it excludes the installation of additional filters or drainage pipes);
- ✓ **High strength** (these are quite strong structures that can withstand floods, ice pressure, landslides, heavy downpours);
- ✓ **Cost-effectiveness** (gabions are more economical compared to other alternatives, both in terms of the use of materials and in terms of labor costs for manufacturing and installation.) As gabions are made of inexpensive materials, the cost of such structures is also low, since local stone materials can be used to fill the baskets. [11]
- ✓ **Environmentally friendly** (recycled materials can be filled into the gabion cage. Gaps in the soil allow plants to grow there. The materials from which gabions are

made do not harm the environment. After dismantling the structure, the material can be reused for various purposes. Using the gabion structure compared to a concrete retaining wall of the same size, can reduce CO₂ emissions by up to 80%; [9]

- ✓ **Fast installation** (for the installation of gabions, special heavy-duty equipment is not required. They can be used to make structures of various complex shapes). In addition, gabion structures are perfectly scalable, as they can be used for both massive structures and small structures); [3]
- ✓ **Reliability** (due to its heavy weight, gabions are securely fixed in place).

Gabion structures do not prevent the growth of vegetation and over time become part of the natural landscape. They fit well to any style of the region, almost completely merging with it, perfectly complementing the aesthetic value of nature. These are stable structures that do not require special care. If all the rules and technologies were taken into account, then gabions can stand for 50 to 100 years. Over the years, the gabion structures don't lose their purpose and color. They are ideal for all types of soils and climatic conditions. Designed constructions are also used as a cooling systems in hot climates and provides passive cooling due to air movement. [17]

Based on the review of literary sources [1,3,9,11,14,15,16,17], it can be confidently stated that gabion structures have practically no disadvantages. But some of them should be noticed:

- Both the cage and its contents will deteriorate over time, which means that you will need to replace them, leading to more expense and greater difficulty locating the resources.
- In instances of high velocity streams and wave interaction, gabion wall wire mesh baskets can abrade and tear open, spilling the rock fill.
- Gabion walls must be inspected on a regular basis to insure their integrity. They must also be immediately inspected and evaluated after any storm, which has caused heavier than normal water flow.

1.5 Gabion retaining walls

An experienced architect know how to turn the weak points of a site with slopes into interesting and profitable solutions in various aspects, so most often in such situations retaining walls are used to fixing the slopes. Gabion structures are most often used as

retaining walls (figure 1.17). All 3 types of gabions (gabion baskets, gabion mattresses, gabion sacks) are suitable for the construction of retaining walls. The structure of the wall can be different, depending on the angle of the slope that will be strengthened and the load that this wall will take. In one case, is used a stepped system, in another case, it can be installed at a certain angle to the slope of the site, in the third case, is used additional fastening (anchoring), which is buried in the ground. In the formation of retaining walls as a reinforcing structure, this is the most optimal option in terms of installation complexity and cost. It is worth noting, however that a large amount of earthworks is required before the installation of the structure. It is necessary to do accurate calculations of height and thickness of the retaining wall, as the reliability and quality of the gabion structure will depend on it. Gabion walls are also very cost effective as they require no maintenance. Moreover gabion walls are very profitable, as they do not need to be maintained. [1,18]



Figure 1.17 Examples of gabion retaining walls [17]

1.6 Description and analysis construction of the gabion structures. Maintenance of gabion walls

In this chapter discusses the technology of construction of the gravity retaining walls, which use their own weight to resist the lateral pressure of earth masses.

1.6.1 Prefabrication and transportation of gabions

The construction of the gabion wall consists in the installation of pre-assembled rectangular containers made of strong double-twisted steel mesh with hexagonal meshes, filled with rocks. Figure 1.18 shows the fundamental geometric elements of gabion baskets and mattresses

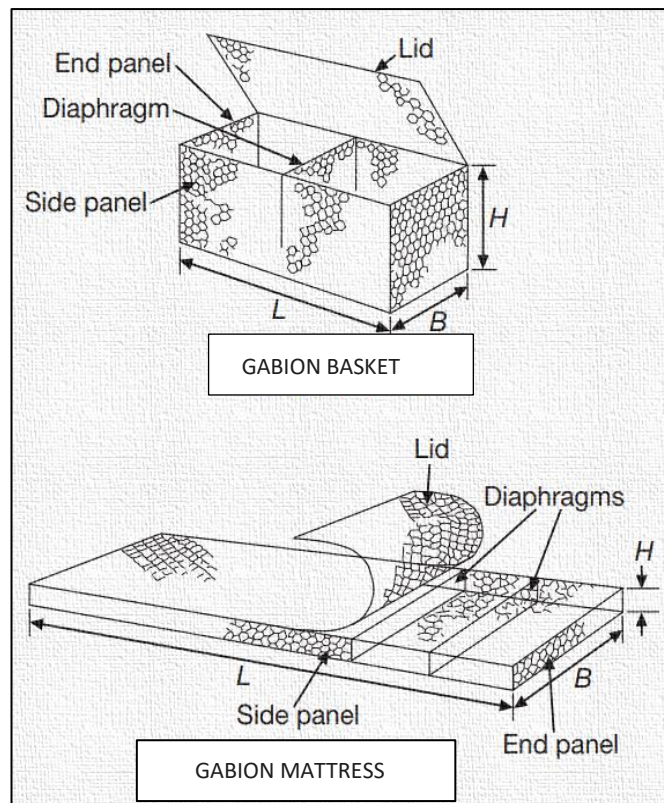


Figure 1.18 Geometric elements of gabion basket and mattress [27]

The prefabrication of gabions assumes that all its elements (base, front and back parts, lid) will be mechanically connected to each other into one whole.

Gabions can be divided into sections using diaphragms located every 1 m. This strengthens the structure of the gabions and facilitates their installation. In the case of possible mechanical damage to one or few cells, the main part of the structure works without reducing strength. Diaphragms have the same characteristics as the mesh that

makes up the gabion, they are fixed directly to the base frame of the gabions during their manufacture. The ends and diaphragm(s) must be factory bonded to the base. The lid can be a separate part of the grid of the same type as the box. All edges of the mesh around the perimeter of the box and lid must be mechanically treated with wire of a larger diameter. Diaphragms must be fixed in such a position to the base that additional lacing is not required at the workplace [24].

Gabion boxes are usually transported in a folded form and rebuilt into boxes of the required sizes on site. These boxes are connected using stainless steel fasteners or lacing or galvanized rings depending on the specifications.

1.7 Sequence and construction technology of gabion gravity retaining walls

1.7.1 Terms

In this work, the recommendations for carrying out work on the installation of a retaining gravity wall were considered. Recommendations are given in [14-25].

In the first stage, the project of carrying out works is developed, in which the technology and basic rules of execution of works on construction of gabion are described in detail. All types of work should be provided for when designing the project and drawing up a calendar schedule for the execution of the works: preparation, basic and finishing works. Methods of their evaluation should be developed to ensure the proper quality of the work. [14]

1.7.2 Preparation of the basis

At the beginning, prepare the base for the future wall and mark the axes. This stage is quite responsible, because it will influence all the further work of the construction. The basic requirements to the foundation depend on a number of factors: Geological conditions of the site, height of the gabion wall, its structure, etc. The upper (fertile) layer of the soil is usually removed to the indicated mark on drawings, that is, to the layer, which has the necessary bearing capacity. If the ground is removed to the desired mark, but the mentioned bearing layer is absent, it is necessary to consult with the responsible engineer for making a responsible decision. The prepared surface is cleaned and leveled, sealing the roller. In places where there is no access to the roller, use vibrobrambivki. Weaknesses must be checked and strengthened. If necessary, a saturated layer can be used, which is

compacted with a window roller weighing 8-10 tons to a minimum of 95% density according to Proctor density. Check the level (mark) before installing the gabion.

Gabions are brought to the installation site packed in bundles, they are unloaded and made on an equal basis on which wood blocks are laid. Check if the bundles and net are damaged. The height should consist of one for one maximum of four bundles [24].

1.7.3 Mounting of gabions

Installation of gabions is performed on the construction site according to the design decision (figure 1.19 shows the stages of installation of the gabions). For this purpose, the flat planed surface is enclosed by the formed gabions, fold them out to make sure that all its parts are equal and without damage. The panels are then stretched, aligned with the walls, and the existing dents. Bend the front, back, and side panels into a vertical position, forming a rectangular box. The top corners of the box are joined together. The top of each of the four sides of the gabion should be at the same level [14, 26,].

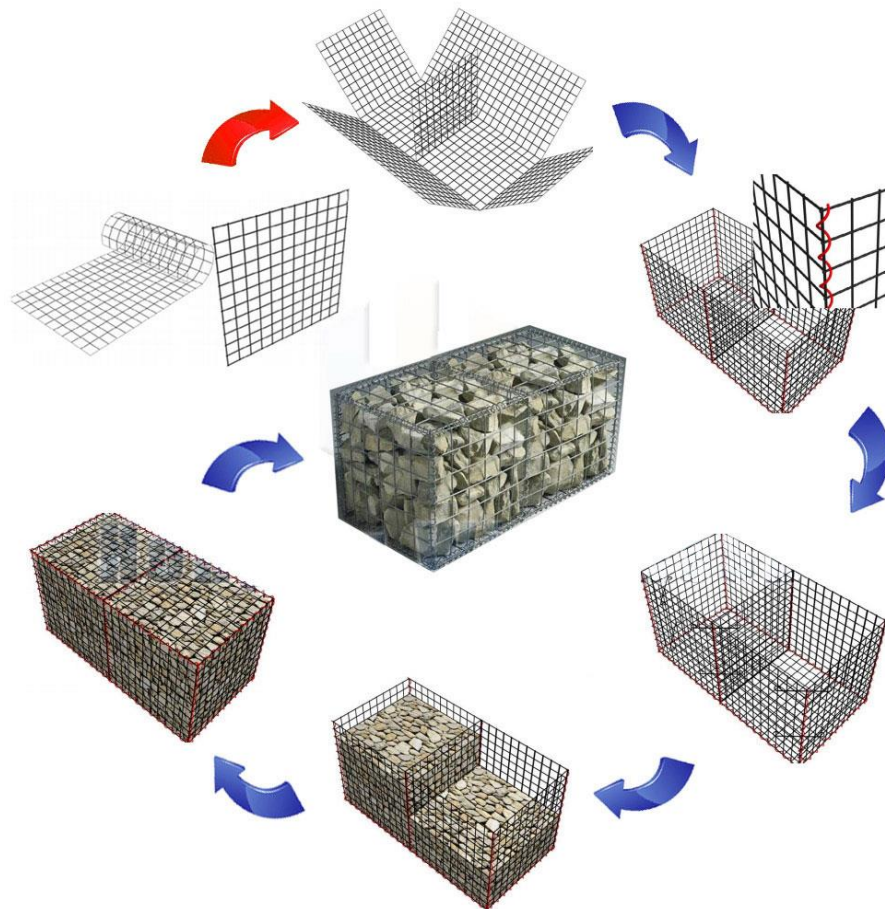


Figure 1.19 Stages of installation of the gabions [34]

The main stages of installation gabion:

1. Prepare materials;
2. Erect panels up;
3. Secure panels with spiral wires;
4. Install stiffeners;
5. Fill gabion with stones;
6. Close the lid.

The correct connection is controlled to create an exact rectangular shape of the specified size ([24], Figure 1.20).

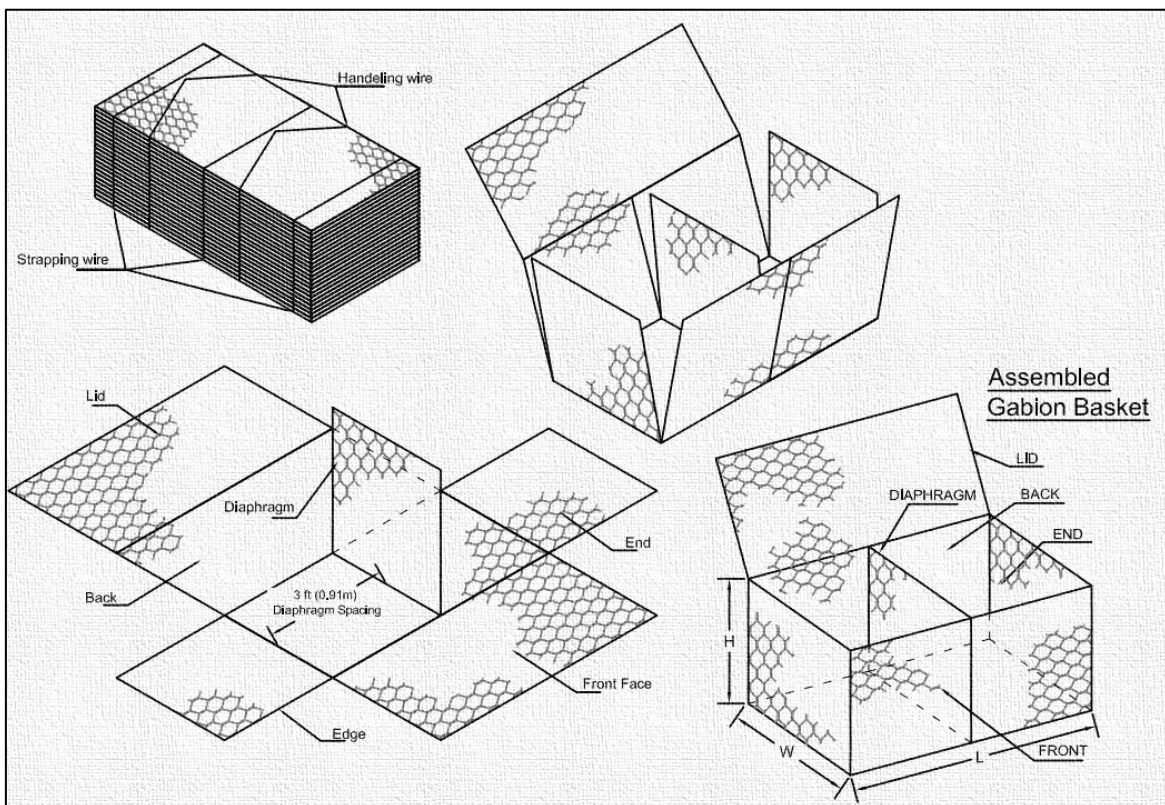


Figure 1.20 Unpacking and assembly process

The edges are connected together, starting from the top, with flicks, continuously, turning the single and double loop through each 100- 125 mm. The ends of the cord are fixed on each corner, and you should use a suitable cord for the entire gabion. The steel ring can be used instead of the cord wire, which are attached with a mechanical tool (figure 1.21a and 1.21b). [24]

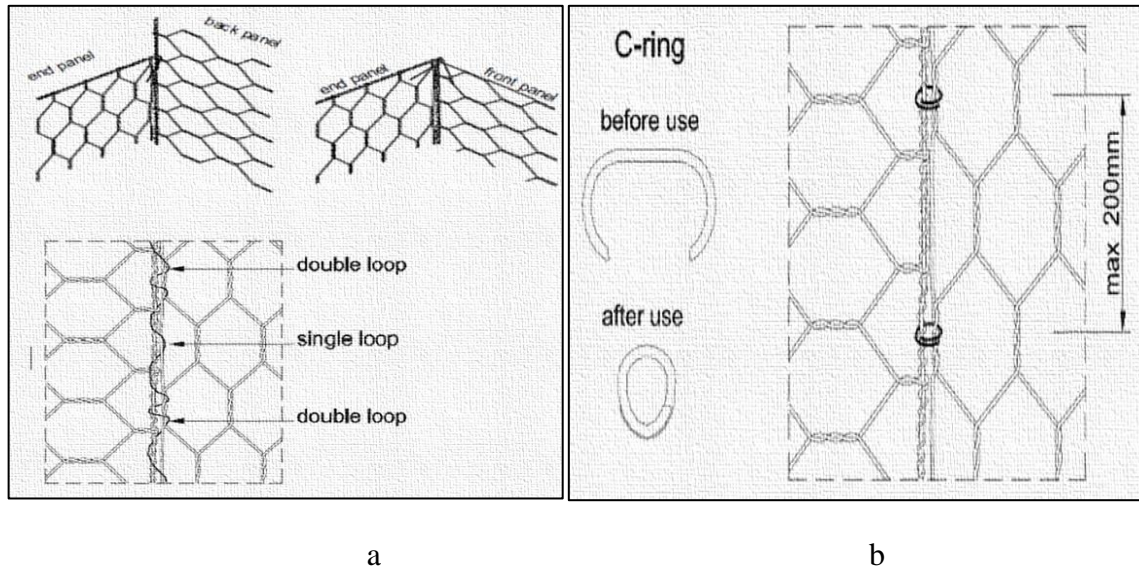


Figure 1.21 Collection of parts: a - with cord; b - with C- rings [24]

All other parties are also bound together. As a result, the frame of the structure (box with an open top), in which the filler will be inserted. Most often it is natural stone of different sizes and shapes.

1.7.4 Installation of gabions

Finished empty gabions are transferred to the place of construction assembly (according to the project). They are installed next to the gabions that are already filled with stones. Until the gabion is empty, it is necessary to connect the empty gabion with the already installed, as shown on picture 1.22. The overall dimensions are grouped together, with a strong stitch along all contact ends. The bottom gabions are fixed in the design position, closing in their corners metal rods, which are used to extract gabion [14, 26].

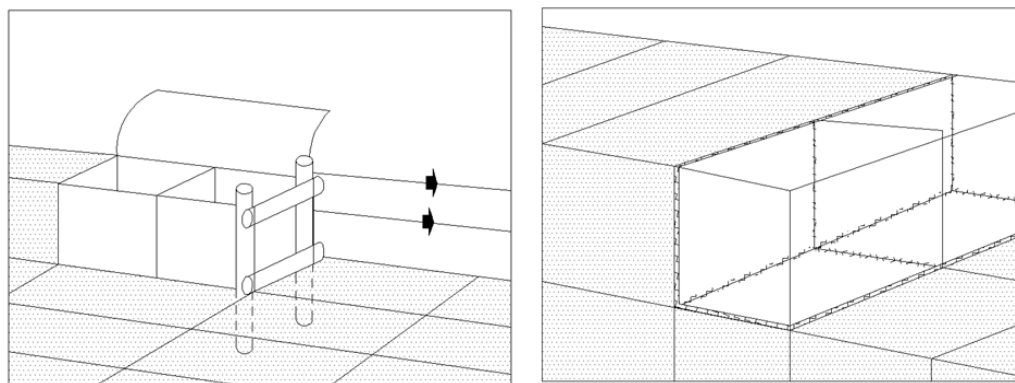


Figure 1.22 Gabion extract before filling [14]

If the gabion underground wall has a significant length, that is, takes a significant load, a compact (manual) winch can be used to tighten each installed gabion with simple adjustment for stretching. It is attached to the side of an empty gabion, the second side is attached to already filled elements. When working, the winch should be securely anchored. After stretching the gabion immediately should be filled with stones [14].

1.7.5 Filling gabions

Filling of gabions is carried out manually or with the help of the appropriate equipment (loader or excavator). The latter significantly increases the productivity of works and reduces their cost.

Before starting to fill with stones it is necessary to check the non-damage of the gabion and its final alignment. If any damage to the facade elements (gabions), armation elements or connections is found during installation or mounting, the damaged element must be replaced [26].

The filler must meet the engineering requirements: to have the appropriate strength on the press and durability, as well as frost resistance to resist loading, atmospheric influences, and under conditions of use on rivers - also influence of water on the course of the whole term of operation of the structure [24, 25].

Gabions are filled with various stone materials. The filler for gabions can be the following types of stones: granite; basalt; shale; sandstone; quartzite; rubble; pebbles, etc.

The size and quality of the mountain pored should correspond to the specifications given in the drawings. The size of the stone must exceed the size of the hole in 1,5 – 2 times. Normally, a stone size of 125 – 200 mm (but not more than 250 mm) is used for filling (filling the gabion box with stones see picture 1.23). The minimum size of the stone must be larger than the size of the net opening, with only 5 – 7% of the smaller diameter of the stone allowed and placed inside the gabion [26] (Fig.1.23).

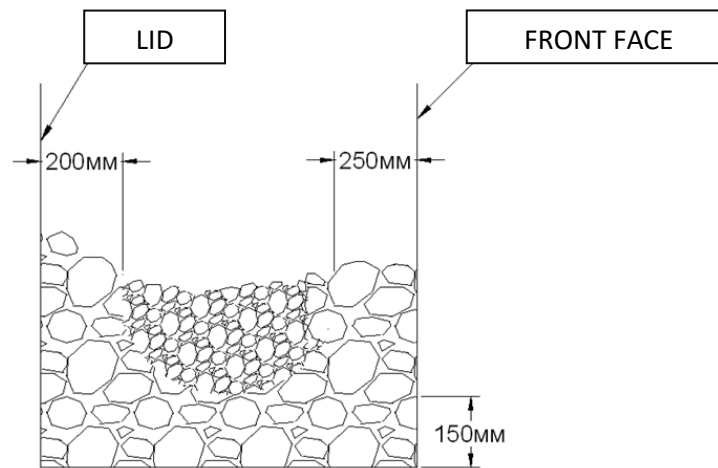


Figure 1.23 Filling the gabion box with stones.

The stones should be put with layers of height not more than 300 mm, more dense to each other, so that the quantity and dimensions of gaps between them were minimal. For this stone is sorted. The size of any large-size breed should ensure placement of at least three layers of stone during filling of blocks with height 1 m and at least two layers - for gabion blocks with height 0,5 m. [24]

To get a beautiful exterior surface of the gabion its front (facade) face must be laid carefully, picking up the stone. In the case of mountain breeds (rubble) it is necessary to choose stone so that at least one face has a flat shape.

It is important to remember that the use of an unsorted filler and/or incorrect filling of the gabion can lead to deformation of the boxes and sludge after completion of construction works. The porous content of the filled gabion box should be within 30-40%. To check the real porosity, it is necessary to weigh the boxes filled with stone and compare the received weight with the calculated weight of the box. [24]

To ensure a flat surface of the facade of the gabion wall, it is advisable to use internal tie wires during filling the gabions. They also prevent the gabions from being deformed at the filling stage. Using boxes with a height of one meter, the gabins fill first one-third of the height, then fix the tie wires (figure 1.24) by fixing the gabion from the middle with a horizontal cross over on top of the stone layer. Then carry out the same operations for the second and third parts. The height of 0,5 m is allowed to fill in two methods, using only one row of tie wires at half the height of the gabion. The height of 0,33 m is filled in one reception without the use of ties.

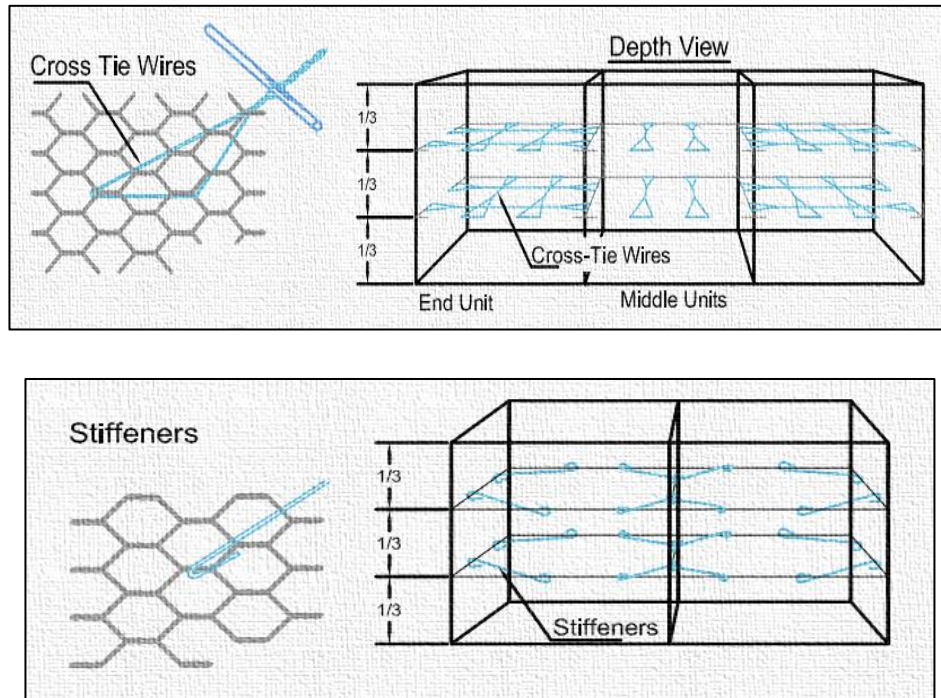


Figure 1.24 Reinforcing details.

To compensate for the settling of the stone, the gabion must be filled with reserve, 2,5 – 5 cm above its top edge. Small stone material is the most suitable for this purpose. Filling of the adjacent boxes should not differ in height more than 300 mm. For this purpose it is necessary to follow the schemes of filling, shown in figure 1.25. [26]

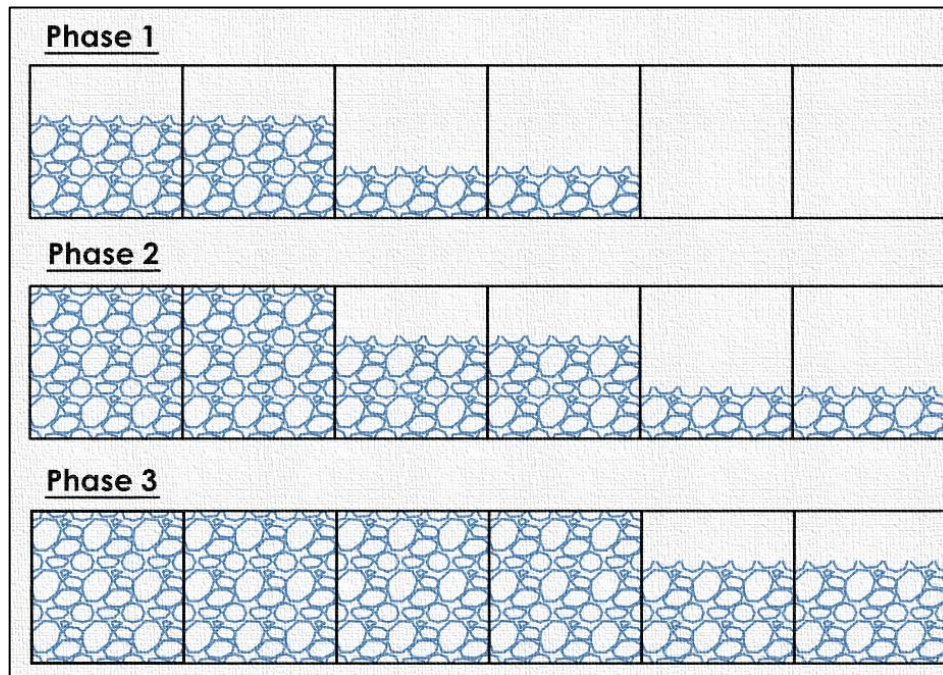


Figure 1.25 Filling pattern of gabion boxes.

Next, the last layer of the stone should be leveled so that the top of the diaphragm is visible, the cover is lowered and fixed on the edges of the gabions and on the top of the diaphragm with the help of a tie or cord. [25]

To ensure an even external surface of the wall and avoid the release of gabions, use temporary formwork (figure 1.26). It ensures the invariability of the size of gabion boxes at the time of stoning and laying of stones.

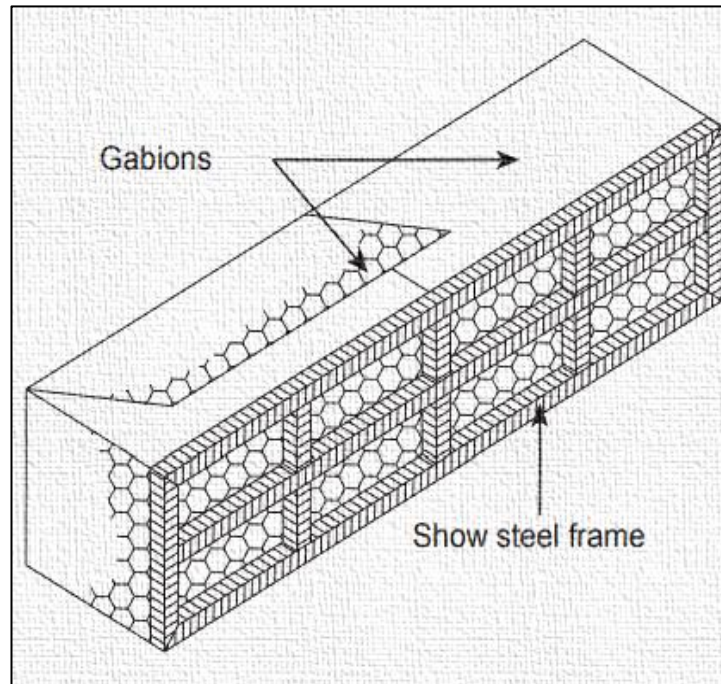


Figure 1.26 Gabion construction frame [28]

1.7.6 Installation of the gabion lid

The lid of the gabion must be tightly attached to the top faces of the gabion and simultaneously wired. To do this, use a special tool (like "stapler") to pull and tie the lid of the gabion. The installation of the gabion lid is shown on the figure 1.27.

First of all, to do a temporary connection of angles, so that there is no collision of the grid around the perimeter of the top of the gabion. If the stone-filler prevents the tight lid attraction, it is necessary to move a little stone inside the gabion. At the end of the lid is tied to the diaphragms [14].

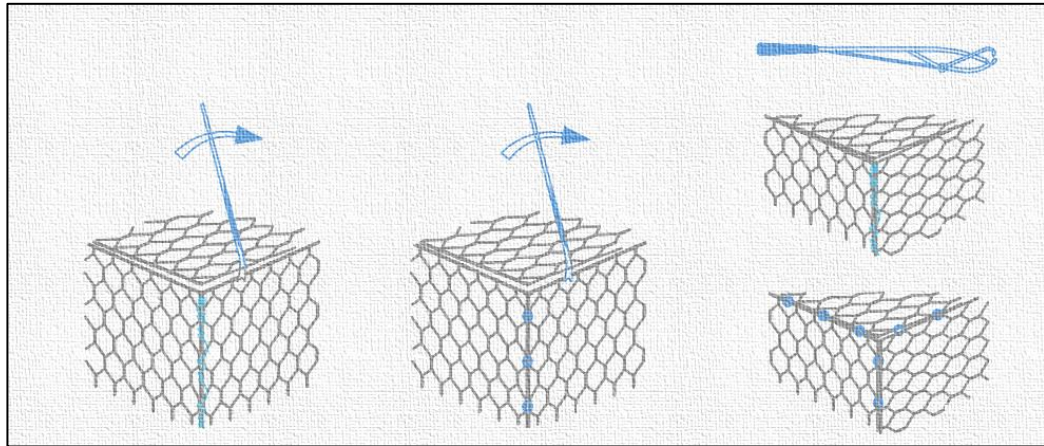


Figure 1.27 Installation of the gabion lid.

To make the lacing and bracing operations easier, it is recommended to use a pair of pliers to create tight joints. The picture 1.28 shows the tools that should be used to help to install the gabion. It is important to be careful not to damage the wire cover. The teeth of the pliers must be smooth. Not recommended to use fencing pliers as they damage the PVC and zinc coating. [28]

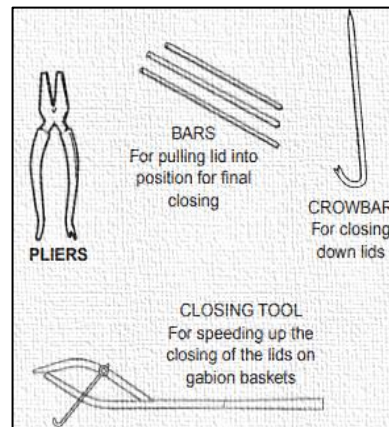


Figure 1.28 Tools for lacing and bracing operations [28]

1.7.7 Arrangement of the following rows / formation of the structure

Installing the next row of collected empty gabions, the top of the filled row should be positioned so that the vertical connections are shifted to each other. Empty boxes connect to the full wire at all outer lower edges. Vertical edges connect with wire or spiral connections. Similar actions, as in arrangement of the first row of gabions, are carried out until the complete completion of works on the installation of gabion wall, as shown in the picture 1.29. After each 10 m. along the wall it is necessary to measure the level of laid boxes. [25]

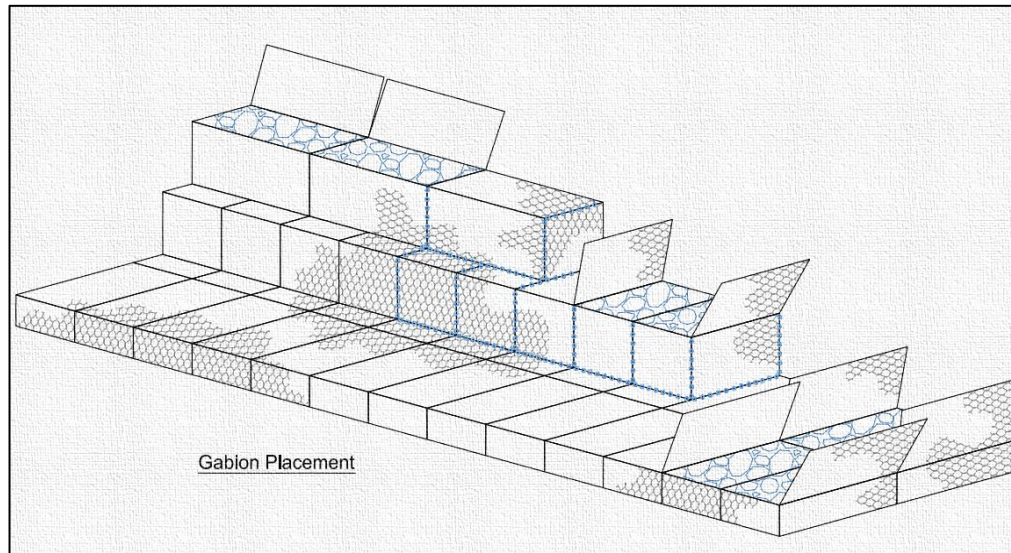


Figure 1.29 Gabion placement.

1.7.8 Placement of the cap

Before laying and sealing of the backfill, the sides of the curtain must be covered with unscanned geotextile. The backfill is compacted with the help of a roller weighing from 8 to 10 tons. The density of the compacted core should be not less than 95% of the modified density of the Proctor for the formation. The seals within 1,5 m from the rear of the end element are carried out with care, with the help of broiler seals or pass-through boilers with a load capacity of 1 t. [24].

1.8 Maintenance of gabion walls

The Gabion wall underfloor does not require special care during operation. The strength of the gabions is determined by the strength of the wire mesh. Lifetime of gabions (in non-aggressive environment) from galvanized wire from 8 to 12 years, from usual – from 3 to 5 years. During this period, gabion laying is usually so dense and colmataged that no longer needed in this mesh. The choice between galvanized and simple wire is made depending on the expected intensity of the colmatage of the gabin masonry and the intensity of the corrosion of the wire in this environment. The period of obtaining the greatest strength of the built gabion structures makes up 1-5 years depending on intensity and volume of accumulation of soil particles in the body of gabion, soil consolidation in the basis of these structures and their boards touching with the surface of the oushes (shores), which are strengthened and other factors.

The lifetime of the zinc coating of the wire, from which the grid of the gabion frame is made, is determined by the corrosion resistance of this coating. At the dense galvanized (260 g/m²) the actual service life of the zinc coating is determined from the experience of previously built gabion structures.

Laboratory-experimental tests show that at tight galvanizing (260 g/m²) the service life of zinc coating is 17-55 years. For the conditions of the marine (aggressive) environment, this figure is 6-25 years. At the density of zinc 50 g/m² the service life of zinc coating in normal conditions makes 4 years, and in marine - 1-2 years. For wire tight galvanized reduction of zinc coating from corrosion action is 10g/m²/year for normal conditions, 25g/m²/year for marine conditions. The lifetime of zinc coating under PVC sometimes reaches 120 years.

The simple double-twist mesh panels are often used to protect highways from rockfall and are also used to restore or initiate revegetation of steep rock slopes. The disclosure and implementation of all the possibilities of gabion structures can be carried out only on the basis of variable processing and comparison with other alternative variants of application of traditional or non-traditional constructions on specific objects of design.

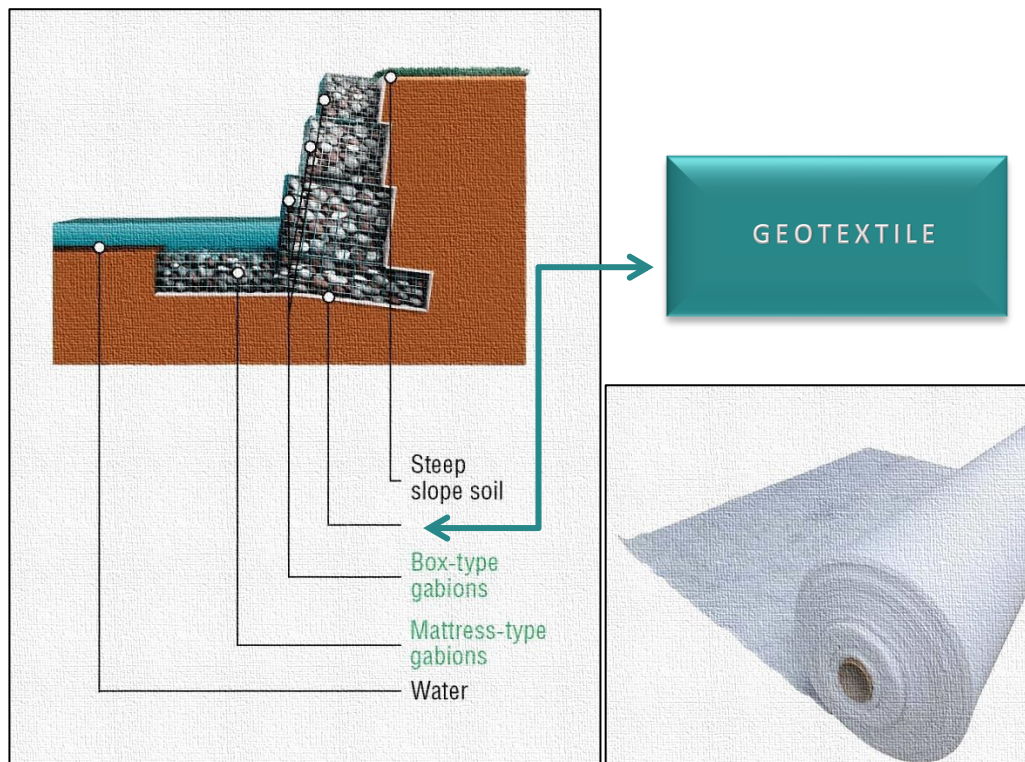


Figure 1.30 Geotextile.

The porosity of gabions prevents the development of pore water pressure behind the walls, which is one of the main advantages of such systems. These structures merge with the environment and allow plants to root through the structure, improving the lifespan of the structure.

In the basis of gabion structures instead of the underlying layer from traditional gravel-sand, rubble and other materials it is possible to use geotextiles. In order to prevent washing due to the gabions of a low or mixed (destroyed) during the operation of the stone material, the geotextile material is deposited in the bottom of the gabion frame. The figure 1.30 shows an example of the use of geotextiles in the structure of a gabion retaining wall.

Chapter 2

2. GABION RETAINING WALL DESIGN GUIDELINES

2.1 General principles for the design of gabion retaining walls

The gabion retaining wall is a simple flexible gravity structure, which in its weight holds the ground. It is designed according to the same principle as the gravitational wall: the mass of stone in the gabions must resist the harsh forces from the ground and external loading.

The Gabion wall is designed so that the gabion grid can keep the stones inside with limited deformation, which does not affect esthetics and internal stability [24].

The design of gabion structures intended for engineering protection of territories, as well as protection of lands, agricultural lands and natural landscapes from the processes of collapse and irrigation should be carried out taking into account the requirements of the current normative documents [25].

The design of gabion constructions and structures should be based on materials of engineering designs and results of hydraulic-hydrologic calculations, as well as on the use of design materials and decisions on those structural elements of earthmoving, which are to be strengthened, reinforced, stabilized, protected and combined with gabion structures and constructions [26].

Retaining walls (type, shape, design dimensions, etc.) should be designed taking into account local conditions, design loads and possible deformations.

The design of retaining walls from gabion constructions consists of construction (assignment of geometrical sizes and quantity of gabions) and calculations of them according to 2 groups of limiting states. The geometrical dimensions, which determine at the stage of construction, specify further calculations [26].

According to the first group of limit states, which involves the loss of bearing capacity or significant damage, the calculation is executed for:

- general stability (external stability):
 - stability of the slope of the embankment with the retaining wall behind the round-cylindrical sliding surface;

- resistance of the wall against displacement on the base;
- wall resistance against overturning;
- strength of the soil base;
- internal stability:
 - displacement of some gabions relative to others;
 - strength of the gabion as a structural element.

According to the second group of limit states (unsuitability for normal operation), the calculation includes a check for permissible deformations during operation of the structure. The calculation according to the second group of limit states is performed for the action of normative loads, that is, the coefficients of the reserve for the load and for the materials are taken to be equal to units. [26]

The geometric dimensions, which are determined at the design stage, are specified by further calculations. [26]

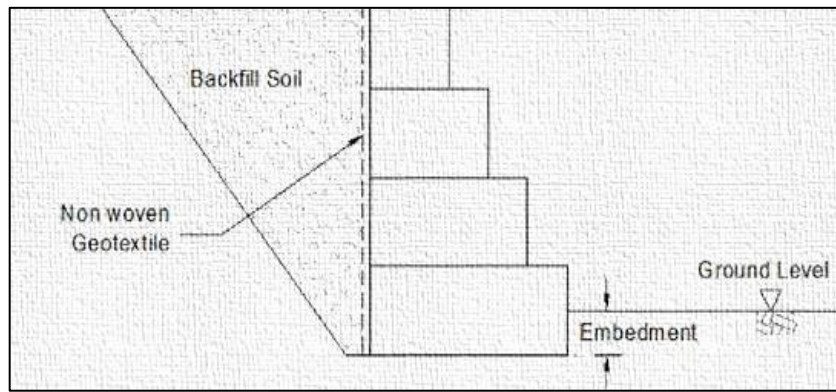
2.2 Types and configuration of gabion walls

These types of gabion retaining walls differ:

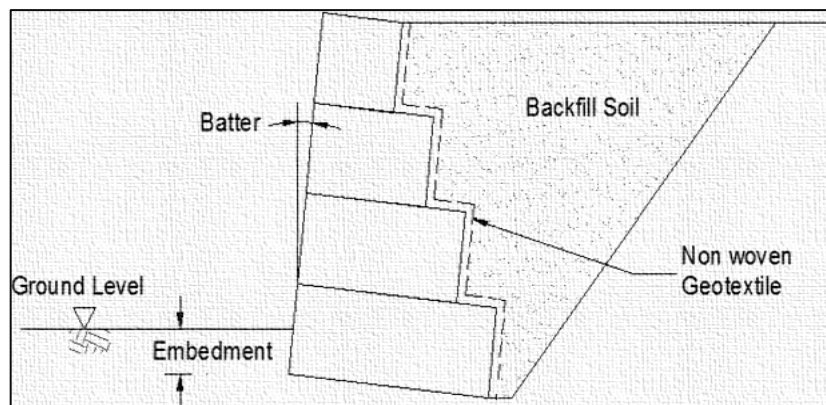
1. Gravity wall;
2. Semi-gravity wall;
3. Stepped wall;
4. Thin wall with anchoring.

The front faces of gabion retaining walls can be stepped (vertical or sloping) and smooth (vertical or sloping).

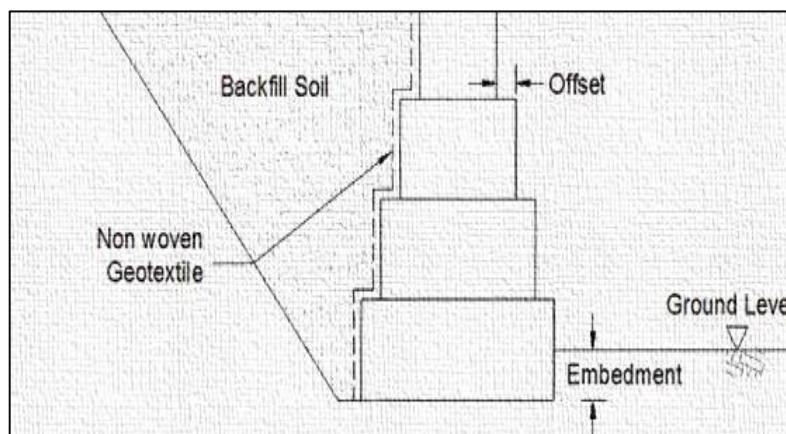
Depending on the site conditions and the initial data, the configuration of the gabion walls can be different, for example (a) with a stepped outside or (b) with batter angle or (c) with an offset, as shown in figure 2.1(a–c). [24]



a



b



c

Figure 2.1 Typical Cross Sections of Gabion Wall: a- with stepped; b- with batter angle; c- with offset. [24]

2.3 Characteristics of materials

2.3.1 Grid specifications

For the design of gravity wall from gabions it is recommended to use box-shaped gabions and gabion mattresses of rectangular shape, made of metal galvanized mesh with hexagonal holes from wire double torsion. The grid used for production of gabions, gabion mattresses, has a strength limit of 380-500 MPa and an extension of less than 12%. The core coating of the wire has a density of 0,240-0,290 kg/ m². In table 2.1 it's showed the density of the zinc coating of the wire. [14]

Table 2.1: Density of the zinc coating of the wire (table according to [14]).

№	Wire diameter, mm	Edges diameter ±, mm	Amount of zinc, kg/m ²
1	2.00	0.06	0.240
2	2.20	0.06	0.240
3	2.40	0.06	0.260
4	2.70	0,08	0.260
5	3.00	0.08	0.275
6	3.40	0.10	0.275
7	3.90	0.10	0.290

The breaking load of the metal mesh made of galvanized wire, depending on the combination between the size of the net openings and the diameter of the wire is 30-53 kN (Table 2.2). [14]

Table 2.2: Strength limit of mesh with hexagonal links of double-twisted steel wire (table according to [14]).

Link type	Strength limit, kN/m				
	Wire diameter, mm				
	2.00	2.20	2.40	2.70	3.00
5x7	35	40	45	-	-
6x8	30	35	42	47	-
8x10	-	-	34	43	53
10x12	-	-	-	35	43

To strengthen metal fittings and facilitate its laying on the edges of the grid is reinforced with a wire, which has a larger diameter than the wire. (Table 2.3, see fig. 2.2).

Table 2.3: The diameter of the grid wires, edges, lacing. (table according to [14]).

№	Wire diameter, mm	Edges diameter, mm	Wire diameter of the lacing, mm
1	2.00	2.40	2.00
2	2.20	2.70	2.00
3	2.40	3.00	2.00
4	2.70	3.40	2.20
5	3.00	3.90	2.40

Tensile strength: the wire used to make the mesh must have a tensile strength of at least $350 \text{ N/mm}^2 - 550 \text{ N/mm}^2$ in accordance with IS 280. Wire tolerances must match IS 16014 (Class T1). Extension: the extension of the wire should not be less than 10%. The test should be carried out as an example of a length of at least 20 cm [24].

The shape of the mesh cells is hexagonal. This helps to distribute efforts evenly. The main requirements to the grid are corrosion resistance and high tensile strength. To ensure corrosion resistance, manufacturers use alloy coatings (e.g. zinc and aluminum, such as Zn 95% Al 5% and Zn 90% Al 10%) that have proven to be better than zinc [24].

Making gabion structures in especially corrosion environment, gabion with polyvinylchloride (PVC) coating (zinc-coated grid, covered with PVC coating 0,4...0,6 mm) is used (figure 2.2c). [14]

Edge wire: a terminal wire used to edge the wire mesh parallel to the double twist (figure 3.2a) by continuously weaving it into the wire mesh.

Selvedge wire: a terminal wire used to edge the wire mesh perpendicular to the double twist by mechanically wrapping the mesh wires around it at least 2.5 times or by inserting it throughout the twists and folding one mesh length (figure 2.2b) [29]

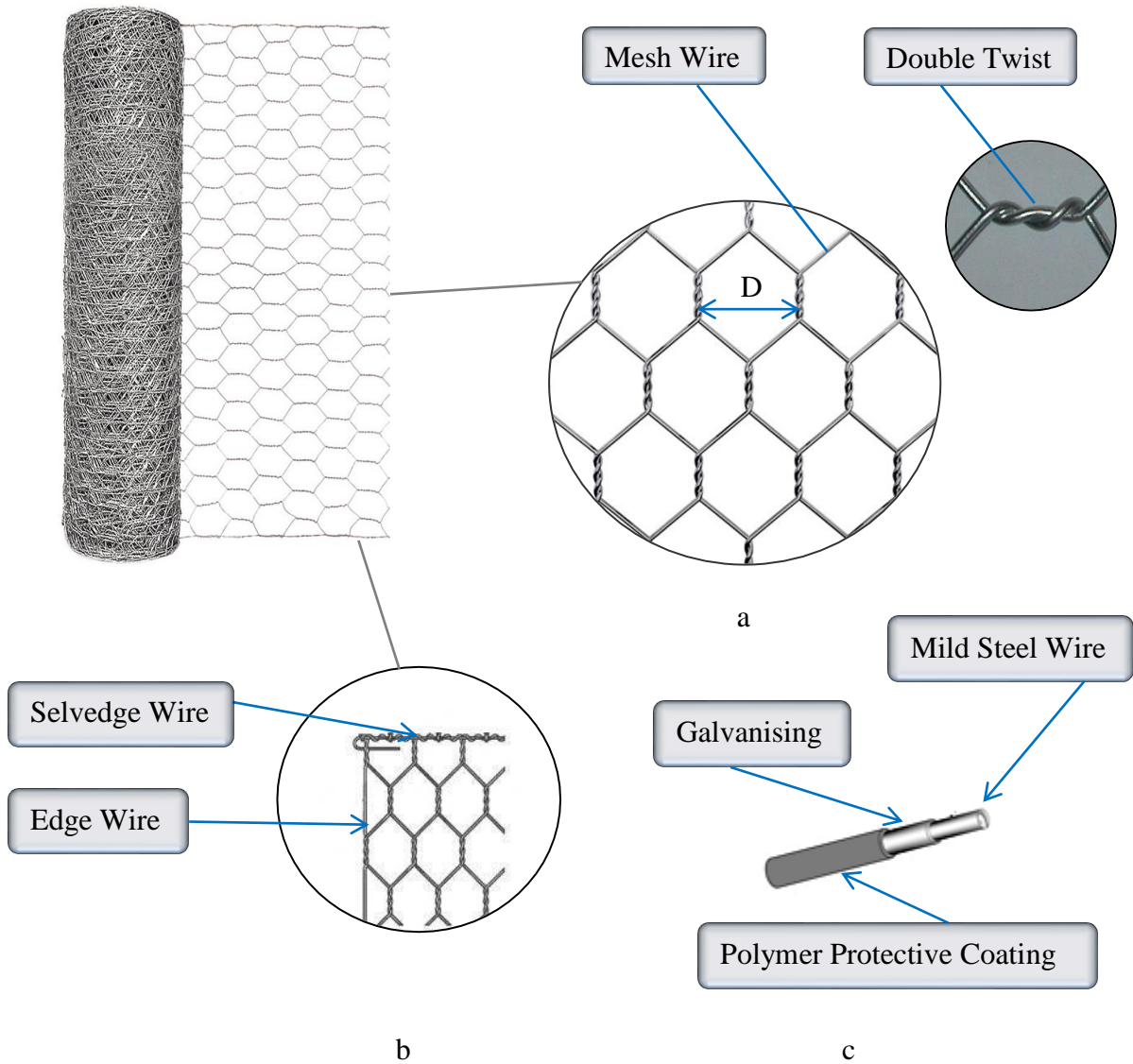


Figure 2.2 Details of mesh wire: a- mesh type and nominal size (D); b- selvedge, edge wire; c- polymer protective coating.

2.3.2 Properties of mountain rocks for filling of gabions

For filling it is recommended to use a material with a high specific weight of soil particles (not less than 17.00 kN/m³) and density 0.30...0.40; frost-free (with a mark on ice-resistance higher than MR 350); strong; non-ozone water; with high hardness.

The type of stone suitable for filling of gabions is given in Table 2.4, figure 2.3. [14]

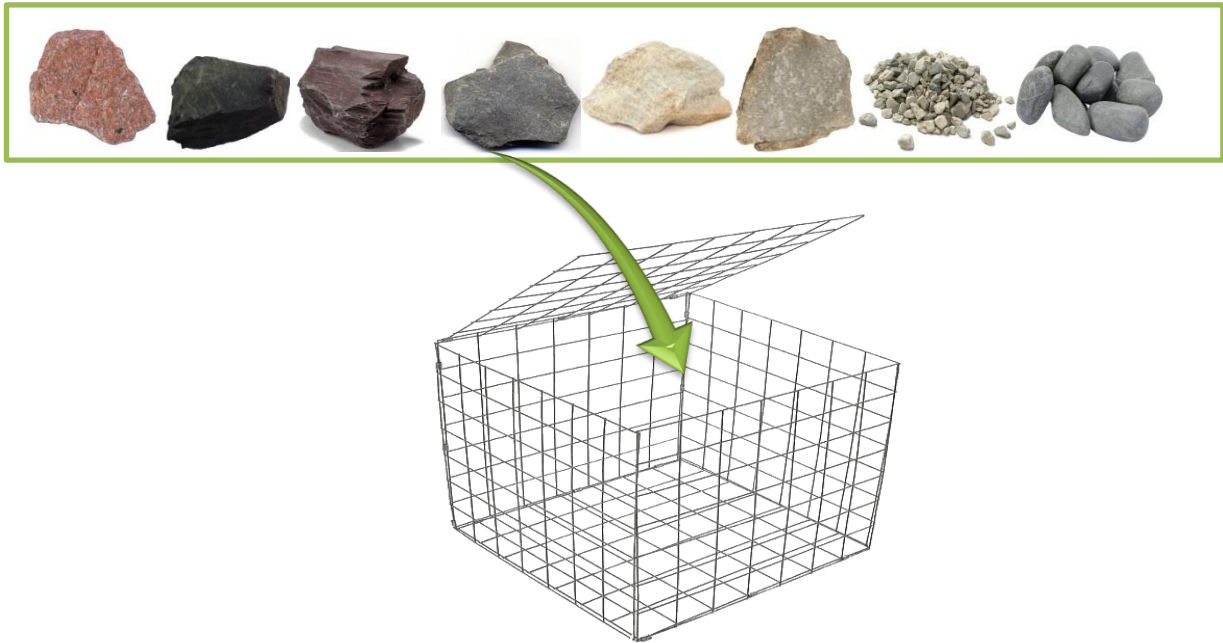


Figure 2.3 Gabion filling with different type of stone.

Table 2.4: Stone types for filling gabions (table according to [24]).

Stone type	Unit weight of soil particles γ_s , kN/m ³
Basalt	29.00
Granite	26.00
Dense limestone	26.00
Sandstones	23.00
Soft limestone	22.00
Tuff	17.00

Table 2.5: Properties of rock to be fill in gabion. (table according to [24]).

Sr No.	Properties of Rockfill	Values
1	Minimum and Maximum size of stone	1.5 to 2.5 times mesh opening
2	Tolerance on size of stone	± 5%.
3	Minimum density	22kN/m ³
4	Los Angeles abrasion value	Not more than 45

Minimum density and Los Angeles abrasion can be changed by designer based on availability of the rock in the area. In places where stones are not available alternate material having good characteristics can be used. (Table 2.5) [24]

2.3.3 Filter material

The filtering material should be non-woven needle or thermally bonded geotextile. Geotextile should be made of polyester or polypropylene. The average values of the geotextile specification should comply according document the IRC - SP-116-2018 - Guidelines for Design and Installation of Gabion Structure [24]

Table 2.6 Minimum geotextile strength of geotextile in terms of MARV under different installation (table according to [24]).

Installation condition	Type	Strength property requirements(MARV)							
		Grab strength in Newton(N) as per ASTM D 4632/IS 13162 Part 5		Tear Strength in Newton (N) as per ASTM D 4533/IS 14293		Puncture Strength in Newton (N)as per IS 13162 Part 4		Burst Strength in Newton (N) as per ASTM D 3786/IS 1966	
		Elongation at failure							
		<50%	<50%	<50%	<50%	<50%	<50%	<50%	<50%
Harsh installation condition	Type 1	1400	900	500	350	500	350	3500	1700
Moderate installation condition	Type 2	1100	700	400	250	400	250	2700	1300
Less severe installation condition	Type 3	800	500	300	180	300	180	2100	950

Table 2.7: Minimum requirement of Puncture Strength in different Condition (table according to [24]).

Installation condition	Strength property requirement (MARV)	
	Puncture Strength in Newton (N) as per ASTM D 6241.	
	Elongation at Failure	
	< 50 %	< 50 %
Harsh installation condition	2800	2000
Moderate Installation condition	2250	1400
Less Severe Installation condition	1700	1000

Table 2.8: Requirements for Ultra Violet Stability (table according to [24]).

Sr No.	Properties of Fabric	Requirements (Retained Strength)
1	Grab Strength	Not less than 70% after 500 hours of exposure.
2	Tear Strength	
3	Puncture Strength	
4	Burst Strength	

Table 2.9: Geotextile Requirements for Subsurface Drainage (table according to [24]).

In-situ passing 0.075 mm sieve (%)	Permittivity, per sec, as per ASTM D 4491/ IS 14324: 1995	Maximum Apparent opening size, mm ASTM D 4751/ IS 14294 : 1995
<15	0.5	0.43
15 to 50	0.2	0.25
>50	0.1	0.22

2.4 Initial data for design

Input data for design should cover all the data necessary for analysis of the state of saturation, determination of the forces operating on supporting gabion structures, calculations of basic parameters of buildings, their arousing, development of technologies of installation of underground walls and their technical and economic estimation [14].

2.4.1 Materials of engineering searches

The following materials of engineering design are required [14]:

- topographic plan of the site;
- transverse and longitudinal engineering and geological cuts;
- hydrogeological and hydrological data;
- climate characteristics;
- physical and mechanical characteristics and soil strength characteristics

2.4.2 Basic parameters

The basic design of the gabion structure is also [24]:

- drainage requirements,
- base width,
- the depth of the laying,
- tilt angle,
- loading,
- density of gabions,
- an amount of backfill,
- presence of seismic influences

2.4.3 Drainage requirements

Usually for gabion walls there is no urgent need to arrange some drainage system, unlike concrete or reinforced concrete walls, because the construction of the gabion is porosity and water can freely wall and drain.

To prevent the wash-off of the fill and the fall of the soil in the pores of the gabion wall (in the case of clay or sandy soils), between the wall and the gabion provide a filter, while applying non-woven geotextile. In this case, it is also necessary to take measures to

improve drainage in the back of the wall, using the bottom coarse material, and water discharge.

The non-woven geotextile (figure 2.4) can also be used under the base of the wall to prevent the washing of a small fraction from the foundation (figure 2.5).



Figure 2.4 Non-woven geotextile.

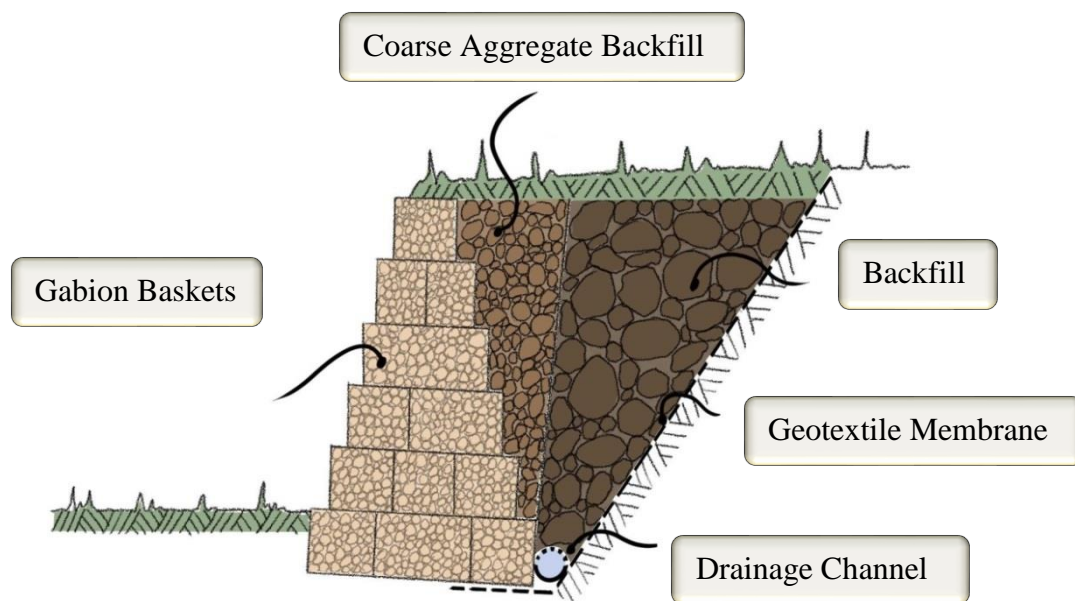


Figure 2.5 Drainage requirements. Use of non-woven geotextile in gabion retaining wall.

2.4.4 Base width.

The width of the base of the gabion wall for height H from 1 m to 6 m is recommended from 0,6 to 0,75 H , and for height above 6 m to 10 m – 0,55-0,65 H and meet the requirements of the project [24].

2.4.5 Depth of laying.

The minimum depth of the bottom wall of the gabions should be not less than 0,5 m for level ground at H from 1 m to 6 m, and 1 m for H from 6 m to 10 m (according to IS 14458 part 1).

Depth of freezing, shrinkage and soil erosion, presence of seismic activity and water washing also influence the depth of laying. Usually, the minimum depth for any design is taken 0,5 m. the exception is the construction, which is built on the glass soil. In this case, the depth of wall depth can be smaller due to the strength of the base and the complication of earthworks. In this case, the depth can be 0,3 m – 0,5 m, and the foundation can be leveled by setting up the dowels and concrete foundation [24].

2.4.6 Tilt angle

Regulations recommend to arrange a gabion wall at an angle of 3-6° to the vertical. The wall can also be vertical, while arranging for the shift of gabions on the outer side (figure 2.6).

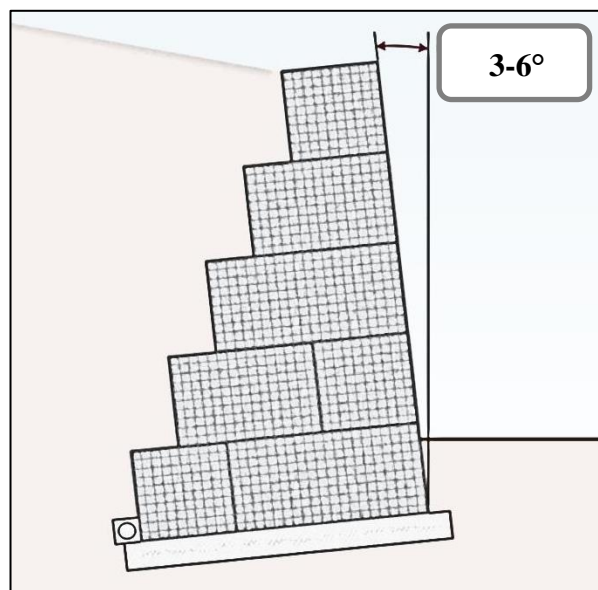


Figure 2.6 Gabion wall with angle.

2.4.7 Density of gabions

Recommended porosity at filling of gabions – from 35% to 40%. This value can be reduced by choosing the size of the mountain rocks and using stone rock and stone crumb of a small size, which fills the empties between the stones.

2.4.8 Amount of backfill

The selected filling must be extended to the intersection of the line $45+\phi/2$ from the toe of the gabion with the horizontal line of the ground surface [according to IRC:78], as shown in figure 2.7 [24]

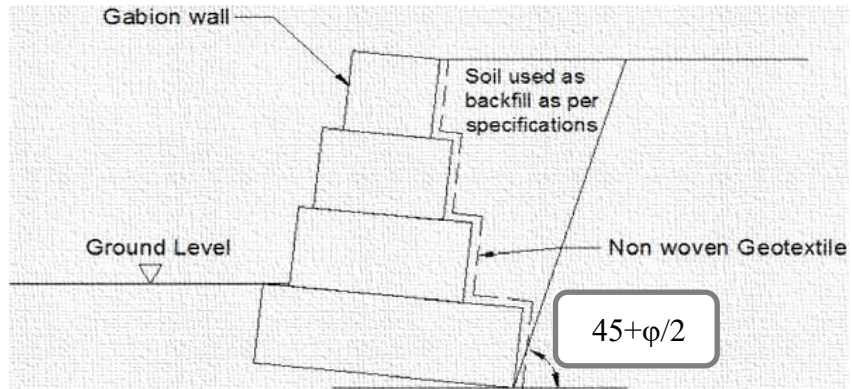


Figure 2.7 Extent of Backfill [24]

2.5 Methodology of construction and calculation of gravity retaining walls

2.5.1 Ultimate limit states to check on a wall

The gabion gravity wall (GGW) should be designed taking into account possible schemes of its ultimate limit states, as shown in figure 2.8 [14, 24]

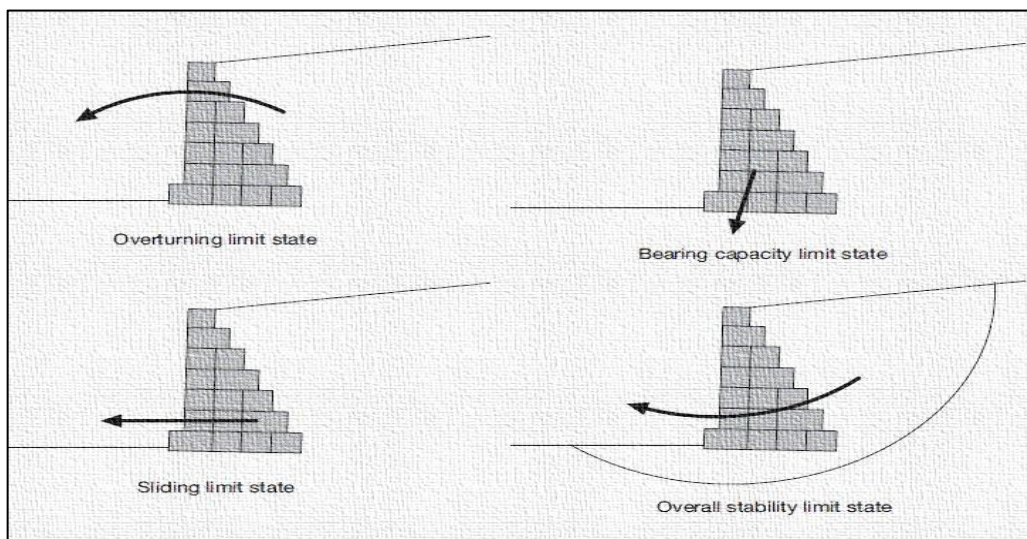


Figure 2.8 Possible schemes of ultimate limit states of gabion gravity wall [available online]

2.5.2 Design technique

First, the type and shape of the retaining wall structure is selected, the connection to local conditions, assign the basic dimensions of the wall, perform the connection to the construction of the saturated saturation. The height of the wall should ensure the stability of the upper part of the pour. The width of the gabions that make up it, and the shape of the wall is established from the condition of the wall stability against the seam and overturning, additionally checked by calculations on the estimation of the bearing capacity of the base and on the estimation of the internal stability of the wall [14, 26].

The external and internal stability of the wall is considered. The external stability of the wall is assessed by the resistance to shear, overturning and loss of the bearing capacity of the base. The internal stability of the wall is checked by calculating the strength at the most dangerous intersections (at the places where the gabions connect to each other). [14]

2.5.3 The main steps on calculation of gabion underground walls

The calculation of the gabion retaining wall was carried out according to the Canadian manual [25], according to which the design begins with the selection of the base dimensions for a typical vertical section of the wall. Then four basic steps should be taken:

1. Determine the forces acting on the wall.
2. Check that resisting moment exceeds the overturning moment by a suitable safety factor.
3. Check that sliding resistance exceeds the active horizontal force by a suitable safety factor.
4. Check that the resultant force falls within the middle third of the wall's base, and that the maximum bearing pressure is within the allowable limit.

These steps are repeated iteratively until a suitable constructive decision is reached, which meets all criteria. The stability of the wall should be checked at the base and at each step in height [25].

2.5.4 Calculated loads

Calculation of the gabion wall should be performed on the calculated load acting on it: constant (from its own weight of the soil and constant evenly distributed load on the surface of the filling) and temporary (from vehicles).

As shown in figure 2.9, the main forces acting on the walls of the gabions are vertical forces from the weight of the gabions and side pressure of the earth acting on the rear surface.

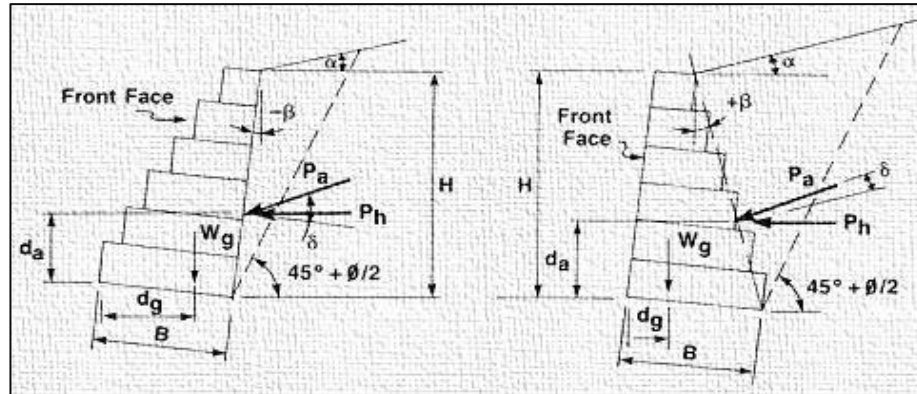


Figure 2.9 Gravity wall design: a- stepped front face; b- stepped back face [25]

If it is necessary to consider other influences, such as transport or seismic loads, then calculate them, that is, they should also be included in the analysis. The own weight of one linear meter of the wall (W_g) determine the multiplication of the area of cross-section of the wall on density of filled gabion. [25]

2.5.5 Determination of the active pressure of the backfill soil.

The Coulomb method is used to calculate the active and passive pressure acting on the retaining structure. It is assumed that the total resistance of the soil is concentrated along the surfaces of forging and destruction, located in the soil mass. The Coulomb method assumes that such surfaces are flat and that the pressure acts on the critical surface of the destruction. Besides that, this method allows to analyze constructions with non-vertical inner front side, it also allows to consider possible friction between the support structure and the ground. In case of a step-by-step filling to determine the point of application of the total active pressure, assume that the parameters of the ground acting on the wall are linear in each layer that crosses the force of the active pressure.

2.5.6 Forces acting on the wall

The side pressure on the ground is determined by the equality of Coulomb. The force of active soil pressure of the P_a (kN/m) on the retaining wall is laid at a distance $H/3$ from the base of the wall.

The active force per meter of the soil of the backfill on the back face of the retaining wall are determined:

$$P_a = K_a w_s H^2 / 2, \quad (3.1)$$

If an additional load (q) is evenly distributed on the surface of the fill, it can be considered as an equivalent layer of soil, which creates an even pressure on the whole height of the wall. Then the equinns (3.1) can be modified as follows:

$$P_a = K_a (w_s H^2 / 2 + qH) \quad (3.1a)$$

The pressure coefficient K_a is: (3.2)

$$K_a = \frac{\cos^2(40 - 5)}{\cos^2 \cos(5 + 5) \left[1 + \sqrt{\frac{\sin(40 + 5) \sin(40 - 20)}{\cos(5 + 5) \cos(20 - 5)}} \right]^2}$$

The horizontal component of P_a is:

$$P_h = P_a \cos\beta \quad (3.3)$$

The vertical component of P_a is usually neglected in calculations, as it reduces the moment of overthrowing and increases the sliding resistance.

2.5.7 External stability of the gabion retaining wall

The moment of overturning is created by side efforts, acting along the walls of gabions. It can overturn the wall if it is not designed properly. The resistance or moments of resistance arise because of the own weight of the gabion wall, vertical component of the force of pressure on the ground, weight of soil on the benches, load acting on the wall, etc. The safety factor against overturning (ratio of overturning and resistance) for a safe condition must be more than 2. [14]

2.5.8 Overturning moment check

Active forces of soil pressure have a tendency to overturn the wall, and this should be properly balanced by the moment of resistance. Using the basic principles of statics, the moment of resistance and the moment of overturning are calculated to check the overturning of the walls. Both moments are calculated by summing the results of the corresponding force on its shoulder (distance perpendicular to the toe of the wall).

This check can be expressed as:

$$M_r = SF_o M_o \quad (3.4)$$

Neglecting the friction of the wall, the active pressure of the soil of the backfill acts normally to the back face at a distance $H/3$ from the base. When there is an additional load (surcharge), the distance to the total active force above the toe is: (3.5)

$$d_a = \frac{H(H + 3q/w_s)}{3(H + 2q/w_s)} + B \sin \beta$$

Overturning moment:

$$M_o = d_a P_h \quad (3.6)$$

The weight of the gabion wall (W_g) acts vertically through the center of the weight of the area of its cross section. The horizontal distance to this point from the toe of the wall (d_g) can be obtained from the static moment of the wall areas. In other words, the moments about the toe is taken, and then divided into the total area. The moment of resistance is the sum of the products of vertical forces or the weight on the unit of length (W) and their distance (d) from the toe of the wall (figure 3.10):

$$M_r = \sum dW \quad (3.7)$$

For a simple gravity wall, the moment of resistance is completely provided by the weight of the wall:

$$M_r = d_g W_g \quad (3.7a)$$

$$d_g = \frac{\sum Ax}{\sum A} \quad (3.7b)$$

Safety factor against sliding:

$$SF_s = \mu W_g / P_h \quad (3.8)$$

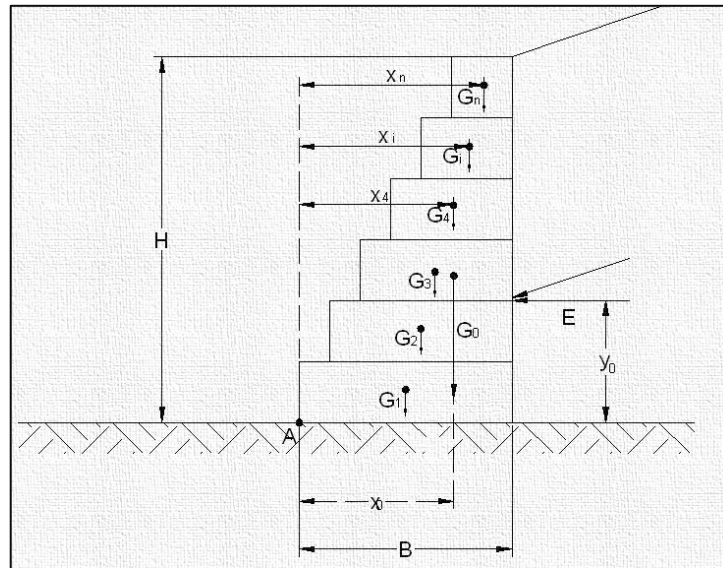


Figure 2.10 Calculation scheme to determine wall resistance to overturning [14]

Check bearing pressure

First, it is checked whether the resulting vertical force is within the middle third of the base. If (B) means the width of the base, then the eccentricity (e) of the vertical force from the middle of the base is equal to:

$$e = B/2 - (M_r - M_o)/W_v \quad (3.10)$$

So that the resulting force lies in the middle third:

$$-B/6 \leq e \leq B/6 \quad (3.11)$$

Then the maximum pressure under the base P :

$$P = (W_v / B)(1 + 6e / B) \quad (3.12)$$

Maximum pressure must not exceed the permissible soil pressure, P_b :

$$P \leq P_b \quad (3.13)$$

The safety factor must be included in P_b .

Note: all formulas and their meanings are taken from the document “Gabion Walls Installation Guide. Modular Gabion Systems” [25].

Chapter 3

3. APPLICATION TO A CASE STUDY AND PARAMETRIC ANALYSIS

Having studied various literature, we can proceed to the practical case of studying a gabion retaining wall. To design a wall, we need to understand what input data we need to design. This section describes the data and parameters that we need to adopt to design the wall

In this section, we are going to design a gabion retaining wall, following the basic steps described in chapter 2 point 2.5.3. Taking into account the main parameters, we can simulate the appearance of our wall and depict it graphically as shown in the figure 3.1. Therefore, we are going to perform the calculation of the gabion retaining wall manually and with the help of a “GAWAC WIN 2003” software package in order to look at the differences in one and another approach to the calculation, and choose the best option, according to which it is possible to correctly design the gabion wall.

Manual calculation is carried out according to the Canadian document, which is described in the previous section “Gabion Walls Installation Guide. Modular Gabion Systems”.

Also we carry out the software calculation according to the document “Obras de contenção. Manual Técnico”. All information about the calculation according to this theory is presented in Annex B.

Also, in order to choose the best parameters for the designed wall, we will change certain parameters in the wall structure to see the effect of certain parameters on the change and behavior of our structure.

The following initial data were chosen for the design of the wall (table 3.1):

3.1 Given data

Table 3.1 Initial data for designing the gabion wall.

SYMBOL	NAME OF VALUE	VALUE	UNIT OF MEASURE
H	Wall Height	7	m
q	Surcharge	5	kN/m
α	Backfill slope angle	20	deg
β	Back Face slope angle	5	deg
φ	Soil friction angle	40	deg
w_s	Soil density	20	kN/m ³
w_g	Gabion fill density	18	kN/m ³
P_b	Soil bearing pressure	300	kPa
B	Width of the base	4.5	m

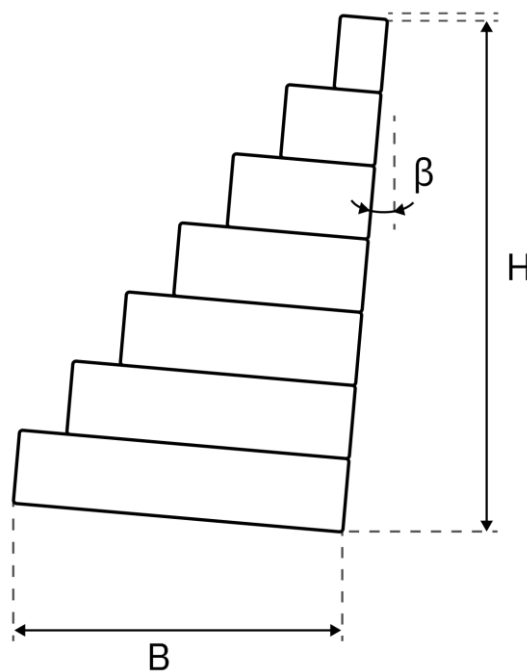


Figure 3.1: Gabion retaining wall

- soil (sand-gravel);
- location of the gabion wall (Bragança);
- filler (granite);
- porosity of gabion – 30%.
- Angle of wall friction 5°

Figure 3.2 shows the view of the designed retaining wall with the initial data presented in the table 3.1

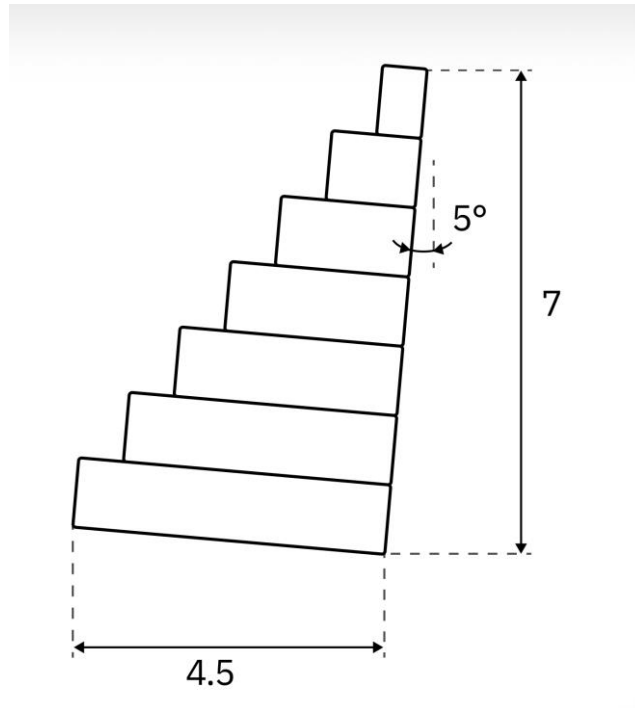


Figure 3.2: Designed gabion retaining wall

3.2 Manual calculation

$$K_a = \frac{0.671}{0.992 \times 0.984 \left[1 + \sqrt{\frac{0.707 \times 0.342}{0.984 \times 0.966}} \right]^2} = \frac{0.671}{0.976 \left[1 + \sqrt{\frac{0.241}{0.951}} \right]^2}$$

$$K_a = 0.31$$

✓ According to (3.2);

$$P_a = 0.31 \left(20 \times \frac{7^2}{2} + 5 \times 7 \right)$$

$$P_a = 162.75$$

✓ According to (3.1a);

$$P_h = 162.75 \times 0.996$$

$$P_h = 162.1$$

✓ According to (3.3);

$$d_a = \frac{7(7 + 3 \times 5/20)}{3(7 + 2 \times 5/20)} + 4.5 \times \sin 5 = \frac{54.25}{22.5} + 0.391 = 2.41 + 0.391$$

$d_a = 2.8$

✓ According to (3.5);

$$M_o = 2.8 \times 162.1$$

$M_o = 453.9$

✓ According to (3.6);

$$W_g = (4.5 + 4 + 3.5 + 3 + 2.5 + 2 + 1.5) \times 18 = 21 \times 18$$

$W_g = 378$

$$d_g = [4.5(2.25 \times 0.996 + 0.0436) + 4(2.5 \times 0.996 + 0.131) + 3.5(2.75 \times 0.996 + 0.218) + 3(3 \times 0.996 + 0.31) + 2.5(3.25 \times 0.996 + 0.4) + 2(3.5 \times 0.996 + 0.48) + 1.5(3.75 \times 0.996 + 0.57)]/21$$

$d_g = 3.08$

✓ According to (3.7b);

$$M_r = 3.08 \times 378$$

$M_r = 1164.24$

✓ According to (3.7a);

$$SF_o = \frac{1164.24}{453.9}$$

$SF_o = 2.56 > 2.00$

✓ According to (3.8);

$$SF_s = \tan 40 \frac{378}{162.1} = 0.839 \times 2.34$$

$SF_s = 1.96 > 1.5$

✓ According to (3.8a);

$$e = \frac{4.5}{2} - \frac{(1164.24 - 453.9)}{378} = 2.25 - 1.87$$

$$e = 0.38$$

✓ According to (3.10);

$$-0.75 \leq 0.38 \leq 0.75$$

✓ According to (3.11);

$$P = \left(\frac{378}{4.5}\right) \left(1 + 6 \times \frac{0.38}{4.5}\right) = 84 \times 1.5$$

$$P = 126$$

✓ According to (3.12);

$$126 \leq 300$$

✓ According to (3.13);

All safety factors are within limits. Stability checks at intermediate levels in the walls show similar results. ✓

Manual calculation was carried out according to the Coulomb principle.

3.3 Calculation using the "Gawac Win 2003" program

Designing a gabion retaining wall, several calculations were carried out, with change of various parameters such as: the angle of inclination of the wall, the porosity of the gabions, the offset of the gabion boxes relative to each other, the height (H) and width (B) of the gabion boxes, the geotextile on the base.

All calculations were carried out using the "GAWAC WIN 2003" software package.

These parameters were taken exclusively in order to see the effect of their change on the construction of the wall. Obviously, we can change various parameters and quantities, so we will have more information to look at different variations in the design of the structure.

Table 3.2 Parameters that were changed to compare the influence of different parameters on the design of a gabion wall.

	Parameters that were changed:
1	
2	- Changed the angle of inclination of the wall from 5° to 6°;
3	- Changed the porosity of gabions from 30% to 40%; - Added geotextile on the base; - Friction reduction reduced by 5.00 %;
4	- Added Layer 8, H- 8.00 m. (original- 7 m.); - Length B - 4 m. (original- 4.5 m.);
5	- Changed the porosity of gabions from 30% to 40%; - Added geotextile on the base; - Friction reduction reduced by 5.00 %; - Added Layer 8, H- 8.00 m. (original- 7 m.); - Length B - 4 m. (original- 4.5 m.);
6	- Changed the porosity of gabions from 30% to 40%; - Added geotextile on the base; - Friction reduction reduced by 5.00 %; - Added Layer 8, H- 8.00 m. (original- 7 m.); - Length B - 4 m. (original- 4.5 m.); - Changed the angle of inclination of the wall from 5° to 6°;
7	-The offset of gabion boxes relative to each other was increased from 0.5 m. to 0.6 m.;
8	-The offset of gabion boxes relative to each other was increased from 0.5 m. to 0.6 m.; - Changed the angle of inclination of the wall from 5° to 6°.

RESULTS OF ANALYSIS OF STRUCTURAL STABILITY WITH THE HELP OF THE PROGRAM “GAWAC WIN 2003”

Table 3.3 Results of analysis of structural stability.

Stability analysis results	1	2	3	4	5	6	7	8
Active and passive thrust								
Active thrust :	79.14	75.42	79.14	107.29	107.29	101.71	60.84	56.64
Point of application ref. To x axis	4.68	4.71	4.68	4.21	4.21	4.25	4.87	4.90
Point of application ref. To y axis	1.88	1.79	1.88	2.24	2.24	2.18	1.83	1.75
Direction of the thrust ref. To x axis :	33.00	32.00	33.00	33.00	33.00	32.00	28.10	27.10
Passive thrust :	0.00	0.00	0.00	0.00	0.00	0.00	0.00	0.00
Point of application ref. To x axis	0.00	0.00	0.00	0.00	0.00	0.00	0.00	0.00
Point of application ref. To y axis	0.00	0.00	0.00	0.00	0.00	0.00	0.00	0.00
Direction of the thrust ref. To x axis	0.00	0.00	0.00	0.00	0.00	0.00	0.00	0.00
Sliding								
Normal force on the base:	429.47	426.54	375.07	392.41	345.79	341.88	413.97	411.04
Point of application ref. To x axis :	2.91	2.96	2.89	2.47	2.42	2.47	3.15	3.20
Point of application ref. To y axis :	0.25	0.31	0.25	0.22	0.21	0.26	0.28	0.34
Shear force on the base	29.05	19.48	33.81	56.00	60.08	50.80	17.65	7.49
Resisting force on the base:	360.36	357.91	298.99	329.27	275.64	272.53	347.36	344.90
Sliding safety coefficient :	6.31	6.69	5.25	4.23	3.55	3.77	7.47	8.11
Overturning								
Overturning moment :	124.78	114.54	124.78	201.81	201.81	188.34	98.02	87.99
Restoring moment :	1374.94	1378.52	1207.35	1170.08	1038.09	1033.73	1400.37	1404.03
Overturning safety coefficient	11.02	12.04	9.68	5.80	5.14	5.49	14.29	15.96
Stresses acting on found.								
Eccentricity :	0.67	0.73	0.65	0.48	0.43	0.49	0.91	0.97
Normal stress on outer border	179.55	184.94	154.06	166.90	140.71	146.08	0.00	0.00
Normal stress on inner border :	1231.39	1239.20	1203.59	1013.21	980.49	991.79	1260.90	1271.24

The calculations were analyzed and the change and influence of the above parameters on the strength and stability of the wall structure was determined. For the general analysis, 2 main values were taken: the safety factor against sliding and the safety factor against overturning (the change of all parameters submitted in table 3.4). After that, the change was monitored relative to the first basic calculation given in column number 1. For better visibility, the analysis of changes in the construction of the wall is presented in a percentage ratio.

Table 3.4 The analysis of changes sliding and overturning safety coefficient in the construction of the gabion wall.

	Sliding safety coefficient	Overturning safety coefficient
1		
2	+ 9,25 %	+ 6 %
3	- 12,2 %	- 16,8 %
4	- 47,4 %	- 33 %
5	- 53,4 %	- 43,8 %
6	- 50,2 %	- 40,3 %
7	+ 29,7 %	+ 18,4 %
8	+ 44 %	+ 28,6 %

Calculations with the changed parameters are presented in Appendix A.

The entire theory that allows to calculate the gabion retaining wall is described in Portuguese and is placed in Appendix B.

3.4 CALCULATION WITH THE HELP OF THE PROGRAM “GAWAC WIN 2003”

GawacWin 1.0

Page 2

Program released in license to: IPB

Project: PRO 05

File: korin

Date: 30.12.1899

Foundation data

Top surface height : 0.00 m
 Top surface init. length : 10.00 m
 Top surface incl. angle : 0.00 deg
 Soil unit weight : 20.00 kN/mi
 Soil friction angle : 40.00 deg
 Soil cohesion : 0.00 kN/ml
 Foundation allowable pressure : kN/ml
 Water table height : m

Additional Foundation Layers

Layer	Depth m	Unit weight kN/mi	Cohesion kN/ml	Friction angle deg

Water profile data

Initial height : m
 Inclination of the 1st stretch : deg
 Length of the 1st stretch : m
 Inclination of the 2nd stretch : deg
 Length of the 2nd stretch : m

Loads data

Distributed loads on backfill
 First stretch : 0.00 kN/ml
 Second stretch : 5.00 kN/ml

Distributed loads on wall
 Load : kN/ml

Line loads on backfill
 Load 1 : kN/m Distance from wall face : m
 Load 2 : kN/m Distance from wall face : m
 Load 3 : kN/m Distance from wall face : m

Line load on wall
 Load : kN/m Distance from wall face : m

Seismic action data

Horizontal coefficient : Vertical coefficient :

is not responsible for the reliability of the geotechnical parameters assumed, or the improper use of the software. The program takes into account the physical characteristics of materials as manufactured by the Maccaferri group; its results will not be realistic if a different material is used.

 Program released in license to: IPB

Project: PRO 05

File: korin

Date: 30.12.1899

STABILITY ANALYSIS RESULTS

Active and Passive Thrust

Active Thrust	:	79.14 kN/m
Point of application ref. to X axis	:	4.68 m
Point of application ref. to Y axis	:	1.88 m
Direction of the thrust ref. to X axis	:	33.00 deg
Passive Thrust	:	0.00 kN/m
Point of application ref. to X axis	:	0.00 m
Point of application ref. to Y axis	:	0.00 m
Direction of the thrust ref. to X axis	:	0.00 deg

Sliding

Normal force on the base	:	429.47 kN/m
Point of application ref. to X axis	:	2.91 m
Point of application ref. to Y axis	:	-0.25 m
Shear force on the base	:	29.05 kN/m
Resisting force on the base	:	360.36 kN/m

Sliding Safety Coefficient : **6.31**

Overturning

Overturning Moment	:	124.78 kN/m x m
Restoring Moment	:	1374.94 kN/m x m

Overturning Safety Coefficient : **11.02**

Stresses Acting on Foundation

Eccentricity	:	-0.67 m
Normal stress on outer border	:	11.33 kN/ml
Normal stress on inner border	:	179.55 kN/ml
Max. allowable stress on the foundation	:	1231.39 kN/ml

is not responsible for the reliability of the geotechnical parameters assumed, or the improper use of the software. The program takes into account the physical characteristics of materials as manufactured by the Maccaferri group; its results will not be realistic if a different material is used.

GawacWin 1.0**Page 4**

Program released in license to: IPB

Project: PRO 05

File: korin

Date: 30.12.1899

Overall Stability

Initial distance at pivot leftside : m
 Initial distance at pivot rightside : m
 Initial depth referred to base : m
 Max depth allowed in calculation : m
 Center of the arch referred to X axis : 0.61 m
 Center of the arch referred to Y axis : 8.83 m
 Radius of the arch : 10.05 m
 Number of search surfaces : 67

Overall Stability Safety Coefficient : 1.98**Internal Stability**

Layer	H m	N kN/m	T kN/m	M kN/m x m	τ_{Max} kN/ml	τ_{All} kN/ml	σ_{Max} kN/ml	σ_{All} kN/ml
1	5.98	329.30	12.41	853.68	3.10	80.50	63.51	
2	4.98	243.95	2.34	552.57	0.67	71.19	53.85	
3	3.98	173.32	-1.29	332.33	-0.43	62.40	45.20	615.79
4	2.99	113.76	-3.14	177.41	-1.26	53.35	36.48	
5	1.99	65.48	-2.96	77.74	-1.48	43.95	27.58	
6	1.00	27.20	-2.38	21.59	-1.59	33.18	17.13	

is not responsible for the reliability of the geotechnical parameters assumed, or the improper use of the software. The program takes into account the physical characteristics of materials as manufactured by the Maccaferri group; its results will not be realistic if a different material is used.

GawacWin 1.0

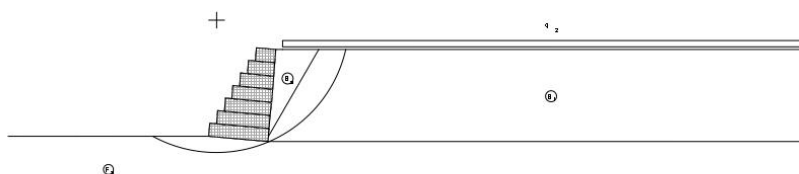
Summary

Program released in license to: IPB

Project: PRO 05

File: korin

Date: 30.12.1899



SOIL DATA

Soil	γ kN/m ³	c kN/m ²	ϕ deg	Soil	γ kN/m ³	c kN/m ²	ϕ deg
B _s	20.00	5.00	40.00	F _s	20.00	0.00	40.00
B ₁	20.00	5.00	35.00				

LOADS

Load	Value kN/m ²	Load	Value kN/m ²
q ₂	5.00		

STABILITY CHECKS

Sliding Safety Coefficient	6.31	Base normal stress (left)	11.33kN/m ²
Overturning Safety Coefficient	11.02	Base normal stress (right)	179.55kN/m ²
Overall Stability Safety Coefficient	1.98	Max. allowable stress	1231.39kN/m ²

is not responsible for the reliability of the geotechnical parameters assumed, or the improper use of the software. The program takes into account the physical characteristics of materials as manufactured by the Maccaferri group; its results will not be realistic if a different material is used.

Chapter 4

4. CONCLUSION AND FUTURE WORKS

As a result of the work, the method of calculating gabion retaining walls was investigated, the wall was calculated manually and with the help of the "GAWAC WIN 2003" program.

Every effort has been made to ensure the accuracy and reliability of the information presented in manual calculation. Nevertheless, manual calculation in this case did not give us accurate conclusions, since this calculation is suitable for the design of ordinary concrete retaining walls. Therefore, the next step was to use the software and another approach (Terzaghi's), since we have a gabion retaining wall and try to design and calculate safety factor. In this case, it is clear why there were deviations in the manual and program results. Application of the information must be based on responsible professional judgment.

Based on the obtained calculation results (tables 3.3 and 3.4), it was established that a positive effect occurs due to changes in parameters related with increasing wall batter inclination and offset relative to each other (2,7,8), which increase the strength of the designed retaining wall and the negative impact occurs due to addition parameters related with an increasing porosity of gabions; geotextile on the base; friction reduction; an additional layer along the height of the wall; reducing the base of the gabion (3,4,5,6), that reduces its stability.

In this case, the wall is negatively affected by a change in the following parameters:

- Increasing the porosity of gabions. This leads to a decrease in the weight of the gabion construction, which in the future may lead to an increase in the risk of overturning. In this case we obtained a value in lower percentage;
- The presence of geotextile on the base. This leads to a decrease in friction, which in turn leads to a worse adhesion of the structure to the ground;
- Increasing the height and decreasing the width of the base almost doubles the overturning moment and reduces the anti-sliding coefficient by (47.4%) and the overturning coefficient by (33%). This means that the wall structure becomes more vulnerable to destruction.

The most negative effect on the wall is the change in factors in the 5th calculation, which is related with increasing porosity of gabions; addition geotextile on the base ; friction reduction; an additional layer along the height of the wall; reducing the base of the gabion.

Changing such parameters as: the angle of inclination of the wall and the offset of gabions relative to each other, the pre-section of the wall and the resistance of the structure to the ground increases, which in turn increases reliability, increases the safety factor against sliding and overturning, and increases the strength of the structure.

The most positive changes are shown in calculations 7 and 8 where we changed such parameters as: offset of gabions relative to each other from 0.5 m to 0.6 m and changed the angle of inclination of the wall in a larger direction from 5 deg. to 6 deg. Therefore, to improve and increase the reliability of the retaining structure, its internal stability and overturning moment, it is important to take into account the change of these parameters.

Instead of using the typical theory of classical concrete retaining walls, it's better to use the Terzaghi's principle, according to the manual "Obras de Contenção. Manual Técnico" [35], where is presented the corrections to obtain the correct theory how to design a gabion retaining wall. My work can serve as the basis, because there is a general information about the appearance and application of gabion walls from the beginning of the appearance, to the present.

In the future work, I propose to conduct calculations according to the theory mentioned above in the technical manual and make multicalculation according to the example given in the annex. Conduct more analyses to compare the impact on the construction of the gabion wall changes of various parameters.

REFERENCES

1. SAVENKO V.YA., DOCTOR OF ENGINEERING, PROFESSOR (NATIONAL TRANSPORT UNIVERSITY, KYIV), PETROVYCH VV, PH.D. IN ENGINEERING, PROFESSOR (NATIONAL TRANSPORT UNIVERSITY, KYIV), KASKIV VI, PH.D. IN ENGINEERING, ASSOCIATE PROFESSOR (NATIONAL TRANSPORT UNIVERSITY, KYIV) and KASKIV SV, ASSIS. (NATIONAL TRANSPORT UNIVERSITY, KYIV). *Development of standards for construction gabions* . Online. "Modern technologies and calculation methods in construction", 2017, No. 6, p. 205–212. ISSN UDC 627.737: 624.01. URL: <https://eforum.lntu.edu.ua/index.php/construction/issue/view/15/20> . (date of access: 31.10.2022);
2. *What are gabions? | Best article* . (2021, April 29). Goodzone. URL: <https://goodzon.com.ua/ua/blog/chto-takoye-gabiony> (date of access: 31.10.2022);
3. *Gabion baskets and the history in military civil engineering - aarsleff ground engineering*. (2017, February 17). Aarsleff Ground Engineering. URL: <https://aarsleff.co.uk/company-news/gabion-baskets-military-civil-engineering/> (date of access: 31.10.2022);
4. *Gabions – a history of changing landscapes*. (2015, July 15). Furnitubes. URL: <https://www.furnitubes.com/blog/2015/07/gabions-a-history-of-changing-landscapes> (date of access: 31.10.2022);
5. *HESCO bastions*. (2010, July 30). Homemade Defense. URL: <http://homemadedefense.blogspot.com/2010/07/hesco-bastions.html> (date of access: 31.10.2022);
6. *Do-it-yourself gabions - step-by-step instructions - Ekobil*. (2021, November 8). Ekobil. URL: <http://ekobil.com.ua/gabioni-svoyimi-rukami-pokrokovaya-instruktsiya/> (date of access: 31.10.2022);
7. *What are gabion structures? | "Liv-energo" Co., Ltd*. (2019, July 22). LLC "LIV-ENERGO". URL: <https://www.liv-energo.com.ua/shho-take-gabionni-konstrukcii/> (date of access: 31.10.2022);
8. Wikimedia project participants. (2008, September 9). *Gabion - Wikipedia* . Wikipedia. URL: <https://uk.wikipedia.org/wiki/Gabion> (date of access: 31.10.2022);
9. *Gabions price - buy gabion constructions in Kyiv, Ukraine, mesh for gabion* . (2022, August 12). Gabions of Ukraine. URL: <https://gabions.com.ua/ua/>

- (date of access: 31.10.2022);
10. *Making a gabion net with your own hands and using it for various purposes. Do-it-yourself gabions: step-by-step instructions for mesh, crushed stone, gravel and stones Do-it-yourself gabions in the garden* . (n.d.). All about kitchen design and repair. Accessories. Furniture. Technique.
URL: <https://24segodnya.ru/uk/technique/proizvodstvo-gabionnoi-setki-svoimi-rukami-i-ee-primenenie-v-razlichnyh-celyah/> (date of access: 31.10.2022);
 11. *Gabioni: Tipi, zastosuvannya that perevagi* . (nd). Modern building technologies.
URL: <https://budtex.com.ua/uk/tehnologii/108-gabioni-tipi-zastosuvannya-ta-perevagi.html> (date of access: 31.10.2022);
 12. *Gabions/gabion mesh - buy gabion structures/mesh | Kyiv. the price* (n.d.). Shore reinforcement, shore reinforcement, slope reinforcement, gabions, geotextile, geogrid — Kyiv. URL: <https://gbservice.com.ua/ua/materialy/gabiony> (date of access: 31.10.2022);
 13. *Viakon Ukraine - manufacturer of prefabricated metal structures :: Design organization* . (nd). Viakon Ukraine - manufacturer of prefabricated metal structures :: Design organization. URL: <http://viacon.ua/> (date of access: 31.10.2022);
 14. *Recommendations for carrying out work, general provisions, temporary technical instructions for the use of gabions for strengthening the ground surface of railways were developed using the materials of CJSC "Gabions Maccaferri"*. Online. Gabions McCaffery. [b. d.].
URL: <https://refdb.ru/look/1931277-pall>. (date of access: 31.10.2022);
 15. *PARFIENTYEVA I.O. and LUGOVSKA T.P. Modern technologies and methods of calculations in construction: a collection of scientific papers - Lutsk* . Online. Lutsk NTU, 2017, No. 7, p. 188.
URL: <https://eforum.lntu.edu.ua/index.php/construction/issue/view/14/13> . (date of access: 31.10.2022);
 16. *Gabion fence: Advantages, selection and installation - VBud* . (2019, September 15). VBud. URL: <https://vbud.in.ua/parkan-z-gabioniv-perevagi-vibir-i-montazh/> (date of access: 31.10.2022);
 17. Tomiša A. (2019, May 6). *Gabion walls - function, application, advantage | Geotech*. Geotech. URL: <https://www.geotech.hr/en/gabion-walls/> (date of access: 31.10.2022);

18. *Gabion: Definition, types, advantages, and applications (with real site photos) - civil engineering magic.* (2021, March 28). Civil Engineering Magic. URL: <https://civilengineeringmagic.com/gabion-wall-types-and-applications/> (date of access: 31.10.2022);
19. *Reno mattress plus / maccaferri corporate.* (nd). Maccaferri Corporate. URL: <https://www.maccaferri.com/reno-mattress-plus/> (date of access: 31.10.2022);
20. *Technical data sheet. sack gabions galvanized.* Online. Maccaferri. (2005, August 8). URL: <https://nebula.wsimg.com/12e69d56c3ba9e5d1c76afc3e24fab5f?AccessKeyId=F1F75E80B1AC978F7606&disposition=0&alloworigin=1>. (date of access: 31.10.2022);
21. *Rock fall protection system.* (n.d.). Indian Railway Institute of Civil Engineering, Pune. URL: https://www.ircen.gov.in/ModelRoom/M10_Rockfall%20Protection%20Systems.html (date of access: 31.10.2022);
22. *Gabion basket 2m x 0.5m x 0.5m / galfan wire mesh stone wall cage.* (n.d.). Wire Mesh | Grass Reinforcement Mesh | Porous Pavers | Ultimate One. URL: <https://www.ultimate-one.co.uk/gabion-mesh-basket-2m-05m-05m-mesh-clips-p-1198> (date of access: 31.10.2022);
23. VIOLLET-LE-DUC, EUGENE-EMMANUEL (1814-1879). *Dictionary of French architecture from the 11th to the 16th century. First volume: AB - ARO.* Online. Paris: Library of the National Institute of Art History, Jacques Doucet collections, 2008. URL: <https://bibliotheque-numerique.inha.fr/collection/item/15484-dictionnaire-raisonne-de-l-architecture-francaise-du-xieme-au-xvieme-siecle-tome-1?offset=5>. (date of access: 31.10.2022);
24. *IRC - SP-116-2018 - guidelines for design and installation of gabion structures.* 24. *INDIAN ROADS CONGRESS/PDF.* (2018, May). URL: <https://www.scribd.com/document/449057904/IRC-SP-116-2018-Guidelines-for-Design-and-Installation-of-Gabion-Structures>. (date of access: 31.10.2022);
25. *GABION WALLS DESIGN/modular gabion systems/ MGS design guide-gabion wall | PDF | physics | building engineering.* (n.d.). Scribd. URL: <https://www.scribd.com/doc/38637356/MGS-Design-Guide-Gabion-Wall>. (date of access: 31.10.2022);

26. NATIONAL TRANSPORT UNIVERSITY (NTU) DEVELOPERS B. KASKIV, CAND. TECH. SCIENCES; C. KASKIV; V. PE. B.2.3-37641918-558:2016, *GBN B.2.3-37641918-558:2016 Roads. Gabion structures. Design and construction* . Online. Kyiv Ministry of Infrastructure of Ukraine: GBN (Industry Building Standards), 2016. URL: http://online.budstandart.com/ua/catalog/doc-page?id_doc=64229 . (date of access: 31.10.2022);
27. *LinkTM gabions and mattresses design booklet*. (2015), p. 40. Global Synthetics Australian Company - Global Expertise. URL: <https://pdfslide.net/documents/linktm-gabions-and-mattresses-design-booklet-many-drainage-issues-and-potential.html?page=1>. (date of access: 31.10.2022);
28. *Assembly manual English version gabion structures* . Online. Designed by: Michelle Neerma, (2012, April) Maccaferri SA (Pty) Ltd, Durban, South Africa. URL: <https://pdfslide.net/documents/assembly-manual-english-version-gabion-structures.html?page=1> . (date of access: 31.10.2022);
29. *Fiji technical workshop. gabion walls. Geofabrics - Australasia's Geosynthetics Specialist* . Online. Geofabrics Smarter Infrastructure, p. 38. URL: <https://www.geofabrics.co/sites/default/files/Gabion%20Walls%20Presentati on%20Fiji.pdf> . (date of access: 31.10.2022);
30. ET PHILLIPS and CA FORTLAGE. *Landscape construction* . Online. USA: by Routledge, (2017). ISBN 13: 978-0-566-09043-1. URL: https://books.google.com.ua/books?id=w29QDwAAQBAJ&printsec=frontcover&hl=uk&source=gbs_ge_summary_r&cad=0#v=onepage&q&f=false . (date of access: 31.10.2022);
31. *Gabion caged basket in bridge abutment & retaining wall behind a galvanized steel mesh formed from recycled concrete crushed to form gabions London UK Stock Photo* - Alamy Online. Get creative with stock photos and videos from Alamy. [b. d.]. URL : <https://www.alamy.com/stock-photo-gabion-caged-basket-in-bridge-abutment-retaining-wall-behind-a-galvanized-89954550.html> . (date of access: 31.10.2022);
32. David Basulto [tricky]. (2013, October 23). *Metropolitan park south access / polidura talhouk architectos*. ArchDaily. URL: https://www.archdaily.com/440276/metropolitan-park-south-access-polidura-talhouk-architectos?ad_medium=gallery . (date of access: 31.10.2022);

33. *Gabion wall project ideas and installation tips of gabion mattress* . Online. Engineering Discoveries. URL: <https://engineeringdiscoveries.com/gabion-wall-project-ideas-and-installation-tips-of-gabion-mattress/> . (date of access: 31.10.2022);
34. *Welded gabions supplier*. (n.d.). Anping Hongyu Wire Mesh Co., Ltd. URL: <https://www.wiremesh-product.com/gabion%20basket/welded-gabions.html> . (date of access: 31.10.2022);
35. Barros, P. D. P. L. d. A. (2011). *Obras de contenção* [Universidade do Estado do Amazonas (UEA)]. p. 223. URL: <https://www.docsity.com/pt/maccaferri-obras-de-contencao/4752345/> (date of access: 31.10.2022).

ANNEX A

RESULTS OF ANALYSIS OF STRUCTURAL STABILITY WITH THE HELP OF
THE PROGRAM “GAWAC WIN 2003”

Program released in license to: IPB

Project: PRO 05

File: korin

Date: 30.12.1899

Foundation data

Top surface height : 0.00 m
 Top surface init. length : 10.00 m
 Top surface incl. angle : 0.00 deg
 Soil unit weight : 20.00 kN/mi
 Soil friction angle : 40.00 deg
 Soil cohesion : 0.00 kN/ml
 Foundation allowable pressure : kN/ml
 Water table height : m

Additional Foundation Layers

Layer	Depth m	Unit weight kN/mi	Cohesion kN/ml	Friction angle deg
-------	------------	----------------------	-------------------	-----------------------

Water profile data

Initial height : m
 Inclination of the 1st stretch : deg
 Length of the 1st stretch : m
 Inclination of the 2nd stretch : deg
 Length of the 2nd stretch : m

Loads data

Distributed loads on backfill
 First stretch : 0.00 kN/ml
 Second stretch : 5.00 kN/ml

Distributed loads on wall
 Load : kN/ml

Line loads on backfill
 Load 1 : kN/m Distance from wall face : m
 Load 2 : kN/m Distance from wall face : m
 Load 3 : kN/m Distance from wall face : m

Line load on wall
 Load : kN/m Distance from wall face : m

Seismic action data

Horizontal coefficient : Vertical coefficient :

is not responsible for the reliability of the geotechnical parameters assumed, or the improper use of the software. The program takes into account the physical characteristics of materials as manufactured by the Maccaferri group; its results will not be realistic if a different material is used.

 Program released in license to: IPB

Project: PRO 05

File: korin

Date: 30.12.1899

STABILITY ANALYSIS RESULTS

Active and Passive Thrust

Active Thrust	:	79.14 kN/m
Point of application ref. to X axis	:	4.68 m
Point of application ref. to Y axis	:	1.88 m
Direction of the thrust ref. to X axis	:	33.00 deg
Passive Thrust	:	0.00 kN/m
Point of application ref. to X axis	:	0.00 m
Point of application ref. to Y axis	:	0.00 m
Direction of the thrust ref. to X axis	:	0.00 deg

Sliding

Normal force on the base	:	429.47 kN/m
Point of application ref. to X axis	:	2.91 m
Point of application ref. to Y axis	:	-0.25 m
Shear force on the base	:	29.05 kN/m
Resisting force on the base	:	360.36 kN/m

Sliding Safety Coefficient : **6.31**

Overturning

Overturning Moment	:	124.78 kN/m x m
Restoring Moment	:	1374.94 kN/m x m

Overturning Safety Coefficient : **11.02**

Stresses Acting on Foundation

Eccentricity	:	-0.67 m
Normal stress on outer border	:	11.33 kN/ml
Normal stress on inner border	:	179.55 kN/ml
Max. allowable stress on the foundation	:	1231.39 kN/ml

is not responsible for the reliability of the geotechnical parameters assumed, or the improper use of the software. The program takes into account the physical characteristics of materials as manufactured by the Maccaferri group; its results will not be realistic if a different material is used.

GawacWin 1.0**Page 4**

Program released in license to: IPB

Project: PRO 05

File: korin

Date: 30.12.1899

Overall Stability

Initial distance at pivot leftside : m
 Initial distance at pivot rightside : m
 Initial depth referred to base : m
 Max depth allowed in calculation : m
 Center of the arch referred to X axis : 0.61 m
 Center of the arch referred to Y axis : 8.83 m
 Radius of the arch : 10.05 m
 Number of search surfaces : 67

Overall Stability Safety Coefficient : 1.98**Internal Stability**

Layer	H m	N kN/m	T kN/m	M kN/m x m	τ_{Max} kN/ml	τ_{All} kN/ml	σ_{Max} kN/ml	σ_{All} kN/ml
1	5.98	329.30	12.41	853.68	3.10	80.50	63.51	
2	4.98	243.95	2.34	552.57	0.67	71.19	53.85	
3	3.98	173.32	-1.29	332.33	-0.43	62.40	45.20	615.79
4	2.99	113.76	-3.14	177.41	-1.26	53.35	36.48	
5	1.99	65.48	-2.96	77.74	-1.48	43.95	27.58	
6	1.00	27.20	-2.38	21.59	-1.59	33.18	17.13	

is not responsible for the reliability of the geotechnical parameters assumed, or the improper use of the software. The program takes into account the physical characteristics of materials as manufactured by the Maccaferri group; its results will not be realistic if a different material is used.

GawacWin 1.0

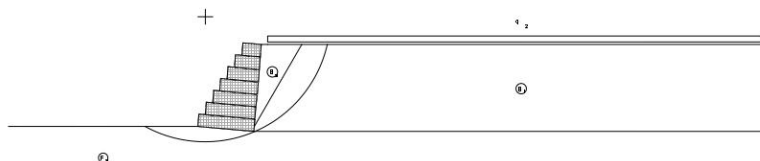
Summary

Program released in license to: IPB

Project: PRO 05

File: korin

Date: 30.12.1899



SOIL DATA

Soil	γ kN/m ³	c kN/m ²	ϕ deg	Soil	γ kN/m ³	c kN/m ²	ϕ deg
B _s	20.00	5.00	40.00	F _s	20.00	0.00	40.00
B ₁	20.00	5.00	35.00				

LOADS

Load	Value kN/m ²	Load	Value kN/m
q ₂	5.00		

STABILITY CHECKS

Sliding Safety Coefficient	6.31	Base normal stress (left)	11.33kN/m ²
Overturning Safety Coefficient	11.02	Base normal stress (right)	179.55kN/m ²
Overall Stability Safety Coefficient	1.98	Max. allowable stress	1231.39kN/m ²

is not responsible for the reliability of the geotechnical parameters assumed, or the improper use of the software. The program takes into account the physical characteristics of materials as manufactured by the Maccaferri group; its results will not be realistic if a different material is used.

Program released in license to: IPB

Project: PRO 05

File: korin

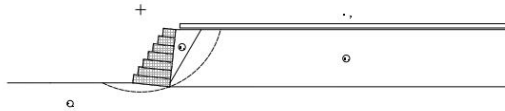
Date: 30.12.1899

INPUT DATA

Wall data

Wall batter : 6.00 deg
 Rockfill unit weight : 26.00 kN/mi
 Porosity of gabions : 30.00 %
 Geotextile in the backfill : Yes
 Friction reduction : 5.00 %
 Geotextile on the base : No
 Friction reduction : %

Layer	Length m	Width m	Offset m
1	4.50	1.00	-
2	4.00	1.00	0.50
3	3.50	1.00	1.00
4	3.00	1.00	1.50
5	2.50	1.00	2.00
6	2.00	1.00	2.50
7	1.50	1.00	3.00



Backfill soil data

Inclination of Stretch 1 : 0.00 deg
 Length of stretch 1 : 0.50 m
 Inclination of Stretch 2 : 0.00 deg
 Soil unit weight : 20.00 kN/mi
 Soil friction angle : 40.00 deg
 Soil cohesion : 5.00 kN/ml

Additional Backfill Layers

Layer	Initial height m	Incl. angle deg	Unit weight kN/mi	Cohesion kN/ml	Friction angle deg
1	0.00	60.00	20.00	5.00	35.00

is not responsible for the reliability of the geotechnical parameters assumed, or the improper use of the software. The program takes into account the physical characteristics of materials as manufactured by the Maccaferri group; its results will not be realistic if a different material is used.

 Program released in license to: IPB

Project: PRO 05

File: korin

Date: 30.12.1899

Foundation data

Top surface height : 0.00 m
 Top surface init. length : 10.00 m
 Top surface incl. angle : 0.00 deg
 Soil unit weight : 20.00 kN/mi
 Soil friction angle : 40.00 deg
 Soil cohesion : 0.00 kN/ml
 Foundation allowable pressure : kN/ml
 Water table height : m

 Additional Foundation Layers

Layer	Depth m	Unit weight kN/mi	Cohesion kN/ml	Friction angle deg
-------	------------	----------------------	-------------------	-----------------------

Water profile data

Initial height : m
 Inclination of the 1st stretch : deg
 Length of the 1st stretch : m
 Inclination of the 2nd stretch : deg
 Length of the 2nd stretch : m

Loads data

Distributed loads on backfill :
 First stretch : 0.00 kN/ml
 Second stretch : 5.00 kN/ml
 Distributed loads on wall :
 Load : kN/ml
 Line loads on backfill :
 Load 1 : kN/m Distance from wall face : m
 Load 2 : kN/m Distance from wall face : m
 Load 3 : kN/m Distance from wall face : m
 Line load on wall :
 Load : kN/m Distance from wall face : m

Seismic action data

Horizontal coefficient : Vertical coefficient :

is not responsible for the reliability of the geotechnical parameters assumed, or the improper use of the software. The program takes into account the physical characteristics of materials as manufactured by the Maccaferri group; its results will not be realistic if a different material is used.

 Program released in license to: IPB

Project: PRO 05

File: korin

Date: 30.12.1899

STABILITY ANALYSIS RESULTS

Active and Passive Thrust

Active Thrust	:	75.42 kN/m
Point of application ref. to X axis	:	4.71 m
Point of application ref. to Y axis	:	1.79 m
Direction of the thrust ref. to X axis	:	32.00 deg
Passive Thrust	:	0.00 kN/m
Point of application ref. to X axis	:	0.00 m
Point of application ref. to Y axis	:	0.00 m
Direction of the thrust ref. to X axis	:	0.00 deg

Sliding

Normal force on the base	:	426.54 kN/m
Point of application ref. to X axis	:	2.96 m
Point of application ref. to Y axis	:	-0.31 m
Shear force on the base	:	19.48 kN/m
Resisting force on the base	:	357.91 kN/m

Sliding Safety Coefficient : **6.69**

Overtipping

Overtipping Moment	:	114.54 kN/m x m
Restoring Moment	:	1378.52 kN/m x m

Overtipping Safety Coefficient : **12.04**

Stresses Acting on Foundation

Eccentricity	:	-0.73 m
Normal stress on outer border	:	4.63 kN/ml
Normal stress on inner border	:	184.94 kN/ml
Max. allowable stress on the foundation	:	1239.20 kN/ml

is not responsible for the reliability of the geotechnical parameters assumed, or the improper use of the software. The program takes into account the physical characteristics of materials as manufactured by the Maccaferri group; its results will not be realistic if a different material is used.

GawacWin 1.0**Page 4**

Program released in license to: IPB

Project: PRO 05

File: korin

Date: 30.12.1899

Overall Stability

Initial distance at pivot leftside : m
 Initial distance at pivot rightside : m
 Initial depth referred to base : m
 Max depth allowed in calculation : m
 Center of the arch referred to X axis : 0.96 m
 Center of the arch referred to Y axis : 8.91 m
 Radius of the arch : 10.04 m
 Number of search surfaces : 60

Overall Stability Safety Coefficient : 2.01

Internal Stability

Layer	H m	N kN/m	T kN/m	M kN/m x m	τ_{Max} kN/ml	τ_{All} kN/ml	σ_{Max} kN/ml	σ_{All} kN/ml
1	5.97	328.09	6.29	864.29	1.57	80.27	62.27	
2	4.97	242.44	-3.06	558.50	-0.88	70.87	52.62	
3	3.98	172.26	-5.15	335.72	-1.72	62.14	44.19	615.79
4	2.98	113.20	-5.53	179.20	-2.21	53.19	35.75	
5	1.99	65.15	-4.36	78.38	-2.18	43.82	27.07	
6	0.99	27.15	-2.85	21.79	-1.90	33.15	16.92	

is not responsible for the reliability of the geotechnical parameters assumed, or the improper use of the software. The program takes into account the physical characteristics of materials as manufactured by the Maccaferri group, its results will not be realistic if a different material is used.

GawacWin 1.0

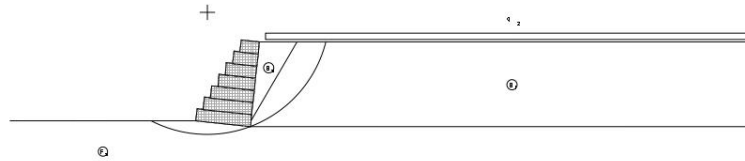
Summary

Program released in license to: IPB

Project: PRO 05

File: korin

Date: 30.12.1899



SOIL DATA

Soil	γ kN/m ³	c kN/m ²	ϕ deg	Soil	γ kN/m ³	c kN/m ²	ϕ deg
B _s	20.00	5.00	40.00	F _s	20.00	0.00	40.00
B ₁	20.00	5.00	35.00				

LOADS

Load	Value kN/m	Load	Value kN/m
q ₂	5.00		

STABILITY CHECKS

Sliding Safety Coefficient	6.69	Base normal stress (left)	4.63kN/ml
Overturning Safety Coefficient	12.04	Base normal stress (right)	184.94kN/ml
Overall Stability Safety Coefficient	2.01	Max. allowable stress	1239.20kN/ml

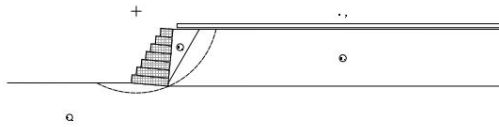
is not responsible for the reliability of the geotechnical parameters assumed, or the improper use of the software. The program takes into account the physical characteristics of materials as manufactured by the Maccaferri group, its results will not be realistic if a different material is used.

INPUT DATA

Wall data

Wall batter : 5.00 deg
 Rockfill unit weight : 26.00 kN/mi
 Porosity of gabions : 40.00 %
 Geotextile in the backfill : Yes
 Friction reduction : 5.00 %
 Geotextile on the base : Yes
 Friction reduction : 5.00 %

Layer	Length m	Width m	Offset m
1	4.50	1.00	-
2	4.00	1.00	0.50
3	3.50	1.00	1.00
4	3.00	1.00	1.50
5	2.50	1.00	2.00
6	2.00	1.00	2.50
7	1.50	1.00	3.00



Backfill soil data

Inclination of Stretch 1 : 0.00 deg
 Length of stretch 1 : 0.50 m
 Inclination of Stretch 2 : 0.00 deg
 Soil unit weight : 20.00 kN/mi
 Soil friction angle : 40.00 deg
 Soil cohesion : 5.00 kN/ml

Additional Backfill Layers

Layer	Initial height m	Incl. angle deg	Unit weight kN/mi	Cohesion kN/ml	Friction angle deg
1	0.00	60.00	20.00	5.00	35.00

is not responsible for the reliability of the geotechnical parameters assumed, or the improper use of the software. The program takes into account the physical characteristics of materials as manufactured by the Maccaferri group; its results will not be realistic if a different material is used.

 Program released in license to: IPB

Project: PRO 05

File: korin

Date: 30.12.1899

Foundation data

Top surface height : 0.00 m
 Top surface init. length : 10.00 m
 Top surface incl. angle : 0.00 deg
 Soil unit weight : 20.00 kN/mi
 Soil friction angle : 40.00 deg
 Soil cohesion : 0.00 kN/ml
 Foundation allowable pressure : kN/ml
 Water table height : m

 Additional Foundation Layers

Layer	Depth m	Unit weight kN/mi	Cohesion kN/ml	Friction angle deg
-------	------------	----------------------	-------------------	-----------------------

Water profile data

Initial height : m
 Inclination of the 1st stretch : deg
 Length of the 1st stretch : m
 Inclination of the 2nd stretch : deg
 Length of the 2nd stretch : m

Loads data

Distributed loads on backfill
 First stretch : 0.00 kN/ml
 Second stretch : 5.00 kN/ml
 Distributed loads on wall
 Load : kN/ml
 Line loads on backfill
 Load 1 : kN/m Distance from wall face : m
 Load 2 : kN/m Distance from wall face : m
 Load 3 : kN/m Distance from wall face : m
 Line load on wall
 Load : kN/m Distance from wall face : m

Seismic action data

Horizontal coefficient : Vertical coefficient :

is not responsible for the reliability of the geotechnical parameters assumed, or the improper use of the software. The program takes into account the physical characteristics of materials as manufactured by the Maccaferri group, its results will not be realistic if a different material is used.

STABILITY ANALYSIS RESULTS**Active and Passive Thrust**

Active Thrust	:	79.14 kN/m
Point of application ref. to X axis	:	4.68 m
Point of application ref. to Y axis	:	1.88 m
Direction of the thrust ref. to X axis	:	33.00 deg
Passive Thrust	:	0.00 kN/m
Point of application ref. to X axis	:	0.00 m
Point of application ref. to Y axis	:	0.00 m
Direction of the thrust ref. to X axis	:	0.00 deg

Sliding

Normal force on the base	:	375.07 kN/m
Point of application ref. to X axis	:	2.89 m
Point of application ref. to Y axis	:	-0.25 m
Shear force on the base	:	33.81 kN/m
Resisting force on the base	:	298.99 kN/m

Sliding Safety Coefficient : **5.25**

Overturning

Overturning Moment	:	124.78 kN/m x m
Restoring Moment	:	1207.35 kN/m x m

Overturning Safety Coefficient : **9.68**

Stresses Acting on Foundation

Eccentricity	:	-0.65 m
Normal stress on outer border	:	12.64 kN/ml
Normal stress on inner border	:	154.06 kN/ml
Max. allowable stress on the foundation	:	1203.59 kN/ml

is not responsible for the reliability of the geotechnical parameters assumed, or the improper use of the software. The program takes into account the physical characteristics of materials as manufactured by the Maccaferri group; its results will not be realistic if a different material is used.

GawacWin 1.0**Page 4**

Program released in license to: IPB

Project: PRO 05

File: korin

Date: 30.12.1899

Overall Stability

Initial distance at pivot leftside : m
 Initial distance at pivot rightside : m
 Initial depth referred to base : m
 Max depth allowed in calculation : m
 Center of the arch referred to X axis : 0.61 m
 Center of the arch referred to Y axis : 8.83 m
 Radius of the arch : 10.05 m
 Number of search surfaces : 57

Overall Stability Safety Coefficient : 1.93**Internal Stability**

Layer	H m	N kN/m	T kN/m	M kN/m x m	τ_{Max} kN/ml	τ_{All} kN/ml	σ_{Max} kN/ml	σ_{All} kN/ml
1	5.98	286.57	16.15	737.93	4.04	60.79	55.64	
2	4.98	211.58	5.17	477.01	1.48	54.38	46.92	
3	3.98	150.01	0.75	286.73	0.25	48.41	39.24	485.79
4	2.99	98.22	-1.78	152.93	-0.71	42.28	31.54	
5	1.99	56.42	-2.16	66.96	-1.08	35.94	23.77	
6	1.00	23.31	-2.04	18.50	-1.36	28.70	14.68	

is not responsible for the reliability of the geotechnical parameters assumed, or the improper use of the software. The program takes into account the physical characteristics of materials as manufactured by the Maccaferri group; its results will not be realistic if a different material is used.

GawacWin 1.0

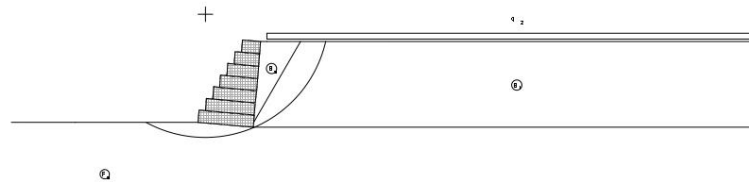
Summary

Program released in license to: IPB

Project: PRO 05

File: korin

Date: 30.12.1899



SOIL DATA

Soil	γ kN/m ³	c kN/m ²	ϕ deg	Soil	γ kN/m ³	c kN/m ²	ϕ deg
B _s	20.00	5.00	40.00	F _s	20.00	0.00	40.00
B ₁	20.00	5.00	35.00				

LOADS

Load	Value kN/m ²	Load	Value kN/m
q ₂	5.00		

STABILITY CHECKS

Sliding Safety Coefficient	5.25	Base normal stress (left)	12.64kN/ml
Overturing Safety Coefficient	9.68	Base normal stress (right)	154.06kN/ml
Overall Stability Safety Coefficient	1.93	Max. allowable stress	1203.59kN/ml

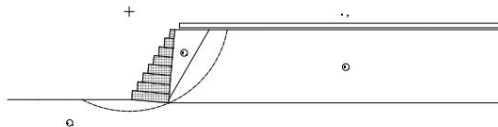
is not responsible for the reliability of the geotechnical parameters assumed, or the improper use of the software. The program takes into account the physical characteristics of materials as manufactured by the Maccaferri group; its results will not be realistic if a different material is used.

INPUT DATA

Wall data

Wall batter : 5.00 deg
 Rockfill unit weight : 26.00 kN/mi
 Porosity of gabions : 30.00 %
 Geotextile in the backfill : Yes
 Friction reduction : 5.00 %
 Geotextile on the base : No
 Friction reduction : %

Layer	Length m	Width m	Offset m
1	4.00	1.00	-
2	3.50	1.00	0.50
3	3.00	1.00	1.00
4	2.50	1.00	1.50
5	2.00	1.00	2.00
6	1.50	1.00	2.50
7	1.00	1.00	3.00
8	0.50	1.00	3.50



Backfill soil data

Inclination of Stretch 1 : 0.00 deg
 Length of stretch 1 : 0.50 m
 Inclination of Stretch 2 : 0.00 deg
 Soil unit weight : 20.00 kN/mi
 Soil friction angle : 40.00 deg
 Soil cohesion : 5.00 kN/ml

Additional Backfill Layers

Layer	Initial height m	Incl. angle deg	Unit weight kN/mi	Cohesion kN/ml	Friction angle deg
1	0.00	60.00	20.00	5.00	35.00

is not responsible for the reliability of the geotechnical parameters assumed, or the improper use of the software. The program takes into account the physical characteristics of materials as manufactured by the Maccaferri group, its results will not be realistic if a different material is used.

 Program released in license to: IPB

Project: PRO 05

File: korin

Date: 30.12.1899

Foundation data

Top surface height : 0.00 m
 Top surface init. length : 10.00 m
 Top surface incl. angle : 0.00 deg
 Soil unit weight : 20.00 kN/mi
 Soil friction angle : 40.00 deg
 Soil cohesion : 0.00 kN/ml
 Foundation allowable pressure : kN/ml
 Water table height : m

 Additional Foundation Layers

Layer	Depth m	Unit weight kN/mi	Cohesion kN/ml	Friction angle deg
-------	------------	----------------------	-------------------	-----------------------

Water profile data

Initial height : m
 Inclination of the 1st stretch : deg
 Length of the 1st stretch : m
 Inclination of the 2nd stretch : deg
 Length of the 2nd stretch : m

Loads data

Distributed loads on backfill :
 First stretch : 0.00 kN/ml
 Second stretch : 5.00 kN/ml
 Distributed loads on wall :
 Load : kN/ml
 Line loads on backfill :
 Load 1 : kN/m Distance from wall face : m
 Load 2 : kN/m Distance from wall face : m
 Load 3 : kN/m Distance from wall face : m
 Line load on wall :
 Load : kN/m Distance from wall face : m

Seismic action data

Horizontal coefficient : Vertical coefficient :

is not responsible for the reliability of the geotechnical parameters assumed, or the improper use of the software. The program takes into account the physical characteristics of materials as manufactured by the Maccaferri group; its results will not be realistic if a different material is used.

 Program released in license to: IPB

Project: PRO 05

File: korin

Date: 30.12.1899

STABILITY ANALYSIS RESULTS

Active and Passive Thrust

Active Thrust	:	107.29 kN/m
Point of application ref. to X axis	:	4.21 m
Point of application ref. to Y axis	:	2.24 m
Direction of the thrust ref. to X axis	:	33.00 deg
Passive Thrust	:	0.00 kN/m
Point of application ref. to X axis	:	0.00 m
Point of application ref. to Y axis	:	0.00 m
Direction of the thrust ref. to X axis	:	0.00 deg

Sliding

Normal force on the base	:	392.41 kN/m
Point of application ref. to X axis	:	2.47 m
Point of application ref. to Y axis	:	-0.22 m
Shear force on the base	:	56.00 kN/m
Resisting force on the base	:	329.27 kN/m

Sliding Safety Coefficient : **4.23**

Overturning

Overturning Moment	:	201.81 kN/m x m
Restoring Moment	:	1170.08 kN/m x m

Overturning Safety Coefficient : **5.80**

Stresses Acting on Foundation

Eccentricity	:	-0.48 m
Normal stress on outer border	:	29.31 kN/ml
Normal stress on inner border	:	166.90 kN/ml
Max. allowable stress on the foundation	:	1013.21 kN/ml

is not responsible for the reliability of the geotechnical parameters assumed, or the improper use of the software. The program takes into account the physical characteristics of materials as manufactured by the Maccaferri group; its results will not be realistic if a different material is used.

GawacWin 1.0**Page 4**

Program released in license to: IPB

Project: PRO 05

File: korin

Date: 30.12.1899

Overall Stability

Initial distance at pivot leftside : m
 Initial distance at pivot rightside : m
 Initial depth referred to base : m
 Max depth allowed in calculation : m
 Center of the arch referred to X axis : -0.29 m
 Center of the arch referred to Y axis : 9.62 m
 Radius of the arch : 10.88 m
 Number of search surfaces : 58

Overall Stability Safety Coefficient : 1.73

Internal Stability

Layer	H m	N kN/m	T kN/m	M kN/m x m	τ_{Max} kN/ml	τ_{All} kN/ml	σ_{Max} kN/ml	σ_{All} kN/ml
1	6.97	296.94	32.97	648.77	9.42	82.35	67.95	
2	5.98	216.82	17.19	412.61	5.73	73.08	56.97	
3	4.98	153.30	10.27	243.46	4.11	65.01	48.26	615.79
4	3.98	100.80	5.05	128.19	2.53	56.96	39.63	
5	2.99	59.37	1.62	56.51	1.08	48.99	31.19	
6	1.99	29.22	0.22	18.14	0.22	41.35	23.53	
7	1.00	9.07	-0.79	2.66	-1.59	33.18	15.43	

is not responsible for the reliability of the geotechnical parameters assumed, or the improper use of the software. The program takes into account the physical characteristics of materials as manufactured by the Maccaferri group; its results will not be realistic if a different material is used.

GawacWin 1.0

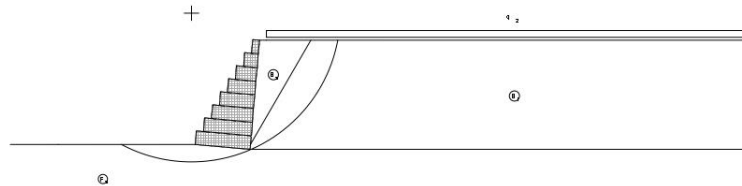
Summary

Program released in license to: IPB

Project: PRO 05

File: korin

Date: 30.12.1899



SOIL DATA

Soil	γ kN/mi	c kN/ml	ϕ deg	Soil	γ kN/mi	c kN/ml	ϕ deg
B _s	20.00	5.00	40.00	F _s	20.00	0.00	40.00
B ₁	20.00	5.00	35.00				

LOADS

Load	Value kN/ml	Load	Value kN/m
q ₂	5.00		

STABILITY CHECKS

Sliding Safety Coefficient	4.23	Base normal stress (left)	29.31kN/ml
Overturning Safety Coefficient	5.80	Base normal stress (right)	166.90kN/ml
Overall Stability Safety Coefficient	1.73	Max. allowable stress	1013.21kN/ml

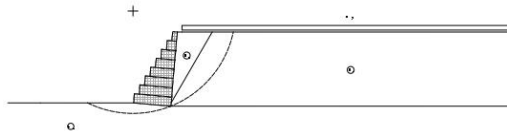
is not responsible for the reliability of the geotechnical parameters assumed, or the improper use of the software. The program takes into account the physical characteristics of materials as manufactured by the Maccaferri group; its results will not be realistic if a different material is used.

INPUT DATA

Wall data

Wall batter : 5.00 deg
 Rockfill unit weight : 26.00 kN/mi
 Porosity of gabions : 40.00 %
 Geotextile in the backfill : Yes
 Friction reduction : 5.00 %
 Geotextile on the base : Yes
 Friction reduction : 5.00 %

Layer	Length m	Width m	Offset m
1	4.00	1.00	-
2	3.50	1.00	0.50
3	3.00	1.00	1.00
4	2.50	1.00	1.50
5	2.00	1.00	2.00
6	1.50	1.00	2.50
7	1.00	1.00	3.00
8	0.50	1.00	3.50



Backfill soil data

Inclination of Stretch 1 : 0.00 deg
 Length of stretch 1 : 0.50 m
 Inclination of Stretch 2 : 0.00 deg
 Soil unit weight : 20.00 kN/mi
 Soil friction angle : 40.00 deg
 Soil cohesion : 5.00 kN/ml

Additional Backfill Layers

Layer	Initial height m	Incl. angle deg	Unit weight kN/mi	Cohesion kN/ml	Friction angle deg
1	0.00	60.00	20.00	5.00	35.00

is not responsible for the reliability of the geotechnical parameters assumed, or the improper use of the software. The program takes into account the physical characteristics of materials as manufactured by the Maccaferri group, its results will not be realistic if a different material is used.

Program released in license to: IPB

Project: PRO 05

File: korin

Date: 30.12.1899

Foundation data

Top surface height : 0.00 m
 Top surface init. length : 10.00 m
 Top surface incl. angle : 0.00 deg
 Soil unit weight : 20.00 kN/mi
 Soil friction angle : 40.00 deg
 Soil cohesion : 0.00 kN/ml
 Foundation allowable pressure : kN/ml
 Water table height : m

Additional Foundation Layers

Layer	Depth m	Unit weight kN/mi	Cohesion kN/ml	Friction angle deg
-------	------------	----------------------	-------------------	-----------------------

Water profile data

Initial height : m
 Inclination of the 1st stretch : deg
 Length of the 1st stretch : m
 Inclination of the 2nd stretch : deg
 Length of the 2nd stretch : m

Loads data

Distributed loads on backfill
 First stretch : 0.00 kN/ml
 Second stretch : 5.00 kN/ml

Distributed loads on wall
 Load : kN/ml

Line loads on backfill
 Load 1 : kN/m Distance from wall face : m
 Load 2 : kN/m Distance from wall face : m
 Load 3 : kN/m Distance from wall face : m

Line load on wall
 Load : kN/m Distance from wall face : m

Seismic action data

Horizontal coefficient : Vertical coefficient :

is not responsible for the reliability of the geotechnical parameters assumed, or the improper use of the software. The program takes into account the physical characteristics of materials as manufactured by the Maccaferri group; its results will not be realistic if a different material is used.

 Program released in license to: IPB

Project: PRO 05

File: korin

Date: 30.12.1899

STABILITY ANALYSIS RESULTS

Active and Passive Thrust

Active Thrust	:	107.29 kN/m
Point of application ref. to X axis	:	4.21 m
Point of application ref. to Y axis	:	2.24 m
Direction of the thrust ref. to X axis	:	33.00 deg
Passive Thrust	:	0.00 kN/m
Point of application ref. to X axis	:	0.00 m
Point of application ref. to Y axis	:	0.00 m
Direction of the thrust ref. to X axis	:	0.00 deg

Sliding

Normal force on the base	:	345.79 kN/m
Point of application ref. to X axis	:	2.42 m
Point of application ref. to Y axis	:	-0.21 m
Shear force on the base	:	60.08 kN/m
Resisting force on the base	:	275.64 kN/m

Sliding Safety Coefficient : **3.55**

Overturning

Overturning Moment	:	201.81 kN/m x m
Restoring Moment	:	1038.09 kN/m x m

Overturning Safety Coefficient : **5.14**

Stresses Acting on Foundation

Eccentricity	:	-0.43 m
Normal stress on outer border	:	32.19 kN/ml
Normal stress on inner border	:	140.71 kN/ml
Max. allowable stress on the foundation	:	980.49 kN/ml

is not responsible for the reliability of the geotechnical parameters assumed, or the improper use of the software. The program takes into account the physical characteristics of materials as manufactured by the Maccaferri group; its results will not be realistic if a different material is used.

GawacWin 1.0**Page 4**

Program released in license to: IPB

Project: PRO 05

File: korin

Date: 30.12.1899

Overall Stability

Initial distance at pivot leftside : m
 Initial distance at pivot rightside : m
 Initial depth referred to base : m
 Max depth allowed in calculation : m
 Center of the arch referred to X axis : -0.08 m
 Center of the arch referred to Y axis : 9.89 m
 Radius of the arch : 11.02 m
 Number of search surfaces : 56

Overall Stability Safety Coefficient : 1.68

Internal Stability

Layer	H m	N kN/m	T kN/m	M kN/m x m	τ_{Max} kN/ml	τ_{All} kN/ml	σ_{Max} kN/ml	σ_{All} kN/ml
1	6.97	260.68	36.14	559.25	10.33	62.41	60.75	
2	5.98	189.62	19.57	355.32	6.52	55.96	50.60	
3	4.98	133.87	11.97	209.59	4.79	50.44	42.75	485.79
4	3.98	87.85	6.19	110.30	3.09	44.93	34.98	
5	2.99	51.60	2.29	48.59	1.53	39.49	27.40	
6	1.99	25.34	0.56	15.59	0.56	34.30	20.58	
7	1.00	7.77	-0.68	2.28	-1.36	28.70	13.23	

is not responsible for the reliability of the geotechnical parameters assumed, or the improper use of the software. The program takes into account the physical characteristics of materials as manufactured by the Maccaferri group, its results will not be realistic if a different material is used.

GawacWin 1.0

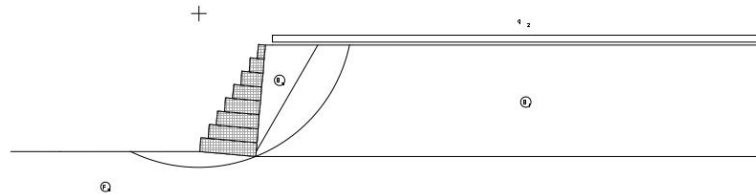
Summary

Program released in license to: IPB

Project: PRO 05

File: korin

Date: 30.12.1899



SOIL DATA

Soil	γ kN/m ³	c kN/m ²	ϕ deg	Soil	γ kN/m ³	c kN/m ²	ϕ deg
B _s	20.00	5.00	40.00	F _s	20.00	0.00	40.00
B ₁	20.00	5.00	35.00				

LOADS

Load	Value kN/m ²	Load	Value kN/m
q ₂	5.00		

STABILITY CHECKS

Sliding Safety Coefficient	3.55	Base normal stress (left)	32.19kN/m ²
Overturning Safety Coefficient	5.14	Base normal stress (right)	140.71kN/m ²
Overall Stability Safety Coefficient	1.68	Max. allowable stress	980.49kN/m ²

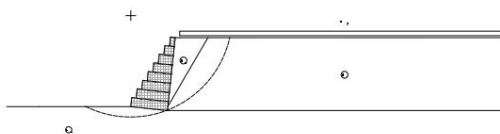
is not responsible for the reliability of the geotechnical parameters assumed, or the improper use of the software. The program takes into account the physical characteristics of materials as manufactured by the Maccaferri group; its results will not be realistic if a different material is used.

INPUT DATA

Wall data

Wall batter : 6.00 deg
 Rockfill unit weight : 26.00 kN/mi
 Porosity of gabions : 40.00 %
 Geotextile in the backfill : Yes
 Friction reduction : 5.00 %
 Geotextile on the base : Yes
 Friction reduction : 5.00 %

Layer	Length m	Width m	Offset m
1	4.00	1.00	-
2	3.50	1.00	0.50
3	3.00	1.00	1.00
4	2.50	1.00	1.50
5	2.00	1.00	2.00
6	1.50	1.00	2.50
7	1.00	1.00	3.00
8	0.50	1.00	3.50



Backfill soil data

Inclination of Stretch 1 : 0.00 deg
 Length of stretch 1 : 0.50 m
 Inclination of Stretch 2 : 0.00 deg
 Soil unit weight : 20.00 kN/mi
 Soil friction angle : 40.00 deg
 Soil cohesion : 5.00 kN/ml

Additional Backfill Layers

Layer	Initial height m	Incl. angle deg	Unit weight kN/mi	Cohesion kN/ml	Friction angle deg
1	0.00	60.00	20.00	5.00	35.00

is not responsible for the reliability of the geotechnical parameters assumed, or the improper use of the software. The program takes into account the physical characteristics of materials as manufactured by the Maccaferri group, its results will not be realistic if a different material is used.

Program released in license to: IPB

Project: PRO 05

File: korin

Date: 30.12.1899

Foundation data

Top surface height : 0.00 m
 Top surface init. length : 10.00 m
 Top surface incl. angle : 0.00 deg
 Soil unit weight : 20.00 kN/mi
 Soil friction angle : 40.00 deg
 Soil cohesion : 0.00 kN/ml
 Foundation allowable pressure : kN/ml
 Water table height : m

Additional Foundation Layers

Layer	Depth m	Unit weight kN/mi	Cohesion kN/ml	Friction angle deg

Water profile data

Initial height : m
 Inclination of the 1st stretch : deg
 Length of the 1st stretch : m
 Inclination of the 2nd stretch : deg
 Length of the 2nd stretch : m

Loads data

Distributed loads on backfill
 First stretch : 0.00 kN/ml
 Second stretch : 5.00 kN/ml

Distributed loads on wall
 Load : kN/ml

Line loads on backfill
 Load 1 : kN/m Distance from wall face : m
 Load 2 : kN/m Distance from wall face : m
 Load 3 : kN/m Distance from wall face : m

Line load on wall
 Load : kN/m Distance from wall face : m

Seismic action data

Horizontal coefficient : Vertical coefficient :

is not responsible for the reliability of the geotechnical parameters assumed, or the improper use of the software. The program takes into account the physical characteristics of materials as manufactured by the Maccaferri group; its results will not be realistic if a different material is used.

 Program released in license to: IPB

Project: PRO 05

File: korin

Date: 30.12.1899

STABILITY ANALYSIS RESULTS

Active and Passive Thrust

Active Thrust	:	101.71 kN/m
Point of application ref. to X axis	:	4.25 m
Point of application ref. to Y axis	:	2.18 m
Direction of the thrust ref. to X axis	:	32.00 deg
Passive Thrust	:	0.00 kN/m
Point of application ref. to X axis	:	0.00 m
Point of application ref. to Y axis	:	0.00 m
Direction of the thrust ref. to X axis	:	0.00 deg

Sliding

Normal force on the base	:	341.88 kN/m
Point of application ref. to X axis	:	2.47 m
Point of application ref. to Y axis	:	-0.26 m
Shear force on the base	:	50.80 kN/m
Resisting force on the base	:	272.53 kN/m

Sliding Safety Coefficient : **3.77**

Overturning

Overturning Moment	:	188.34 kN/m x m
Restoring Moment	:	1033.73 kN/m x m

Overturning Safety Coefficient : **5.49**

Stresses Acting on Foundation

Eccentricity	:	-0.49 m
Normal stress on outer border	:	24.86 kN/ml
Normal stress on inner border	:	146.08 kN/ml
Max. allowable stress on the foundation	:	991.79 kN/ml

is not responsible for the reliability of the geotechnical parameters assumed, or the improper use of the software. The program takes into account the physical characteristics of materials as manufactured by the Maccaferri group; its results will not be realistic if a different material is used.

GawacWin 1.0**Page 4**

Program released in license to: IPB

Project: PRO 05

File: korin

Date: 30.12.1899

Overall Stability

Initial distance at pivot leftside : m
 Initial distance at pivot rightside : m
 Initial depth referred to base : m
 Max depth allowed in calculation : m
 Center of the arch referred to X axis : -0.01 m
 Center of the arch referred to Y axis : 9.91 m
 Radius of the arch : 11.08 m
 Number of search surfaces : 56

Overall Stability Safety Coefficient : 1.70**Internal Stability**

Layer	H m	N kN/m	T kN/m	M kN/m x m	τ_{Max} kN/ml	τ_{All} kN/ml	σ_{Max} kN/ml	σ_{All} kN/ml
1	6.96	259.18	30.89	567.33	8.83	62.16	59.20	
2	5.97	187.80	14.75	360.29	4.92	55.61	48.95	
3	4.97	132.54	8.49	212.59	3.39	50.13	41.32	485.79
4	3.98	86.93	3.82	111.94	1.91	44.67	33.75	
5	2.98	51.14	0.99	49.38	0.66	39.31	26.48	
6	1.99	25.07	-0.15	15.88	-0.15	34.15	19.79	
7	0.99	7.76	-0.82	2.35	-1.63	28.68	12.82	

is not responsible for the reliability of the geotechnical parameters assumed, or the improper use of the software. The program takes into account the physical characteristics of materials as manufactured by the Maccaferri group; its results will not be realistic if a different material is used.

GawacWin 1.0

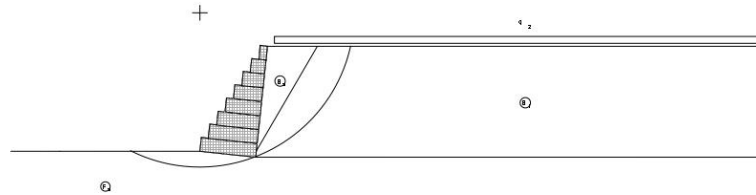
Summary

Program released in license to: IPB

Project: PRO 05

File: korin

Date: 30.12.1899



SOIL DATA

Soil	γ kN/m ³	c kN/m ²	ϕ deg	Soil	γ kN/m ³	c kN/m ²	ϕ deg
B _s	20.00	5.00	40.00	F _s	20.00	0.00	40.00
B ₁	20.00	5.00	35.00				

LOADS

Load	Value kN/m ²	Load	Value kN/m
q ₂	5.00		

STABILITY CHECKS

Sliding Safety Coefficient	3.77	Base normal stress (left)	24.86kN/m ²
Overturning Safety Coefficient	5.49	Base normal stress (right)	146.08kN/m ²
Overall Stability Safety Coefficient	1.70	Max. allowable stress	991.79kN/m ²

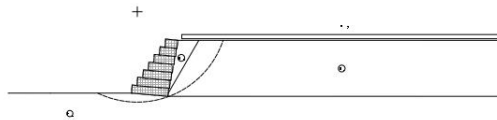
is not responsible for the reliability of the geotechnical parameters assumed, or the improper use of the software. The program takes into account the physical characteristics of materials as manufactured by the Maccaferri group, its results will not be realistic if a different material is used.

INPUT DATA

Wall data

Wall batter : 5.00 deg
 Rockfill unit weight : 26.00 kN/mi
 Porosity of gabions : 30.00 %
 Geotextile in the backfill : Yes
 Friction reduction : 5.00 %
 Geotextile on the base : No
 Friction reduction : %

Layer	Length m	Width m	Offset m
1	4.50	1.00	-
2	4.00	1.00	0.60
3	3.50	1.00	1.20
4	3.00	1.00	1.80
5	2.50	1.00	2.40
6	2.00	1.00	3.00
7	1.50	1.00	3.60



Backfill soil data

Inclination of Stretch 1 : 0.00 deg
 Length of stretch 1 : 0.50 m
 Inclination of Stretch 2 : 0.00 deg
 Soil unit weight : 20.00 kN/mi
 Soil friction angle : 40.00 deg
 Soil cohesion : 5.00 kN/ml

Additional Backfill Layers

Layer	Initial height m	Incl. angle deg	Unit weight kN/mi	Cohesion kN/ml	Friction angle deg
1	0.00	60.00	20.00	5.00	35.00

is not responsible for the reliability of the geotechnical parameters assumed, or the improper use of the software. The program takes into account the physical characteristics of materials as manufactured by the Maccaferri group; its results will not be realistic if a different material is used.

Program released in license to: IPB

Project: PRO 05

File: korin

Date: 30.12.1899

Foundation data

Top surface height : 0.00 m
 Top surface init. length : 10.00 m
 Top surface incl. angle : 0.00 deg
 Soil unit weight : 20.00 kN/mi
 Soil friction angle : 40.00 deg
 Soil cohesion : 0.00 kN/ml
 Foundation allowable pressure : kN/ml
 Water table height : m

Additional Foundation Layers

Layer	Depth m	Unit weight kN/mi	Cohesion kN/ml	Friction angle deg
-------	------------	----------------------	-------------------	-----------------------

Water profile data

Initial height : m
 Inclination of the 1st stretch : deg
 Length of the 1st stretch : m
 Inclination of the 2nd stretch : deg
 Length of the 2nd stretch : m

Loads data

Distributed loads on backfill
 First stretch : 0.00 kN/ml
 Second stretch : 5.00 kN/ml

Distributed loads on wall
 Load : kN/ml

Line loads on backfill
 Load 1 : kN/m Distance from wall face : m
 Load 2 : kN/m Distance from wall face : m
 Load 3 : kN/m Distance from wall face : m

Line load on wall
 Load : kN/m Distance from wall face : m

Seismic action data

Horizontal coefficient : Vertical coefficient :

is not responsible for the reliability of the geotechnical parameters assumed, or the improper use of the software. The program takes into account the physical characteristics of materials as manufactured by the Maccaferri group; its results will not be realistic if a different material is used.

 Program released in license to: IPB

Project: PRO 05

File: korin

Date: 30.12.1899

STABILITY ANALYSIS RESULTS

Active and Passive Thrust

Active Thrust	:	60.84 kN/m
Point of application ref. to X axis	:	4.87 m
Point of application ref. to Y axis	:	1.83 m
Direction of the thrust ref. to X axis	:	28.10 deg
Passive Thrust	:	0.00 kN/m
Point of application ref. to X axis	:	0.00 m
Point of application ref. to Y axis	:	0.00 m
Direction of the thrust ref. to X axis	:	0.00 deg

Sliding

Normal force on the base	:	413.97 kN/m
Point of application ref. to X axis	:	3.15 m
Point of application ref. to Y axis	:	-0.28 m
Shear force on the base	:	17.65 kN/m
Resisting force on the base	:	347.36 kN/m

Sliding Safety Coefficient : **7.47**

Overturning

Overturning Moment	:	98.02 kN/m x m
Restoring Moment	:	1400.37 kN/m x m

Overturning Safety Coefficient : **14.29**

Stresses Acting on Foundation

Eccentricity	:	-0.91 m
Normal stress on outer border	:	87.72 kN/ml
Normal stress on inner border	:	0.00 kN/ml
Max. allowable stress on the foundation	:	1260.90 kN/ml

Warning. Not all base is used!

is not responsible for the reliability of the geotechnical parameters assumed, or the improper use of the software. The program takes into account the physical characteristics of materials as manufactured by the Maccaferri group; its results will not be realistic if a different material is used.

GawacWin 1.0**Page 4**

Program released in license to: IPB

Project: PRO 05

File: korin

Date: 30.12.1899

Overall Stability

Initial distance at pivot leftside : m
 Initial distance at pivot rightside : m
 Initial depth referred to base : m
 Max depth allowed in calculation : m
 Center of the arch referred to X axis : 0.71 m
 Center of the arch referred to Y axis : 10.04 m
 Radius of the arch : 11.16 m
 Number of search surfaces : 50

Overall Stability Safety Coefficient : 2.00**Internal Stability**

Layer	H m	N kN/m	T kN/m	M kN/m x m	τ_{Max} kN/ml	τ_{All} kN/ml	σ_{Max} kN/ml	σ_{All} kN/ml
1	5.93	320.98	7.13	892.66	1.78	78.96	57.71	
2	4.95	237.48	-3.40	576.62	-0.97	69.83	48.90	
3	3.96	169.51	-4.79	345.79	-1.60	61.46	41.55	615.79
4	2.97	111.96	-4.84	183.70	-1.94	52.82	34.12	
5	1.98	64.72	-3.75	79.45	-1.88	43.67	26.36	
6	1.00	27.20	-2.38	21.59	-1.59	33.18	17.13	

is not responsible for the reliability of the geotechnical parameters assumed, or the improper use of the software. The program takes into account the physical characteristics of materials as manufactured by the Maccaferri group; its results will not be realistic if a different material is used.

GawacWin 1.0

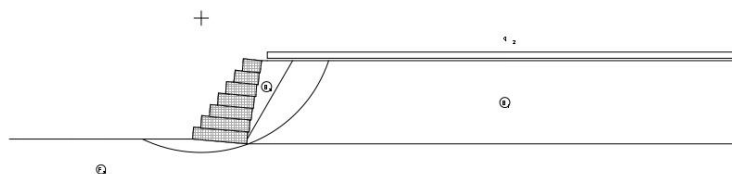
Summary

Program released in license to: IPB

Project: PRO 05

File: korin

Date: 30.12.1899



SOIL DATA

Soil	γ kN/m ³	c kN/m ²	ϕ deg	Soil	γ kN/m ³	c kN/m ²	ϕ deg
B _s	20.00	5.00	40.00	F _s	20.00	0.00	40.00
B ₁	20.00	5.00	35.00				

LOADS

Load	Value kN/m ²	Load	Value kN/m
q ₂	5.00		

STABILITY CHECKS

Sliding Safety Coefficient	7.47	Base normal stress (left)	87.72kN/m ²
Overturing Safety Coefficient	14.29	Base normal stress (right)	0.00kN/m ²
Overall Stability Safety Coefficient	2.00	Max. allowable stress	1260.90kN/m ²

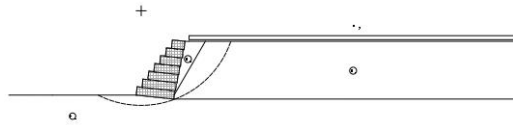
is not responsible for the reliability of the geotechnical parameters assumed, or the improper use of the software. The program takes into account the physical characteristics of materials as manufactured by the Maccaferri group; its results will not be realistic if a different material is used.

INPUT DATA

Wall data

Wall batter : 6.00 deg
 Rockfill unit weight : 26.00 kN/mi
 Porosity of gabions : 30.00 %
 Geotextile in the backfill : Yes
 Friction reduction : 5.00 %
 Geotextile on the base : No
 Friction reduction : %

Layer	Length m	Width m	Offset m
1	4.50	1.00	-
2	4.00	1.00	0.60
3	3.50	1.00	1.20
4	3.00	1.00	1.80
5	2.50	1.00	2.40
6	2.00	1.00	3.00
7	1.50	1.00	3.60



Backfill soil data

Inclination of Stretch 1 : 0.00 deg
 Length of stretch 1 : 0.50 m
 Inclination of Stretch 2 : 0.00 deg
 Soil unit weight : 20.00 kN/mi
 Soil friction angle : 40.00 deg
 Soil cohesion : 5.00 kN/ml

Additional Backfill Layers

Layer	Initial height m	Incl. angle deg	Unit weight kN/mi	Cohesion kN/ml	Friction angle deg
1	0.00	60.00	20.00	5.00	35.00

is not responsible for the reliability of the geotechnical parameters assumed, or the improper use of the software. The program takes into account the physical characteristics of materials as manufactured by the Maccaferri group; its results will not be realistic if a different material is used.

Program released in license to: IPB

Project: PRO 05

File: korin

Date: 30.12.1899

Foundation data

Top surface height : 0.00 m
 Top surface init. length : 10.00 m
 Top surface incl. angle : 0.00 deg
 Soil unit weight : 20.00 kN/mi
 Soil friction angle : 40.00 deg
 Soil cohesion : 0.00 kN/ml
 Foundation allowable pressure : kN/ml
 Water table height : m

Additional Foundation Layers

Layer	Depth m	Unit weight kN/mi	Cohesion kN/ml	Friction angle deg
-------	------------	----------------------	-------------------	-----------------------

Water profile data

Initial height : m
 Inclination of the 1st stretch : deg
 Length of the 1st stretch : m
 Inclination of the 2nd stretch : deg
 Length of the 2nd stretch : m

Loads data

Distributed loads on backfill
 First stretch : 0.00 kN/ml
 Second stretch : 5.00 kN/ml

Distributed loads on wall
 Load : kN/ml

Line loads on backfill
 Load 1 : kN/m Distance from wall face : m
 Load 2 : kN/m Distance from wall face : m
 Load 3 : kN/m Distance from wall face : m

Line load on wall
 Load : kN/m Distance from wall face : m

Seismic action data

Horizontal coefficient : Vertical coefficient :

is not responsible for the reliability of the geotechnical parameters assumed, or the improper use of the software. The program takes into account the physical characteristics of materials as manufactured by the Maccaferri group; its results will not be realistic if a different material is used.

Program released in license to: IPB

Project: PRO 05

File: korin

Date: 30.12.1899

STABILITY ANALYSIS RESULTS**Active and Passive Thrust**

Active Thrust	:	56.64 kN/m
Point of application ref. to X axis	:	4.90 m
Point of application ref. to Y axis	:	1.75 m
Direction of the thrust ref. to X axis	:	27.10 deg
Passive Thrust	:	0.00 kN/m
Point of application ref. to X axis	:	0.00 m
Point of application ref. to Y axis	:	0.00 m
Direction of the thrust ref. to X axis	:	0.00 deg

Sliding

Normal force on the base	:	411.04 kN/m
Point of application ref. to X axis	:	3.20 m
Point of application ref. to Y axis	:	-0.34 m
Shear force on the base	:	7.49 kN/m
Resisting force on the base	:	344.90 kN/m

Sliding Safety Coefficient : **8.11**

Overturning

Overturning Moment	:	87.99 kN/m x m
Restoring Moment	:	1404.03 kN/m x m

Overturning Safety Coefficient : **15.96**

Stresses Acting on Foundation

Eccentricity	:	-0.97 m
Normal stress on outer border	:	85.59 kN/ml
Normal stress on inner border	:	0.00 kN/ml
Max. allowable stress on the foundation	:	1271.24 kN/ml

Warning. Not all base is used!

is not responsible for the reliability of the geotechnical parameters assumed, or the improper use of the software. The program takes into account the physical characteristics of materials as manufactured by the Maccaferri group; its results will not be realistic if a different material is used.

GawacWin 1.0**Page 4**

Program released in license to: IPB

Project: PRO 05

File: korin

Date: 30.12.1899

Overall Stability

Initial distance at pivot leftside : m
 Initial distance at pivot rightside : m
 Initial depth referred to base : m
 Max depth allowed in calculation : m
 Center of the arch referred to X axis : 0.58 m
 Center of the arch referred to Y axis : 10.10 m
 Radius of the arch : 11.32 m
 Number of search surfaces : 51

Overall Stability Safety Coefficient : 2.05

Internal Stability

Layer	H m	N kN/m	T kN/m	M kN/m x m	τ_{Max} kN/ml	τ_{All} kN/ml	σ_{Max} kN/ml	σ_{All} kN/ml
1	5.91	319.73	0.77	903.29	0.19	78.73	56.59	
2	4.93	236.60	-8.11	583.43	-2.32	69.64	47.97	
3	3.95	168.64	-8.52	349.48	-2.84	61.25	40.69	615.79
4	2.96	111.39	-7.30	185.52	-2.92	52.66	33.44	
5	1.98	64.39	-5.19	80.10	-2.59	43.54	25.88	
6	0.99	27.15	-2.85	21.79	-1.90	33.15	16.92	

is not responsible for the reliability of the geotechnical parameters assumed, or the improper use of the software. The program takes into account the physical characteristics of materials as manufactured by the Maccaferri group; its results will not be realistic if a different material is used.

GawacWin 1.0

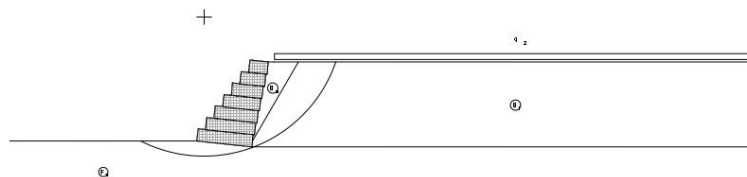
Summary

Program released in license to: IPB

Project: PRO 05

File: korin

Date: 30.12.1899



SOIL DATA

Soil	γ kN/mi	c kN/ml	ϕ deg	Soil	γ kN/mi	c kN/ml	ϕ deg
B _s	20.00	5.00	40.00	F _s	20.00	0.00	40.00
B ₁	20.00	5.00	35.00				

LOADS

Load	Value kN/ml	Load	Value kN/m
q ₂	5.00		

STABILITY CHECKS

Sliding Safety Coefficient	8.11	Base normal stress (left)	85.59kN/ml
Overturning Safety Coefficient	15.96	Base normal stress (right)	0.00kN/ml
Overall Stability Safety Coefficient	2.05	Max. allowable stress	1271.24kN/ml

is not responsible for the reliability of the geotechnical parameters assumed, or the improper use of the software. The program takes into account the physical characteristics of materials as manufactured by the Maccaferri group; its results will not be realistic if a different material is used.

ANNEX B

THEORY AND AN EXAMPLE OF GABION WALL CALCULATION
ACCORDING TO THE MANUAL
“OBRAS DE CONTENÇÃO. MANUAL TÉCNICO”

3. TEORIA E CÁLCULOS DE ESTABILIDADE

3.1 Resistência ao cisalhamento dos solos

A resistência ao cisalhamento pode ser definida como o máximo valor que a tensão cisalhante pode alcançar ao longo de um plano qualquer no interior do maciço sem que haja ruptura da estrutura do solo. Como uma grande parte dessa resistência provém do atrito entre as partículas do solo, ela depende da tensão normal que age sobre este plano. Por outro lado, a maioria dos problemas de empuxo pode ser aproximada a um estado plano de deformação considerando apenas a seção principal do conjunto solo-estrutura e admitindo que todas as outras seções são iguais a esta.

3.1.1 Critério de Mohr-Coulomb

A lei que determina a resistência ao cisalhamento do solo é o critério de ruptura ou de plastificação do material. Trata-se de um modelo matemático aproximado que relaciona a resistência ao estado de tensão atuante. No caso dos solos, o critério mais amplamente utilizado é o critério de Mohr-Coulomb, que estabelece uma relação entre a resistência ao cisalhamento e a tensão normal. O critério de Mohr-Coulomb se baseia na lei de Coulomb e no critério de ruptura de Mohr.

O critério de Mohr-Coulomb assume que a envoltória de resistência ao cisalhamento do solo tem a forma de uma reta dada por:

$$s = c + \sigma \cdot \tan \phi$$

(01)

onde “s” é a resistência ao cisalhamento, “c” é chamada de coesão e “ ϕ ” o ângulo de atrito interno (figura 3.1.1).

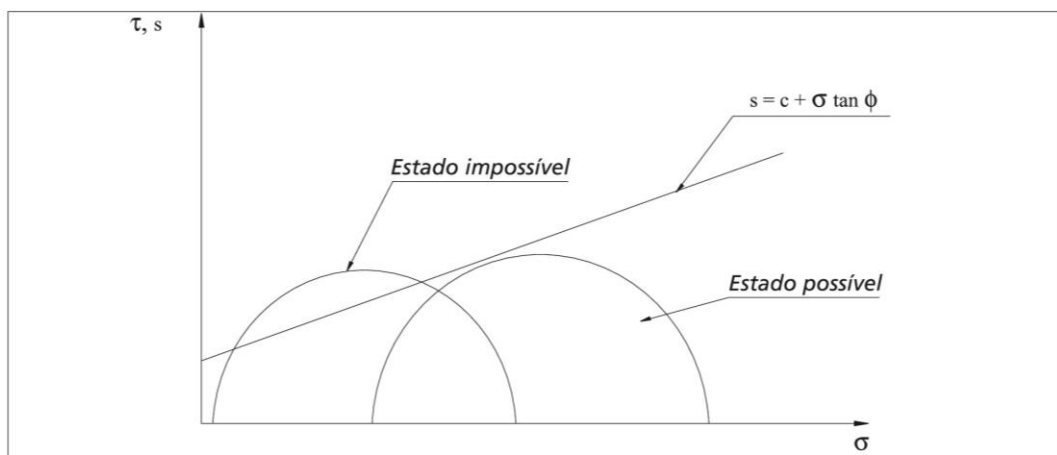


Figura 3.1.1 - Critério de Mohr-Coulomb

Assim, a coesão e o ângulo de atrito interno são os parâmetros da resistência ao cisalhamento do solo, segundo este critério de ruptura, e a sua determinação é fundamental na determinação do empuxo. Esta determinação pode ser feita por ensaios de laboratório, como o ensaio de cisalhamento direto e o ensaio de compressão triaxial. Podem também ser estimados a partir de ensaios de campo, ou mesmo a partir de outras características do material.

É importante notar que “c” e “ ϕ ” não são parâmetros intrínsecos do solo, mas parâmetros do modelo adotado como critério de ruptura. Além disso, o valor desses parâmetros depende de outros fatores, como teor de umidade, velocidade e forma de carregamento e condições de drenagem. Estes valores podem, inclusive, variar com o tempo, o que leva à conclusão de que o valor do empuxo também pode variar com o tempo. Isto torna a análise muito mais complexa e cabe ao projetista identificar o momento em que as condições do problema são mais desfavoráveis.

3.1.2 Cisalhamento dos solos não coesivos

Solos não coesivos são representados pelas areias e pedregulhos, também chamados de solos granulares. A resistência ao cisalhamento desses solos se deve principalmente ao atrito entre as partículas que os compõem. Assim, a envoltória de resistência pode ser expressa por:

$$s = \sigma \cdot \tan \phi$$

(02)

ou seja, a coesão “c” é nula, e o ângulo de atrito interno é o único parâmetro de resistência.

Os principais fatores que determinam o valor do ângulo de atrito interno “ ϕ ” são:

1. Compacidade: é o principal fator. Quanto maior a compacidade (ou menor índice de vazios), maior o esforço necessário para se romper a estrutura das partículas e, conseqüentemente, maior o valor de “ ϕ ”.

2. Granulometria: nas areias bem graduadas as partículas menores ocupam os vazios formados pelas partículas maiores, conduzindo a um arranjo mais estável, com maior resistência. Além disso, as areias mais grossas tendem a se dispor naturalmente de forma mais compacta, devido ao peso próprio de cada partícula. Isto faz com que, em geral, o valor de “ ϕ ” seja um pouco maior nas areias grossas e pedregulhos.

3. Forma das partículas: partículas mais arredondadas oferecem menos resistência do que partículas mais irregulares. Assim, estas últimas apresentam “ ϕ ” maior.

4. Teor de umidade: a umidade do solo tem pequena influência na resistência das areias. Isto se deve ao fato de a água funcionar como um lubrificante nos contatos entre as partículas, diminuindo o valor de “ ϕ ”. Além disso, quando a areia está parcialmente saturada, surgem tensões capilares entre as partículas, o que provoca o aparecimento de uma pequena coesão, chamada de coesão aparente. No entanto esta coesão desaparece quando o solo é saturado ou seco.

Na tabela 3.1.1 estão mostrados valores típicos do ângulo de atrito interno “ ϕ ” de alguns materiais granulares.

Solo	Ângulo de atrito efetivo [graus]	
	Fofo	Compacto
Pedra britada	36-40	40-50
Pedregulho de cava	34-38	38-42
Pedrisco (angular)	32-36	35-45
Areia de cava (subangular)	30-34	34-40
Areia de praia (arredondada)	28-32	32-38
Areia siltosa	25-35	30-36
Silte	25-35	30-35

Tabela 3.1.1 - Valores típicos de “ ϕ ” de alguns materiais

3.1.3 Cisalhamento dos solos coesivos

O comportamento dos solos argilosos no cisalhamento é muito mais complexo do que o dos solos granulares apresentados no item anterior. Isto se deve ao tamanho das partículas que compõem as argilas. Define-se como argila a fração do solo composta por partículas de tamanho menor que 0,002 mm. Nestas condições, a superfície específica, definida como a relação entre a superfície total de todas as partículas e o volume total dos sólidos, é muito maior no caso das argilas. Isto faz com que forças de superfície de natureza físico-químicas se tornem preponderantes no comportamento do solo. Estas forças dependem muito da distância entre as partículas. Assim, a resistência ao cisalhamento aumenta com o adensamento, quando as partículas são aproximadas umas das outras por efeito de um carregamento. Quando este carregamento é retirado, as forças de superfície impedem o retorno das partículas à situação anterior e surge então a coesão.

A presença de água nos vazios do solo argiloso também influencia muito a sua resistência. Isto se deve em parte ao fato de a água provocar um afastamento entre as partículas, diminuindo a coesão. Por outro lado, em solos argilosos parcialmente saturados, o efeito da sucção causada por forças de capilaridade tende a aumentar a coesão.

Outra característica importante ligada à presença de água, que influi no comportamento dos solos argilosos, é a sua baixa permeabilidade. Enquanto nas areias qualquer excesso de poro-pressão provocado pelo carregamento se dissipa quase imediatamente, no caso das argilas esta dissipação é muito mais lenta. Assim, a poro-pressão originada pelo carregamento continua agindo, mesmo após o término da construção, às vezes por anos. Distinguem-se, assim, duas situações extremas. A situação imediatamente posterior à aplicação da carga, quando pouca ou nenhuma dissipação de poro-pressão ocorreu, chamada de situação de curto prazo ou não drenada e aquela de longo prazo ou drenada, após a total dissipação de toda a poro-pressão causada pelo carregamento. O comportamento do solo em cada uma dessas duas condições é diferente, e o projeto deve levar em conta esta diferença.

A envoltória de resistência que representa a situação de curto prazo é denominada envoltória rápida ou não drenada " s_u ". Esta envoltória é utilizada na análise quando se admite que no campo não ocorreu qualquer dissipação da poro-pressão ocasionada pela carga aplicada sobre o solo. Além disso, admite-se também que o valor da poro-pressão que age no campo é semelhante ao que age nos ensaios de resistência e, portanto, não necessita ser determinado. No caso de solos saturados, a envoltória rápida não apresenta atrito:

$$s_u = c_u \quad (03)$$

onde " c_u " é chamada de coesão não drenada. Isto ocorre porque o aumento de pressão confinante não se traduz num aumento da resistência do solo já que sem drenagem não ocorre adensamento e então o aumento do confinamento é transferido para a água e se traduz num aumento igual da poro-pressão.

A tabela 3.1.2 mostra valores típicos da resistência não drenada " s_u " de argilas saturadas em função de sua consistência.

Consistência	s_u [kPa]	Características
Muito mole	0-10	Flui por entre os dedos quando a mão é fechada
Mole	10-20	Facilmente moldada pelos dedos
Firme	20-40	Moldada por forte pressão dos dedos
Rija	40-60	Deformada por forte pressão dos dedos
Muito rija	60-80	Pouco deformada por forte pressão dos dedos
Dura	> 80	Pouco deformada pela pressão de um lápis

Tabela 3.1.2 - Resistência não drenada " s_u " de argilas saturadas

Para solos parcialmente saturados, porém, há um aumento da resistência com o aumento do confinamento. Isto faz com que a envoltória " s_u " apresente uma parcela de atrito. Em geral se considera que a situação de saturação completa é mais crítica e, então, se despreza este atrito.

No outro extremo, a situação de longo prazo é caracterizada pela dissipação de toda a poro-pressão causada pela carga. A envoltória de resistência que representa essa situação é chamada de envoltória efetiva " s " e é utilizada para se analisar situações em que toda a poro-pressão causada pelo carregamento se dissipou. Neste caso a análise é feita em termos de tensões efetivas e é necessário determinar as poro-pressões devidas ao lençol freático, quando presente.

Em argilas normalmente adensadas e saturadas a envoltória efetiva " s " não apresenta coesão:

$$s' = \sigma' \cdot \tan \phi'$$

(04)

onde " σ " é a tensão normal efetiva e " ϕ " é o ângulo de atrito efetivo do solo. A tabela 3.1.3 mostra valores do ângulo de atrito efetivo " ϕ " de argilas em função do seu índice de plasticidade.

Índice de plasticidade [%]	ϕ [graus]
15	30
30	25
50	20
80	15

Tabela 3.1.3 - Ângulo de atrito efetivo " ϕ " de argilas

A coesão efetiva surge apenas nas argilas pré-adensadas, como efeito do sobreadensamento do solo. Para pressões confinantes abaixo da pressão de pré-adensamento, a resistência ao cisalhamento é superior à da argila normalmente adensada. Ao se aproximar esta envoltória de uma reta num intervalo de tensões de trabalho que inclui tensões abaixo da pressão de pré-adensamento, a envoltória efetiva fica:

$$s' = c' + \sigma' \cdot \tan' \phi'$$

onde “c” é a coesão efetiva.

Na determinação de empuxos atuantes sobre estruturas de arrimo, em geral é mais indicada a análise em termos de tensões efetivas, utilizando-se a envoltória de resistência efetiva do solo. Isto porque a hipótese de empuxo ativo caracteriza um descarregamento do solo, e a situação de longo prazo é, em geral, mais desfavorável. Dessa forma, mesmo no caso de maciços formados por solos argilosos, a coesão efetiva é muito pequena, ou mesmo nula. Assim, é comum desprezar-se completamente a coesão no cálculo do empuxo ativo sobre estruturas de arrimo.

3.2 Percolação d'água e drenagem

A presença de água no solo influencia o comportamento das estruturas de contenção de várias maneiras. Em primeiro lugar, os parâmetros de resistência ao cisalhamento do solo, em particular a coesão, diminuem quando a umidade aumenta. Também o peso específico do solo é aumentado pela presença de água nos vazios.

Além dessas influências, a pressão na água altera o valor do empuxo que atua sobre a estrutura. Como exemplo, veja a estrutura esquematizada na figura 3.2.1. Trata-se de um muro de arrimo que suporta um maciço saturado por efeito de chuvas intensas. Como a estrutura é impermeável e na base desse maciço há uma camada também impermeável, não há drenagem da água e, assim, esta exerce pressões hidrostáticas sobre o muro. Estas pressões podem, em muitos casos, superar o próprio empuxo exercido pelo solo.

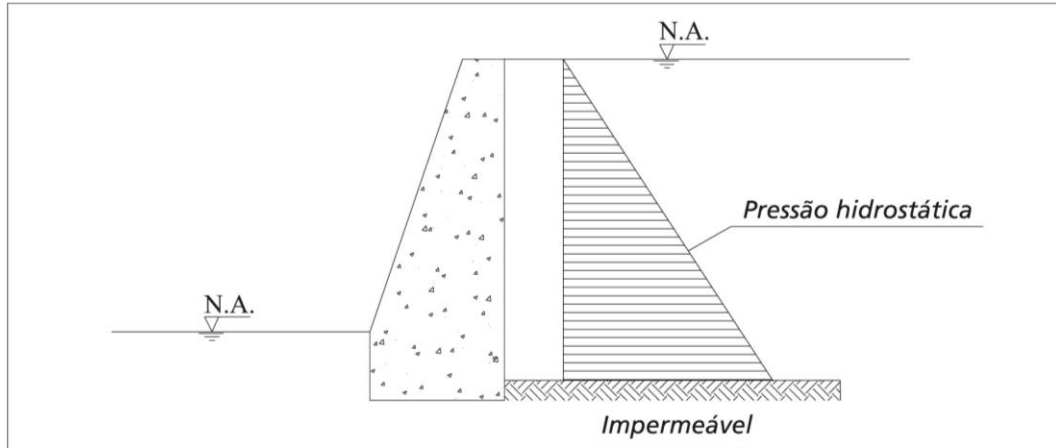


Figura 3.2.1 - Muro de arrimo sob a ação de um maciço saturado

Caso não haja a camada impermeável na base do maciço arrimado, a água irá percolar através dos vazios do solo e, então, a distribuição de pressões deixará de ser hidrostática. Além disso, no caso de estruturas de arrimo em gabiões, o próprio muro é permeável e, assim, a água também percola através dele.

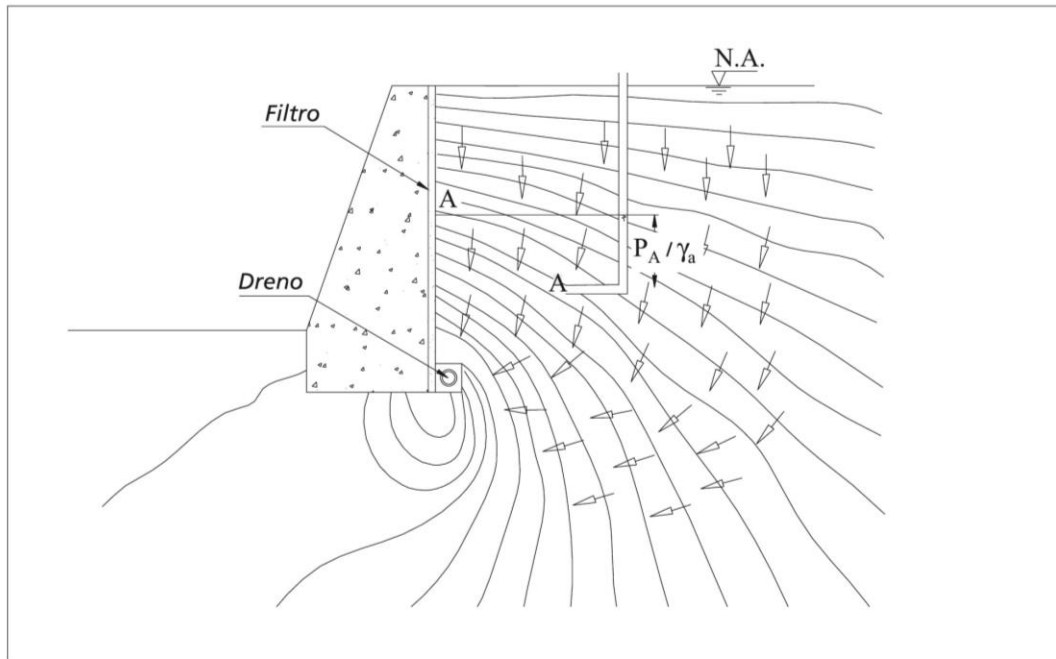


Figura 3.2.2 - Estrutura de arrimo com sistema de drenagem vertical

A pressão da água sobre a estrutura de arrimo, neste caso, é completamente eliminada como mostrado na figura 3.2.2. Neste caso há percolação de água através do solo e do muro. Foram traçadas equipotenciais com o auxílio de um programa de elementos finitos. As equipotenciais são curvas de mesma carga hidráulica total, que, por sua vez, resulta da soma das cargas altimétrica e piezométrica. Esta última expressa a pressão da água no interior do solo.

Ao longo do contato solo-estrutura a carga piezométrica é nula. No interior do maciço, porém, a água ainda estará sob pressão. Para se determinar a carga piezométrica em um ponto "A" qualquer no interior do maciço basta tomar a equipotencial que passa por esse ponto e localizar o ponto "A" no extremo dessa equipotencial onde a carga piezométrica é nula. A carga piezométrica em "A" é dada pela diferença de cota entre os pontos "A" e "A". Isto porque a carga hidráulica total, que é a soma das cargas piezométrica e altimétrica, é a mesma em "A" e "A".

Mesmo não atuando diretamente sobre a estrutura, a pressão da água no interior do maciço influencia o empuxo, aumentando seu valor.

3.3 Coeficientes de segurança

O projeto de estruturas em geral visa a estabelecer segurança contra a ruptura e contra a deformação excessiva. No projeto são utilizados, então, estados limites a fim de estabelecer esta segurança. Estados limites são definidos como estados além dos quais a estrutura não mais satisfaz aos requisitos de estabilidade e usabilidade impostos pelo projeto. Estes estados limites são classificados em:

- 1. Estado limite último:** define o ponto a partir do qual ocorre a ruína da estrutura de contenção, quer por ruptura do maciço, quer por ruptura dos elementos que compõem a própria estrutura.
- 2. Estado limite de utilização:** define o ponto de máxima deformação aceitável, em termos de utilização, tanto para a estrutura, quanto para o solo.

A segurança da estrutura de contenção pode ser definida genericamente como a "distância mínima" que a estrutura se encontra desses estados limites. Normalmente esta segurança é expressa em termos de coeficientes adimensionais que relacionam o estado atual da estrutura aos estados limites.

Há duas formas gerais de se estabelecer estes coeficientes de segurança:

1. Coeficientes de segurança global: os estados limites são determinados com base nos parâmetros reais de resistência e de solicitação do conjunto, e os coeficientes de segurança são definidos como a relação entre a resistência total disponível contra uma dada condição de colapso e a resistência efetivamente mobilizada para se contrapor a esta condição. Os valores mínimos dos coeficientes de segurança global a serem satisfeitos pela estrutura são definidos com base na prática de projeto.

2. Coeficientes de segurança parcial: aos parâmetros de resistência e de solicitação são aplicados coeficientes de segurança no sentido de minorar (no caso da resistência) ou majorar (no caso da solicitação) seus valores. Os estados limites obtidos com a utilização destes parâmetros modificados são impostos como condição limite para o estado atual da estrutura. Os valores dos coeficientes de segurança parcial são estabelecidos com base em estudos estatísticos da dispersão dos valores dos parâmetros a que são aplicados.

No caso do projeto de estruturas de contenção, os coeficientes de segurança global são tradicionalmente mais utilizados. No entanto, a utilização de coeficientes de segurança parcial tem aumentado, e muitos países têm adotado este tipo de análise em seus códigos de projeto.

3.4 Determinação do empuxo

3.4.1 Conceitos básicos

Empuxo de terra é a resultante das pressões laterais exercidas pelo solo sobre uma estrutura de arrimo ou de fundação. Estas pressões podem ser devido ao peso próprio do solo ou a sobrecargas aplicadas sobre ele.

O valor do empuxo sobre uma estrutura depende fundamentalmente da deformação que esta sofre sob a ação deste empuxo. Pode-se visualizar esta interação efetuando-se um experimento que utiliza um anteparo vertical móvel, como mostrado na figura 3.4.1, suportando um desnível de solo. Verifica-se que a pressão exercida pelo solo sobre o anteparo varia com o deslocamento deste último.

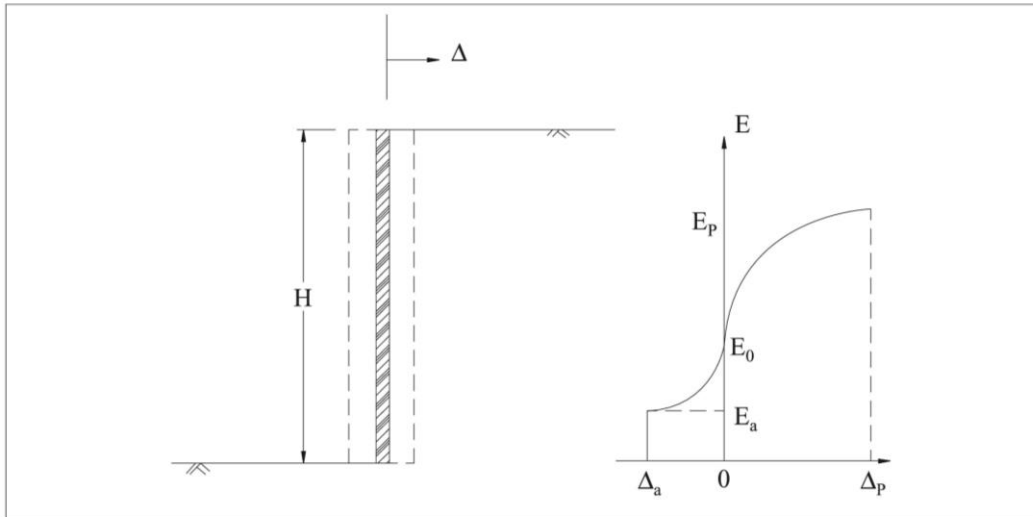


Figura 3.4.1 - Empuxo sobre um anteparo

Quando o anteparo se afasta do solo arrimado, há uma diminuição do empuxo até um valor mínimo que corresponde à total mobilização da resistência interna do solo. Esta condição é atingida mesmo com um pequeno deslocamento do anteparo e é chamada de estado ativo. O empuxo atuante neste instante então é chamado empuxo ativo “ E_a ”.

Se ao contrário, o anteparo for movido contra o solo arrimado, haverá um aumento no empuxo até um valor máximo onde haverá novamente a mobilização total da resistência do solo. A este valor máximo é dado o nome de empuxo passivo “ E_p ”, e a condição de deformação em que ocorre é chamada estado passivo. Diferentemente do estado ativo, o estado passivo só é atingido após um deslocamento bem maior do anteparo.

Caso o anteparo, porém, se mantenha imóvel na posição inicial, o empuxo em repouso “ E_0 ”, se manterá entre os valores do empuxo ativo e do empuxo passivo. Nesta condição não há uma completa mobilização da resistência do solo.

Na tabela 3.4.1 estão mostrados valores típicos do deslocamento “ Δ ” da estrutura necessários para se alcançar a completa mobilização da resistência do solo e se alcançar os estados ativo e passivo. Verifica-se que para se alcançar o estado passivo é necessário um deslocamento dez vezes superior ao necessário para o estado ativo.

Tipo de solo	Valores de Δ / H	
	Ativo	Passivo
Areia compactada	0,001	-0,01
Areia mediamente compactada	0,002	-0,02
Areia fofa	0,004	-0,04
Silte compactado	0,002	-0,02
Argila compactada	0,01	-0,05

Tabela 3.4.1 - Valores de Δ/H necessários para se alcançar os estados ativos e passivos para vários tipos de solos

Os muros de arrimo de gravidade, em geral, e em particular os flexíveis, caso dos construídos com gabiões, permitem a deformação do solo arrimado suficiente para que sua resistência seja totalmente mobilizada. Assim, devem ser dimensionados sob a ação do empuxo ativo.

O problema da determinação da magnitude e distribuição da pressão lateral do solo é, porém, estaticamente indeterminado e são necessárias hipóteses entre a relação entre as tensões e as deformações do solo para que se possa chegar à solução.

Os métodos clássicos empregados na geotecnia na determinação dos empuxos ativos ou passivos adotam uma relação do tipo rígido-plástica entre as tensões e deformações do solo. Este modelo apresenta a vantagem de dispensar o cálculo dos deslocamentos da estrutura, já que qualquer deformação é suficiente para se alcançar a plastificação do material.

Como critério de plastificação, é empregado quase que exclusivamente o critério de Mohr-Coulomb. Segundo este critério, a tensão cisalhante " τ " ao longo de uma superfície de ruptura deve se igualar à resistência " s " que é dada por:

$$s = c + \sigma \cdot \tan \phi \quad (06)$$

onde: " σ " é a tensão normal que age sobre a superfície de ruptura e " c " e " ϕ " são constantes características do solo conhecidas como coesão e ângulo de atrito interno.

No desenvolvimento da solução, geralmente são tomadas fatias unitárias do maciço e da estrutura de arrimo, admitindo-se que todas as seções são iguais, o que equivale a se aproximar a um problema bidimensional de deformação. Esta aproximação simplifica bastante a análise e, além disso, é em geral mais conservativa que a análise tridimensional.

Quanto ao empuxo em repouso "E₀", que age sobre estruturas que não permitem qualquer deslocamento, sua determinação é feita normalmente através de expressões empíricas, baseadas na determinação, em laboratório ou no campo, das pressões laterais. A expressão mais utilizada está baseada nas teorias de Jàky [7], e, neste caso, é dada por:

$$K_0 = p_0/p_v = 1 - \text{sen } \phi \quad (07)$$

onde "p₀" é a pressão lateral em repouso, "p_v" é a pressão vertical atuante e "K₀" é denominado coeficiente de empuxo em repouso. Esta expressão é válida apenas para solos normalmente adensados. Para solos pré-adensados o valor da pressão lateral é mais elevado, dependendo principalmente do grau de pré-adensamento do material.

3.4.2 Teoria de Rankine

Ao analisar o estado de tensão de um elemento de solo localizado a uma profundidade "z" junto ao anteparo da figura 3.4.2, pode-se determinar a tensão vertical "σ_v" dada por:

$$\sigma_v = \gamma \cdot z \quad (08)$$

Onde "γ" é o peso específico do solo.

Enquanto o anteparo permanece em repouso, a tensão horizontal atuante sobre o elemento é indeterminada. Mas ao ser afastado do solo, até a formação do estado ativo, esta tensão pode ser determinada a partir da envoltória de resistência do material, como mostrado na figura 3.4.2.

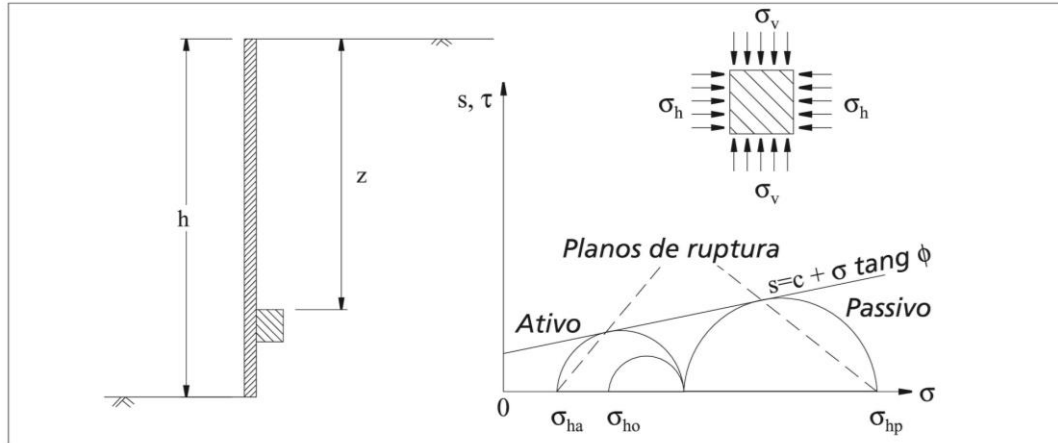


Figura 3.4.2 - Determinação da pressão lateral

Neste instante a tensão horizontal “ σ_h ” é dada por:

$$\sigma_h = K_a \cdot \gamma \cdot z - 2 \cdot c \cdot \sqrt{K_a} \quad (09)$$

Onde:

$$K_a = \tan^2 \left(\frac{\pi}{4} - \frac{\phi}{2} \right) = \frac{1 - \text{sen } \phi}{1 + \text{sen } \phi} \quad (10)$$

Sendo “ K_a ” denominado coeficiente de empuxo ativo.

Através desse resultado pode-se determinar o valor do empuxo ativo resultante “ E_a ” sobre o anteparo:

$$E_a = \frac{1}{2} \cdot \gamma \cdot H^2 \cdot K_a - 2 \cdot c \cdot H \cdot \sqrt{K_a} \quad (11)$$

Onde “ H ” é a altura total do desnível de solo.

No caso de o anteparo se mover contra o solo até o estado passivo, obtém-se:

$$\sigma_h = K_p \cdot \gamma \cdot z + 2 \cdot c \cdot \sqrt{K_p} \quad (12)$$

Onde:

$$K_p = \tan^2 \left(\frac{\pi}{4} + \frac{\phi}{2} \right) = \frac{1 + \sin \phi}{1 - \sin \phi} \quad (13)$$

É denominado coeficiente de empuxo passivo, e o empuxo resultante “E_p” é dado por:

$$E_p = \frac{1}{2} \cdot \gamma \cdot H^2 \cdot K_p - 2 \cdot c \cdot H \sqrt{K_p} \quad (14)$$

Verifica-se por esses resultados que o solo coesivo fica sujeito a tensões de tração na sua porção superior no estado ativo. Estas tensões de tração se prolongam até uma profundidade “z₀” dada por:

$$z_0 = \frac{2 \cdot c}{\gamma} \cdot \frac{1}{\sqrt{K_a}} \quad (15)$$

Ocorre, porém, que o solo normalmente não resiste a tensões de tração. Assim, abrem-se fendas na superfície até esta profundidade. Sendo assim, não se pode contar com estas tensões que diminuiriam o valor do empuxo ativo resultante. Além disso, estas fendas podem estar preenchidas com água proveniente de chuvas, o que pode aumentar ainda mais o valor do empuxo. O resultado é a distribuição de tensões mostrada na figura 3.4.3. Pode-se adotar para efeito de cálculo uma distribuição aproximada como a mostrada na mesma figura e sugerida por Bowles [8].

Estas tensões de tração não ocorrem, porém, no estado passivo, como se pode ver na figura 3.4.3. Assim, não há a formação de fendas de tração no estado passivo.



Figura 3.4.3 - Distribuição de " σ_h " no estado ativo e passivo (solo coesivo)

As direções das superfícies de ruptura nos estados ativo e passivo são dadas pelo gráfico da figura 3.4.1 e mostradas na figura 3.4.4.

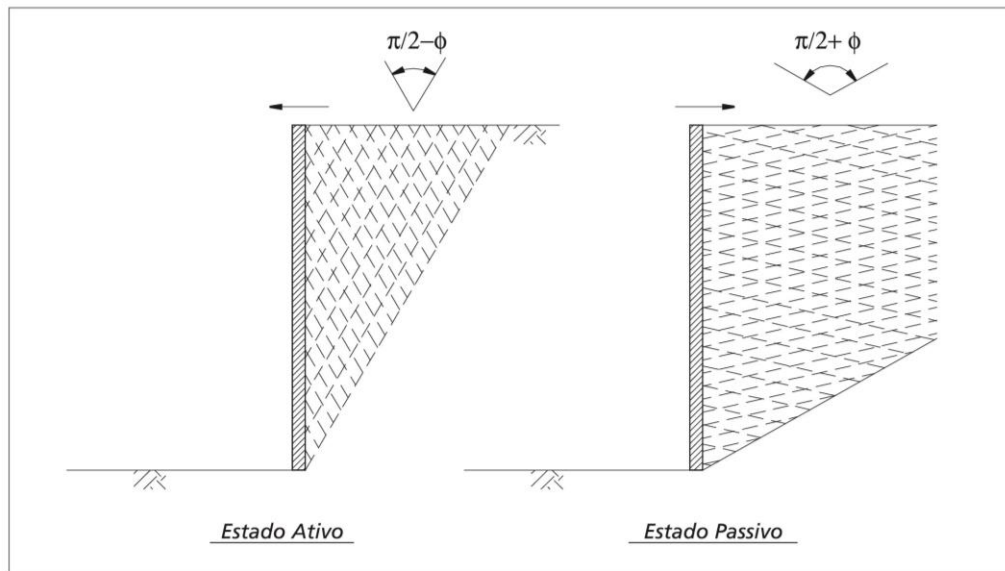


Figura 3.4.4 - Planos de ruptura nos estados ativo e passivo.

Caso a superfície do solo não seja horizontal, exibindo uma inclinação "i", o valor da pressão vertical " p_v " será dado por (figura 3.4.5):

$$p_v = \gamma \cdot z \cdot \cos i \quad (16)$$

Como a tensão vertical " P_v " possui uma obliquidade " i " em relação à superfície do elemento de solo mostrado, esta pode ser decomposta em uma tensão normal " σ " e uma tensão de cisalhamento " τ " :

$$\sigma = p_v \cdot \cos i = \gamma \cdot z \cdot \cos^2 i \quad (17)$$

e

$$\tau = p_v \cdot \sin i = \gamma \cdot z \cdot \sin i \cdot \cos i \quad (18)$$

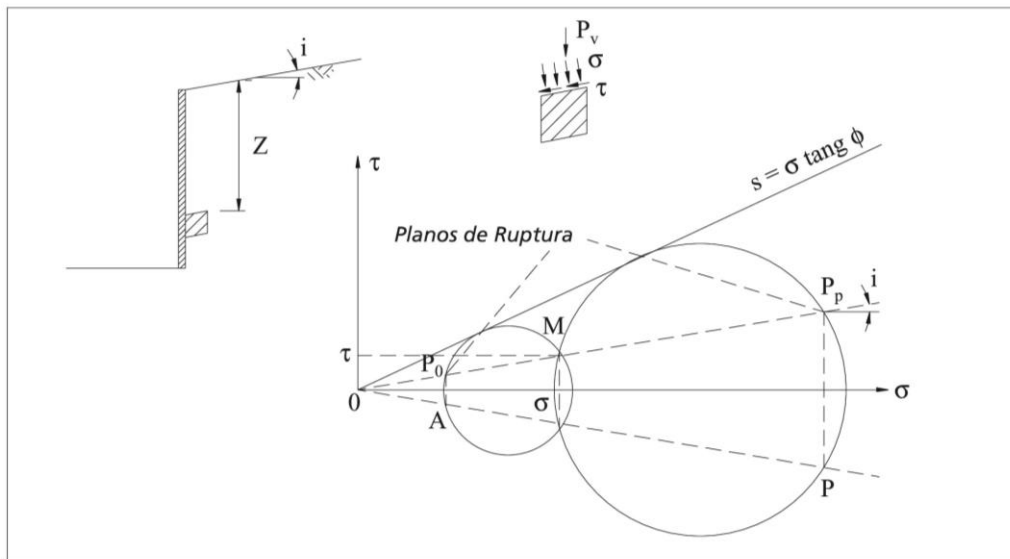


Figura 3.4.5 - Determinação da pressão lateral para " $i \neq 0$ " ($c=0$).

Na figura 3.4.5 estão mostrados os círculos de Mohr correspondentes aos estados ativo e passivo, para o caso de um solo não coesivo " $c = 0$ ". Dali pode-se verificar que a pressão lateral " p_l " sobre o anteparo possui uma obliquidade " i " nos dois estados e que a relação entre esta e a pressão vertical é dada por:

$$\frac{P_{la}}{P_v} = \frac{OA}{OM} = \frac{\cos i - \sqrt{\cos^2 i - \cos^2 \phi}}{\cos i + \sqrt{\cos^2 i - \cos^2 \phi}} = K_a \quad (19)$$

para o caso ativo e

$$\frac{P_{lp}}{P_v} = \frac{\overline{OP}}{\overline{OM}} = \frac{\cos i + \sqrt{\cos^2 i - \cos^2 \phi}}{\cos i - \sqrt{\cos^2 i - \cos^2 \phi}} = K_p \quad (20)$$

para o caso passivo.

Portanto, as pressões laterais e os empuxos ativo e passivo serão dados por:

$$p_{la} = \gamma \cdot H \cdot K_a \cdot \cos i \quad (21)$$

$$E_a = \frac{1}{2} \cdot \gamma \cdot H^2 \cdot K_a \cdot \cos i \quad (22)$$

e

$$p_{lp} = \gamma \cdot H \cdot K_p \cdot \cos i \quad (23)$$

$$E_p = \frac{1}{2} \cdot \gamma \cdot H^2 \cdot K_p \cdot \cos i \quad (24)$$

Em ambos os casos a direção do empuxo será paralela à da superfície do solo arrimado.

Para o caso de solo coesivo, não há uma expressão analítica simples quando a superfície do solo não é horizontal, sendo necessária a determinação da pressão lateral graficamente com o uso dos círculos de Mohr correspondentes aos estados ativo e passivo, ou se desenvolvendo as equações analíticas correspondentes. Para isto utiliza-se a construção mostrada na figura 3.4.6.

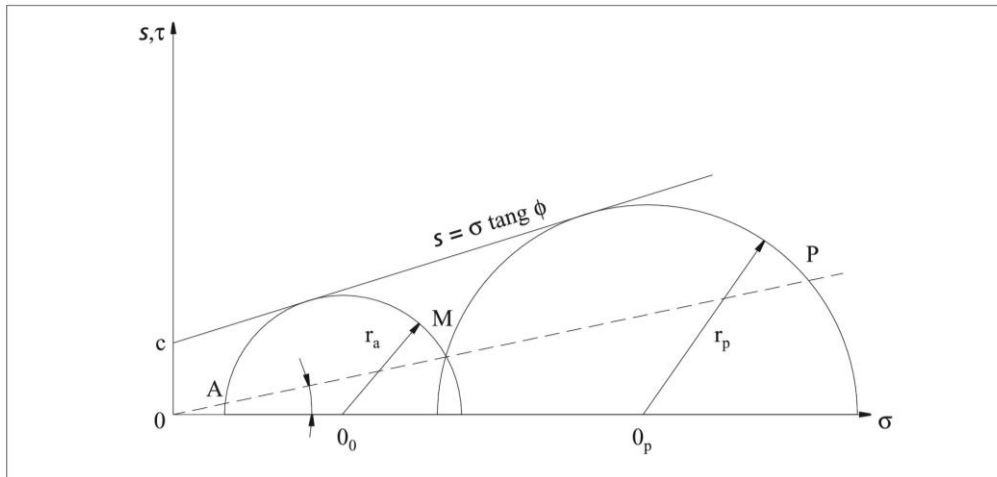


Figura 3.4.6 - Determinação das pressões laterais para solos coesivos

Inicialmente determina-se o ponto "M" dado por:

$$\sigma_M = \gamma \cdot z \cdot \cos^2 i \quad (25)$$

$$\tau_M = \gamma \cdot z \cdot \sin i \cdot \cos i \quad (26)$$

O centro "O" e o raio "r" do círculo que passa por "M" e é tangente à envoltória de resistência são dados por:

$$O = \frac{\phi_M \cdot \tan^2 \phi + c \cdot (\sin^2 \phi \cdot \tan \phi) \pm \sqrt{\Delta}}{1 - \cos^2 \phi} \quad (27)$$

$$r = \left(O + \frac{c}{\tan \phi} \right) \cdot \sin \phi \quad (28)$$

$$\overline{OM} = p_v = \gamma \cdot z \cdot \cos i \quad (29)$$

onde o sinal positivo se refere ao estado passivo e o sinal negativo, ao estado ativo e:

$$\Delta = 2.c.\sigma_M.\tan^3 \sigma.\text{sen}^2 \sigma + c^2.\tan^2 \sigma.\text{sen}^2 \sigma - \tau_M^2.\tan^4 \sigma + (\sigma_M^2 + \tau_M^2).\text{sen}^2 \sigma.\tan^4 \sigma \quad (30)$$

As coordenadas dos pontos "A" e "P" serão dadas, finalmente, por:

$$\sigma_A = 0.\cos^2 i - \cos i.\sqrt{(r^2 - 0^2 + 0^2.\cos^2 i)} \quad (31)$$

$$\tau_A = \sigma_A.\tan i \quad (32)$$

$$\sigma_p = 0.\cos^2 i - \cos i.\sqrt{(r^2 - 0^2 + 0^2.\cos^2 i)} \quad (33)$$

$$\tau_p = \sigma_p.\tan i \quad (34)$$

$$r = \sqrt{(\sigma_A - 0)^2 + \tau_A^2} \quad (35)$$

$$\tau_A = \sigma_A.\tan \alpha \quad (36)$$

Os valores das pressões laterais ativa e passiva, para a profundidade "z", serão dados por:

$$p_{la} = \overline{0A} = \sqrt{\sigma_A^2 + \tau_A^2} \quad (37)$$

$$p_{lp} = \overline{0P} = \sqrt{\sigma_p^2 + \tau_p^2} \quad (38)$$

Também neste caso ocorrem fendas de tração no estado ativo até a profundidade "Z₀" dada por:

$$z_0 = \frac{2.c}{\gamma} \cdot \frac{1}{\tan\left(\frac{\pi}{4} - \frac{\sigma}{2}\right)} \quad (39)$$

Quando há sobrecarga uniforme "q" sobre o maciço, seu efeito sobre o anteparo é dado por um aumento constante da pressão lateral que, assim, ficará:

$$p_{la} = (\gamma.z + q).K_a.\cos i \quad (40)$$

$$p_{la} = (\gamma.z + q).K_q.\cos i \quad (41)$$

Portanto os empuxos ativo e passivo, neste caso, são dados por:

$$E_a = \frac{1}{2} \cdot \gamma.H^2.K_a.\cos i + q.H.K_a.\cos i \quad (42)$$

$$E_p = \frac{1}{2} \cdot \gamma.H^2.K_p.\cos i + q.H.K_p.\cos i \quad (43)$$

O ponto de aplicação do empuxo, em todos esses casos, está localizado no centro de gravidade dos diagramas de pressão lateral descritos. Assim, no caso de solo não coesivo e sobrecarga nula, o diagrama de pressão lateral é triangular, e o ponto de aplicação do empuxo, tanto ativo como passivo, está localizado a uma altura igual a "H/3" da base do anteparo.

3.4.3 Teoria de Coulomb

Outra maneira de se quantificar o empuxo ativo ou o passivo sobre uma estrutura de arrimo é se admitir que no instante da mobilização total da resistência do solo formam-se superfícies de deslizamento ou de ruptura no interior do maciço. Estas superfícies

delimitariam então uma parcela do maciço que se movimentaria em relação ao restante do solo no sentido do deslocamento da estrutura. Se esta parcela do solo for considerada como um corpo rígido, o empuxo pode então ser determinado do equilíbrio das forças atuantes sobre este corpo rígido.

O método de Coulomb admite que tais superfícies de ruptura são planas e o empuxo é aquele que age sobre a mais crítica das superfícies de ruptura planas.

A vantagem deste método reside no fato de que se pode considerar a ocorrência de atrito entre a estrutura de arrimo e o solo, além de possibilitar a análise de estruturas com o paramento não vertical.

Para o caso de solo não coesivo, as forças que agem sobre a cunha de solo formada no estado ativo estão mostradas na figura 3.4.7. Estas forças são o seu peso próprio "P", a reação do maciço "R", que devido ao atrito interno do solo tem uma obliquidade "φ" em relação à superfície de ruptura, e o empuxo ativo "E_a", que exibe também uma obliquidade "δ" em relação ao paramento da estrutura de arrimo. Esta última obliquidade é o ângulo de atrito entre o solo e a estrutura de arrimo. A superfície potencial de ruptura forma um ângulo "ρ" com a direção horizontal.

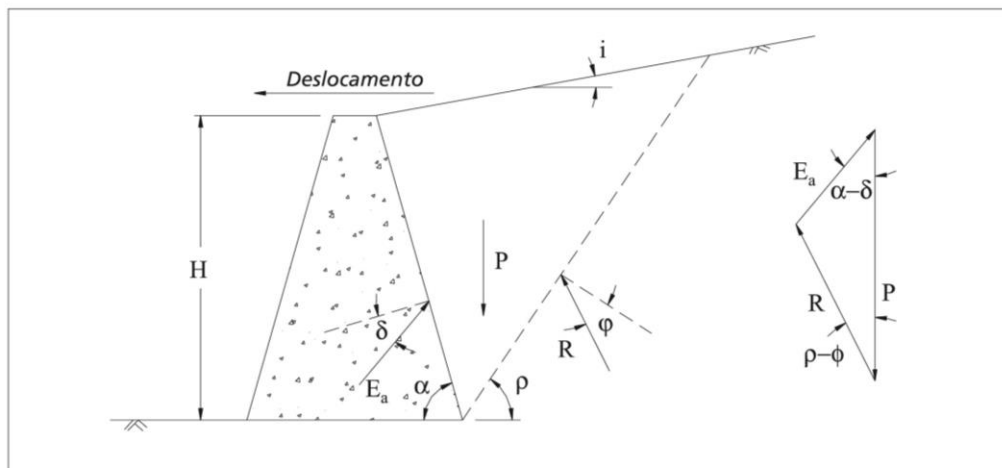


Figura 3.4.7 - Forças que agem sobre a cunha de solo no caso ativo

O valor do peso próprio é:

$$P = \frac{\gamma \cdot H^2}{2 \cdot \text{sen}^2 \alpha} \cdot \left[\text{sen}(\alpha + \rho) \cdot \frac{\text{sen}(\alpha + i)}{\text{sen}(\rho - i)} \right] \quad (44)$$

O empuxo ativo pode ser determinado a partir do equilíbrio de forças:

$$\frac{E_a}{\text{sen}(\rho - \phi)} = \frac{P}{\text{sen}(\pi - \alpha - \rho + \phi + \delta)} \quad (45)$$

ou

$$E_a = \frac{P \cdot \text{sen}(\rho - \phi)}{\text{sen}(\pi - \alpha - \rho + \phi + \delta)} \quad (46)$$

A superfície mais crítica, no caso ativo, é aquela que leva o valor de “E_a” a um máximo, ou seja, é obtida da derivada da expressão anterior em relação ao ângulo da superfície de ruptura “ρ”:

$$\frac{dE_a}{d\rho} = 0 \quad (47)$$

Daí se obtém o valor máximo de “E_a”:

$$E_a = \frac{1}{2} \cdot \gamma \cdot H^2 \cdot K_a \quad (48)$$

onde:

$$K_a = \frac{\text{sen}^2(\alpha + \phi)}{\text{sen}^2 \alpha \cdot \text{sen}(\alpha - \delta) \cdot \left[1 + \sqrt{\frac{\text{sen}(\phi + \delta) \cdot \text{sen}(\phi - i)}{\text{sen}(\alpha - \delta) \cdot \text{sen}(\alpha + i)}} \right]^2} \quad (49)$$

No estado passivo há uma inversão nas obliquidades das forças “R” e “E_p” devido à inversão no sentido do deslocamento da estrutura, e a superfície mais crítica é aquela que leva “E_p” a um valor mínimo (figura 3.4.8).

da sobrecarga que ocorre sobre a cunha de solo delimitada pela superfície de ruptura (figura 3.4.9). Esta parcela "Q" se somará ao peso da cunha "P" e, assim, provocará um aumento proporcional nas outras forças que agem sobre a cunha.

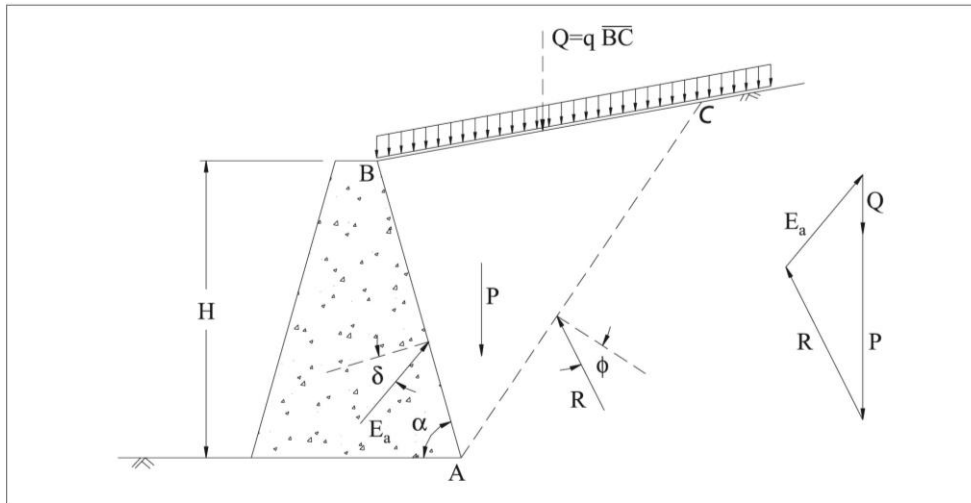


Figura 3.4.9 - Empuxo devido à sobrecarga distribuída uniforme

Então, o empuxo "E_a" será dado por:

$$E_a = \frac{1}{2} \cdot \gamma \cdot H^2 \cdot K_a \cdot \text{sen } i + q \cdot H \cdot K_a \cdot \frac{\text{sen } \alpha}{\text{sen } (\alpha + i)}$$

(52)

Dessa expressão percebe-se que o efeito da sobrecarga distribui-se de maneira uniforme ao longo do paramento, o que permite a determinação do ponto de aplicação do empuxo sobre a estrutura de arrimo. A primeira parcela da expressão acima " $\frac{1}{2} \cdot \gamma \cdot H^2 \cdot K_a$ " é devida apenas ao solo, e, portanto, está aplicada a "H/3" da base da estrutura, enquanto a segunda parcela " $q \cdot H \cdot K_a \cdot \frac{\text{sen } \alpha}{\text{sen } (\alpha + i)}$ " é devida à sobrecarga e estará aplicada a uma altura igual a "H/2". O ponto de aplicação do empuxo total pode, então, ser obtido do centro de gravidade das duas parcelas.

3.4.4 Método de Equilíbrio Limite

Caso o solo seja coesivo ou a superfície do maciço não seja plana, não há como aplicar diretamente a teoria de Coulomb. Nestes casos pode-se adotar um método de análise semelhante ao de Coulomb, mas voltado ao problema específico em questão.

Tome-se como exemplo o caso mostrado na figura 3.4.10. Como a superfície do maciço não possui uma inclinação "i" constante, não é possível se utilizar as expressões deduzidas no item anterior para a determinação do empuxo. Neste caso, pode-se fazer uma análise por tentativas. Consideram-se várias posições para a superfície de ruptura e para cada uma delas determina-se o valor do empuxo pelo equilíbrio de forças. Estes valores são colocados em função da superfície de ruptura que lhes deu origem e assim pode-se estimar a variação correspondente. Pode-se então determinar a posição mais crítica da superfície de ruptura e o empuxo correspondente.

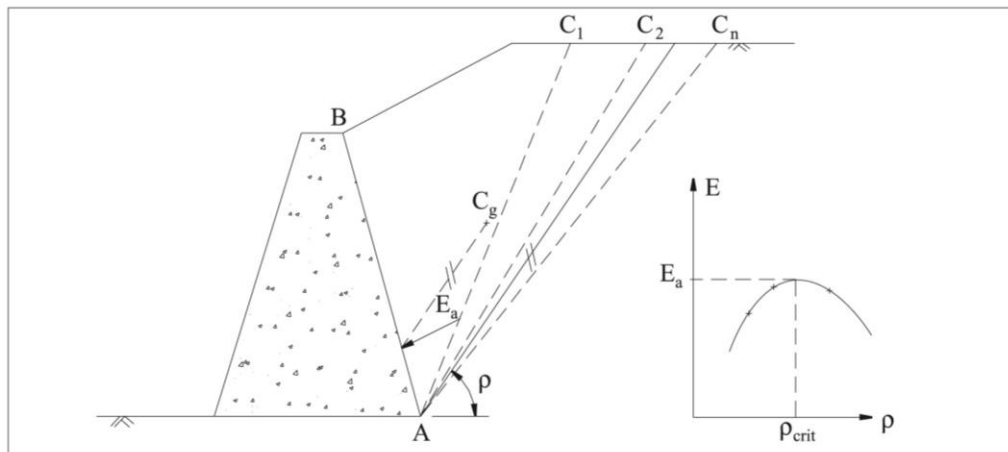


Figura 3.4.10 - Método do equilíbrio limite

O ponto de aplicação do empuxo sobre a estrutura de arrimo é determinado através de uma paralela à superfície de ruptura mais crítica, passando pelo centro de gravidade da cunha crítica.

A vantagem deste método se encontra na grande variedade de casos que podem ser analisados, tais como solo coesivo, ocorrência de sobrecargas não uniformes sobre o maciço, de pressões neutras no interior do solo, etc.

Porém, para se determinar o empuxo aplicado por um maciço composto de camadas de solos com características diferentes, é necessária a extensão deste método, de modo que se considere superfícies de ruptura formadas por mais de um plano e, portanto, formando mais de uma cunha de solo.

3.4.5 Efeito de sobrecargas no empuxo ativo

Muitas vezes ocorrem sobrecargas sobre o solo arrimado. Essas sobrecargas provêm de várias fontes tais como estruturas construídas sobre o maciço, tráfego de veículos, etc. e provocam um aumento no empuxo.

O caso mais simples de sobrecarga é a carga uniforme distribuída sobre o maciço (figura 3.4.11). Na análise pelo método do equilíbrio limite, deve ser adicionada ao peso da cunha de solo formada pela superfície de ruptura a porção da carga distribuída que se encontra sobre ela.

Quanto ao ponto de aplicação do empuxo resultante, pode-se obtê-lo através de uma paralela à superfície de ruptura passando pelo centro de gravidade do conjunto solo-sobrecarga. Outra alternativa é se separar o efeito do solo do efeito da sobrecarga e determinar o ponto de aplicação de cada parcela através de paralelas pelos centros de gravidade de cada parcela.

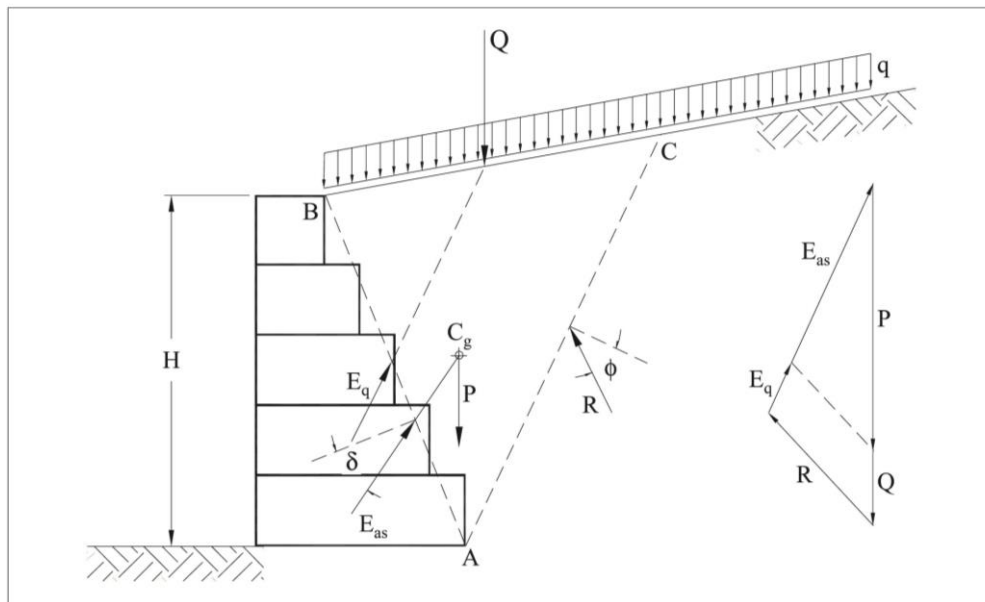


Figura 3.4.11 - Carga uniforme sobre o maciço

Caso as condições do problema permitam a utilização direta da teoria de Coulomb, o efeito da sobrecarga uniformemente distribuída pode ser determinado de acordo com as expressões do item 3.4.3.

Outro caso bastante comum de sobrecarga é o da linha de carga "Q" paralela à estrutura de arrimo como na figura 3.4.12

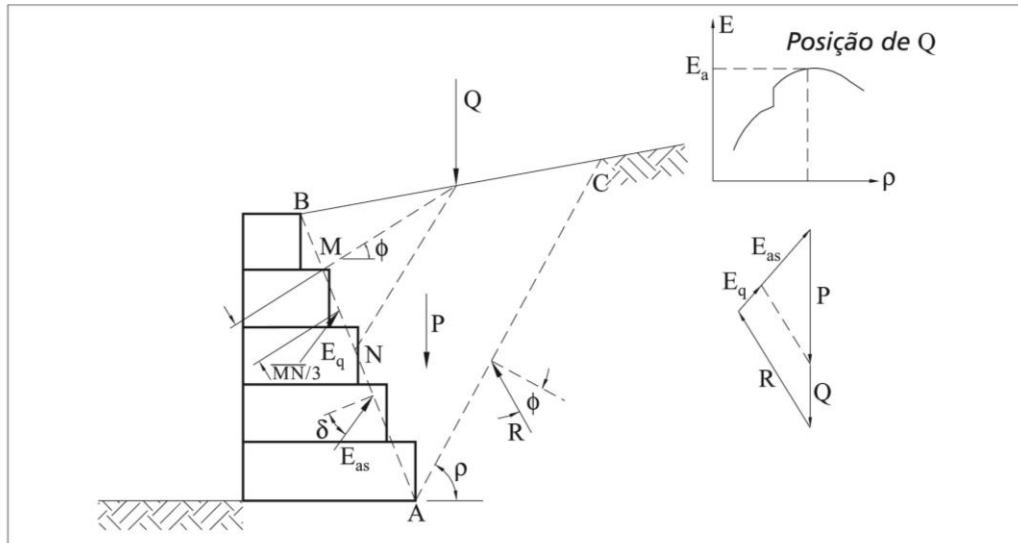


Figura 3.4.12 - Linha de carga paralela à estrutura de arrimo

Neste caso, ao se utilizar o método do equilíbrio limite, deve-se adicionar o valor de “Q” ao peso da cunha de solo apenas no caso de a superfície de ruptura terminar num ponto posterior ao ponto de aplicação da linha de carga. Assim, a variação do empuxo com a posição da superfície de deslizamento apresentará uma descontinuidade no ponto correspondente à posição de “Q”.

Também neste caso deve-se separar do empuxo máximo “E_a” os efeitos do solo “E_{as}” e o efeito da linha de carga “E_q”. O ponto de aplicação deste último é determinado segundo as teorias de Terzaghi & Peck [9] conforme mostrado na figura 3.4.12.

Outra alternativa na determinação do efeito da linha de carga sobre o empuxo é pela utilização de equações da teoria da elasticidade obtidas por Boussinesq [10]. Por este método, determina-se separadamente o empuxo devido ao solo, ignorando-se a presença da linha de carga. O efeito da carga é simplesmente adicionado ao do solo, sendo determinado pela teoria da elasticidade:

$$\sigma_h = \frac{2 \cdot Q}{\pi \cdot H} \cdot \frac{m^2 \cdot n}{(m^2 \cdot n^2)^2} \quad (53)$$

onde “σ_h” é o acréscimo da pressão horizontal devida à linha de carga “Q” e “H”, “m” e “n” estão indicados na figura 3.4.13.

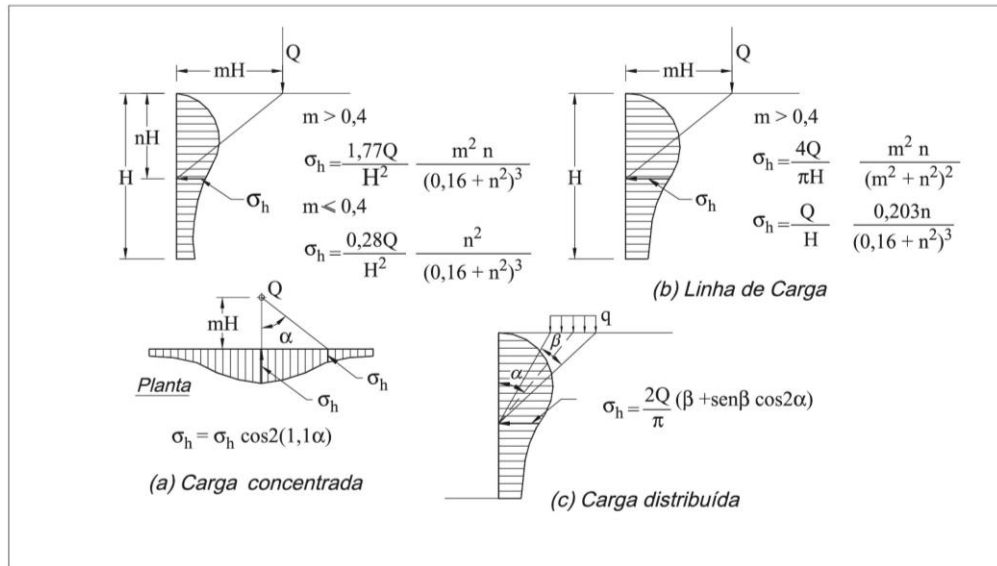


Figura 3.4.13 - Efeito de sobrecargas pela teoria da elasticidade

A expressão anterior, no entanto é válida apenas para meios semi-infinitos. Como a estrutura de arrimo possui uma rigidez muito maior que a do solo, este valor deve ser duplicado conforme as expressões da figura 3.4.13. Nesta figura estão também mostradas as expressões para os casos de carga concentrada e carga parcialmente distribuída. Em todos esses casos, a expressões mostradas estão majoradas conforme explicado acima.

Caso a estrutura de arrimo seja deformável, como é o caso das estruturas construídas em gabiões, pode-se reduzir o valor obtido por essas expressões.

Finalmente, deve-se notar que para este último método assume-se que a existência da sobrecarga não tem influência no empuxo devido ao solo, ou seja, não é analisada a influência da carga na posição da superfície de ruptura crítica.

Na verdade, trata-se de uma superposição de efeitos que não é de todo válida, pois o efeito do solo é determinado assumindo a plastificação do material enquanto o efeito da carga é determinado assumindo-se um modelo elástico linear para o material. De qualquer forma, apesar destes problemas, os resultados obtidos por esta análise apresentam boa concordância com medições feitas em modelos experimentais.

3.4.6 Solo coesivo

Quando o solo que compõe o maciço arrimado é coesivo ($c > 0$), há a ocorrência de tensões de tração na porção superior do maciço no estado ativo, como já visto no item 3.4.2.

Estas tensões provocam o aparecimento de fendas de tração que diminuem a área útil resistente da superfície de ruptura, aumentando assim o empuxo final sobre a estrutura.

Dessa forma, a posição mais crítica para a ocorrência de uma fenda de tração é no final da superfície de ruptura, diminuindo o comprimento desta (figura 3.4.14).

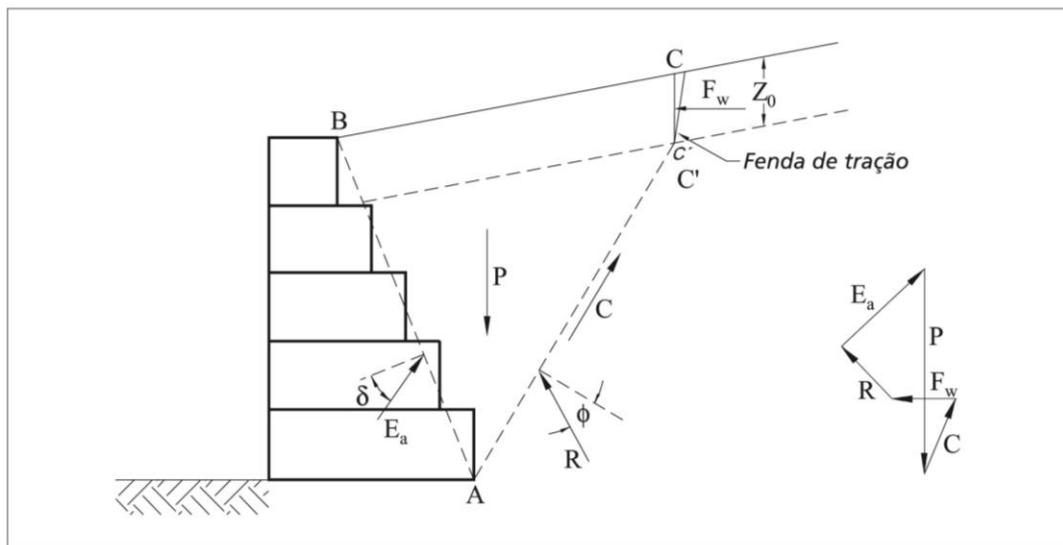


Figura 3.4.14 - Empuxo ativo em solos coesivos

Além disso, como também já foi citado, as fendas de tração podem estar preenchidas com água proveniente de chuvas, o que provoca um aumento suplementar no empuxo devido à pressão hidrostática no interior dessas fendas de tração. Assim, as forças atuantes sobre a cunha de solo formada pela superfície de ruptura incluem esta força " F_w ", devido à pressão da água no interior das fendas de tração, além da força resistente " C ", devido à coesão do solo. Estas forças são determinadas por:

$$F_w = \frac{1}{2} \cdot \gamma_a \cdot Z_0^2$$

(54)

$$C = c \cdot \overline{AC}^1$$

(55)

onde “ z_0 ” é a profundidade das fendas de tração, “ γ_a ” é o peso específico da água e “ c ”, a coesão do solo.

Utilizando-se o método do equilíbrio limite, o empuxo é determinado do equilíbrio de forças para cada superfície de ruptura hipotética até que se encontre a mais crítica. A cada uma dessas superfícies deve corresponder uma fenda de tração, pois a distribuição real destas fendas é aleatória, e a localização mais crítica é aquela que coincide com a superfície de ruptura mais crítica.

O ponto de aplicação do empuxo ativo “ E_a ” resultante sobre a estrutura de arrimo pode ser adotado como estando a “ $H/3$ ” da base da estrutura. Isto se justifica pelo fato de que este empuxo inclui o efeito da pressão da água no interior das fendas de tração e pela distribuição aproximada de pressões laterais apresentada no item 3.4.2.

3.4.7 Efeitos da água no empuxo ativo

3.4.7.1 Estrutura parcialmente submersa

Em obras de regularização de cursos d'água, é bastante comum a construção de estruturas de arrimo parcialmente submersas. Na figura 3.4.15 pode-se ver um exemplo.

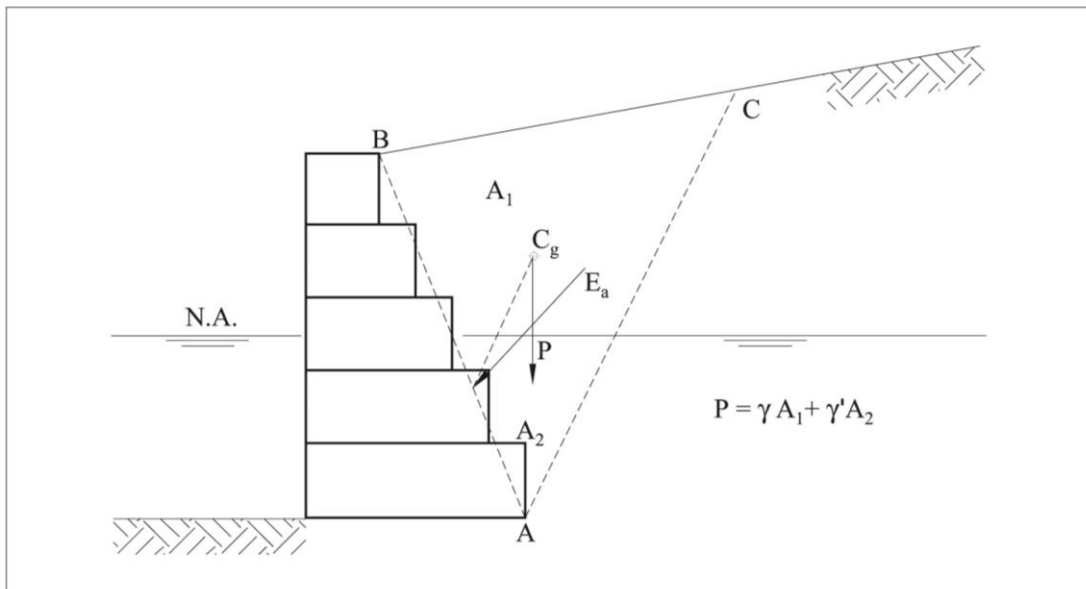


Figura 3.4.15 - Estrutura de arrimo parcialmente submersa

Nestes casos, deve-se separar do efeito do solo o efeito da água existente nos seus vazios. Isto porque a resistência do solo é devido à pressão entre suas partículas (pressão efetiva) enquanto a água não possui resistência alguma ao cisalhamento. Este tipo de análise é conhecida como análise em termos de tensão efetiva.

Assim, para se empregar o método do equilíbrio limite neste tipo de estrutura deve-se determinar o equilíbrio de forças utilizando o peso submerso da cunha de solo, ou seja, para se calcular o peso da parte submersa da cunha de solo deve-se utilizar o peso específico submerso " γ " do material.

O empuxo " E_a ", assim obtido, é então aquele devido apenas ao peso das partículas do solo, sendo necessário adicionar-se a este a pressão da água sobre a estrutura. A determinação desta pressão é trivial e obedece às leis da hidrostática. No caso específico de muro de arrimo de gabiões, devido à sua natureza altamente drenante, a análise de estabilidade pode ser feita em termos de pressões efetivas.

O ponto de aplicação do empuxo " E_a " é determinado por uma reta paralela à superfície de ruptura crítica passando pelo centro de gravidade (do peso submerso) da cunha crítica.

Caso se considere que há diferença entre as resistências do material acima e abaixo do nível d'água o problema deve ser analisado como no item 3.4.2.

3.4.7.2 Maciço sob influência de percolação d'água

Outro caso bastante comum é a ocorrência de percolação d'água através do maciço arrimado. Isto acontece, por exemplo, quando o nível do lençol freático que se encontrava pouco abaixo da fundação da estrutura se eleva por ocasião da época das chuvas ou, ainda quando em estruturas do tipo das descritas no item anterior, ocorre uma brusca redução do nível do curso d'água. Nestes casos há percolação d'água através do maciço na direção da estrutura de arrimo, o que faz aumentar o valor do empuxo sobre esta. Para que a água não fique retida atrás do muro, aumentando ainda mais o valor do empuxo, deve-se usar estruturas autodrenantes, como por exemplo os gabiões, ou prover a estrutura de drenos e filtros que impeçam o carreamento das partículas do solo.

Para se analisar este tipo de problema deve-se determinar inicialmente a rede de fluxo formada como mostrado na figura 3.4.16.

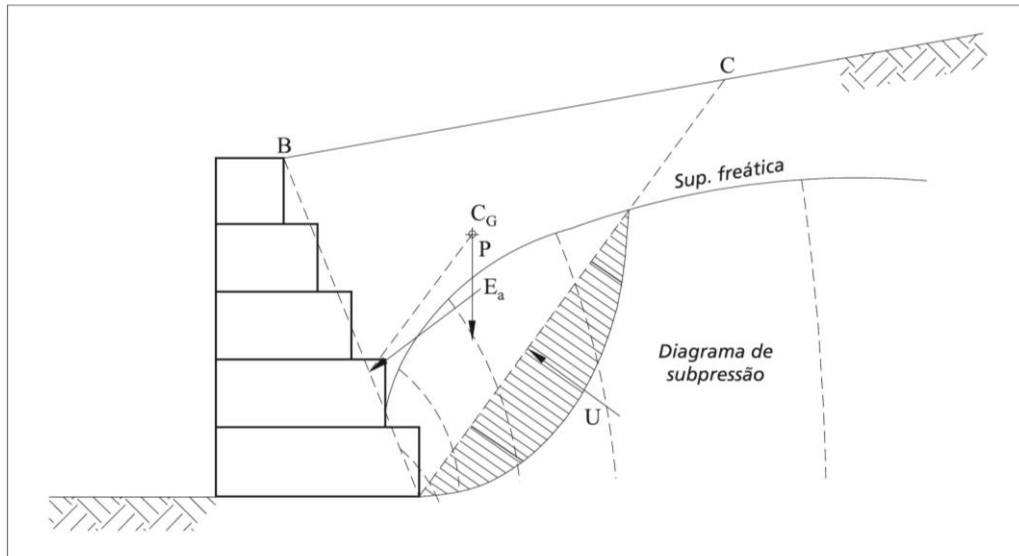


Figura 3.4.16 - Rede de fluxo através do maciço arrimado

A seguir pode-se fazer a análise pelo método do equilíbrio limite. As forças que atuam sobre a cunha de solo formada pela superfície de ruptura incluem o peso próprio desta (aqui determinado utilizando-se o peso específico saturado " γ_{sat} " do solo) e a força "U" devido à pressão neutra que age sobre a superfície de escorregamento. Esta última é determinada a partir do diagrama de subpressões atuantes na superfície de ruptura.

Uma forma simplificada de determinação da força "U" consiste na adoção de um parâmetro de subpressão " r_u " definido como:

$$r_u = \frac{U}{P} \quad (56)$$

que pode ser estimado a partir da altura do lençol freático.

O ponto de aplicação do empuxo " E_a " pode ser determinado como no item anterior. Deve-se notar, porém, que aqui o empuxo " E_a " inclui o efeito da água. Então o centro de gravidade da cunha crítica deve ser determinado pelo seu peso saturado.

3.4.8 Maciço em camadas (não homogêneo)

Caso o maciço arrimado seja formado por camadas de solos diferentes (figura 3.4.17), o método do equilíbrio limite pode ainda ser utilizado.

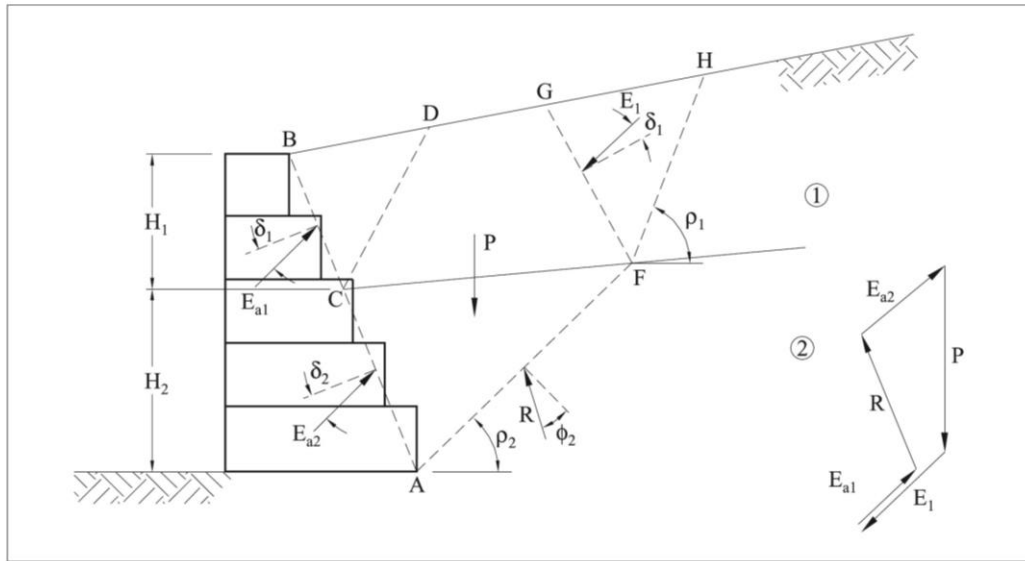


Figura 3.4.17 - Maciço não homogêneo

Primeiramente determina-se o empuxo " E_{a1} " provocado sobre a estrutura pela primeira camada de solo ao longo de "BC" utilizando o método já citado anteriormente.

Em seguida considera-se uma superfície de ruptura formada por três planos. O primeiro destes planos parte do ponto "A" na base da estrutura (ou da base da segunda camada do solo, no caso de haver mais de duas camadas) e se estende até o limite entre a segunda e a primeira camadas (ponto "F"), com uma inclinação " ρ_2 " em relação à horizontal. O segundo plano parte deste ponto e prossegue até a superfície do maciço (ponto "G"), numa direção paralela à face interna da estrutura de arrimo ("AB"). O terceiro plano parte do mesmo ponto ("F") e se estende até a superfície do maciço (ponto "H") numa direção inclinada de " ρ_1 " em relação à horizontal.

Formam-se assim, duas cunhas de solo. Uma delas com vértices em A, B, G e F, e outra com vértices em F, G e H. O efeito da cunha menor sobre a maior pode então ser determinado como o empuxo " E_1 ", calculado também pelo método do equilíbrio limite, considerando um ângulo de atrito entre as duas cunhas igual ao ângulo de atrito " δ_1 " que atua entre o solo da camada superior e a estrutura de arrimo.

Conhecido o valor de " E_1 ", o empuxo aplicado pela camada inferior pode ser determinado pelo equilíbrio das forças que atuam sobre a cunha de solo maior.

A inclinação “ ρ_2 ” deve ser então pesquisada a fim de se encontrar a posição mais crítica para a superfície de ruptura.

Caso o número de camadas seja superior a dois, o processo deve ser repetido para incluir as camadas inferiores até se alcançar a base da estrutura.

O ponto de aplicação de “ E_{a1} ” é determinado como já mencionado nos itens anteriores, ou seja, a “ $H_1/3$ ” da base da camada, onde “ H_1 ” é a espessura desta camada em contato com a estrutura de arrimo, caso a superfície do maciço seja plana e não haja sobrecargas. Quanto ao ponto de aplicação de “ E_{a2} ”, pode-se assumir que a distribuição da pressão lateral sobre a estrutura de arrimo é linear e que a taxa de variação desta pressão com a altura da estrutura é:

$$\frac{dp_{l2}}{dh_2} = \gamma_2 \cdot K_{a2} \quad (57)$$

onde “ K_{a2} ” é o coeficiente de empuxo ativo determinado pela teoria de Coulomb. Assim, pode-se determinar a pressão lateral no topo e na base da segunda camada e, em seguida, o centro de gravidade do diagrama de pressão lateral obtido (figura 3.4.18).

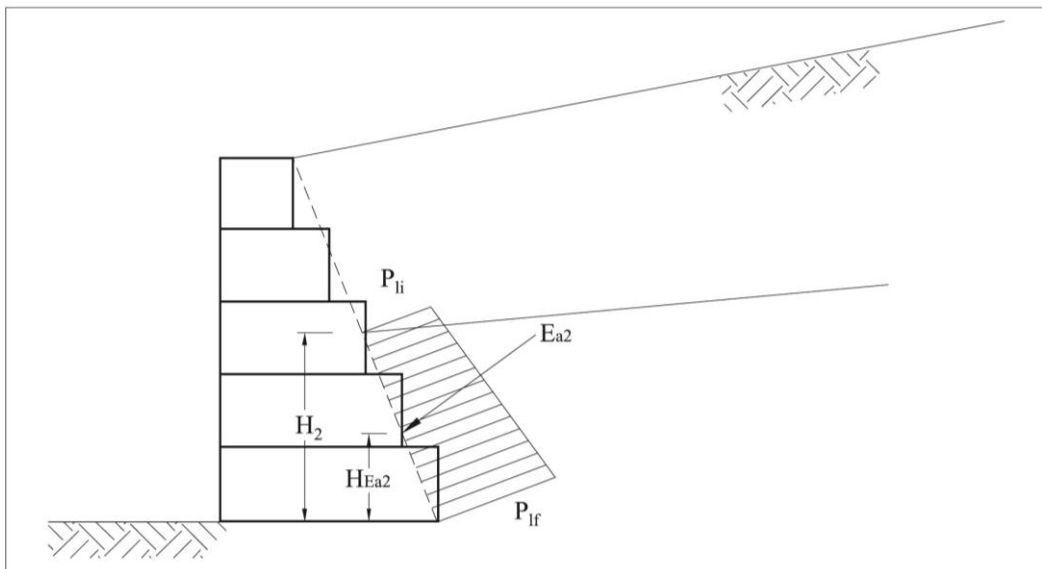


Figura 3.4.18 - Distribuição da pressão lateral na segunda camada de solo

$$dp_{li} = \frac{E_{a2}}{H_2} - \frac{\gamma_2 \cdot K_{a2} \cdot H_2}{2} \quad (58)$$

$$dp_{lr} = \frac{E_{a2}}{H_2} + \frac{\gamma_2 \cdot K_{a2} \cdot H_2}{2} \quad (59)$$

então:

$$H_{E2} = \frac{H_2}{2} - \frac{\gamma_2 \cdot K_{a2} \cdot H_2}{H_{a2}} \cdot \frac{H_2^3}{12} \quad (60)$$

Na determinação de “ K_{a2} ” pela teoria de Coulomb pode-se adotar, caso seja necessário, valores aproximados para a inclinação “ i ” da superfície do talude.

A execução deste processo só é viável com a utilização de um programa de computador. O programa GawacWin[®] foi desenvolvido com a capacidade de analisar também estes casos.

3.4.9 Efeito sísmico

Durante um abalo sísmico, o empuxo ativo pode sofrer um incremento devido às acelerações horizontal e vertical do solo. Estas acelerações provocam o aparecimento de forças inerciais nas direções vertical e horizontal que devem ser consideradas no equilíbrio de forças (figura 3.4.19).

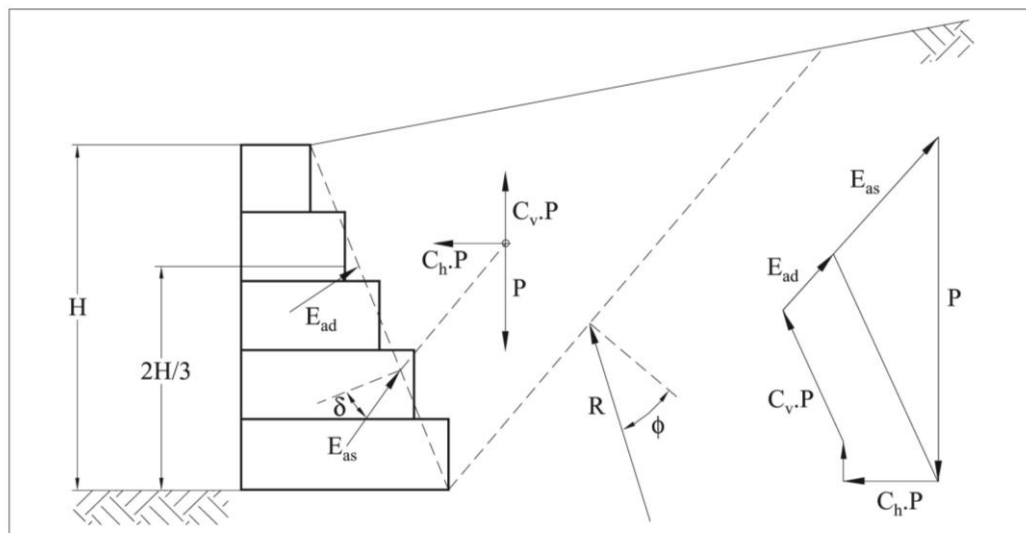


Figura 3.4.19 - Forças de inércia que agem sobre a cunha de solo

Estas acelerações normalmente são expressas em relação à aceleração da gravidade “g” e são função do risco sísmico local. Assim, as forças de inércia serão calculadas como parcelas do peso da cunha de solo “P”:

$$I_h = C_h \cdot P \quad (61)$$

e

$$I_v = C_v \cdot P \quad (62)$$

onde “C_h” e “C_v” são as relações de aceleração nas direções horizontal e vertical.

A aceleração na direção horizontal apresenta uma maior influência no valor do empuxo ativo e, assim, geralmente é a única considerada na análise.

O empuxo ativo calculado, então, dessa forma pode ser dividido em duas parcelas. A primeira, igual ao empuxo estático “E_{ac}”, tem seu ponto de aplicação sobre a estrutura de arrimo determinado como nos itens anteriores. A segunda parcela “E_{ad}” é o efeito do abalo sísmico, e seu ponto de aplicação está situado a “2.H/3” da base da estrutura [13].

Caso o maciço esteja submerso, deve-se utilizar o peso específico submerso “γ” do solo no cálculo do peso específico da cunha, como já citado no item 3.4.7.1. Então, é necessária também a consideração do efeito sísmico na massa de água existente no interior do solo.

Esta massa provocará uma pressão adicional ao efeito estático, resultando num empuxo adicional “U_d” devido à água, dado por:

$$U_d = \frac{7}{12} \cdot H_a^2 \cdot \gamma_a \cdot C_h \quad (63)$$

onde “γ_a” e “H_a” são o peso específico e a altura da água respectivamente. Este empuxo está aplicado a “H_a/3” da base da estrutura [14].

Caso as condições do problema permitam a utilização direta da teoria de Coulomb e, além disso, considere-se apenas a aceleração na direção horizontal, o efeito sísmico pode ser determinado pelas expressões do item 3.4.3 corrigindo-se os valores dos ângulos “ α ” e “ i ” da figura 3.4.7.

$$i' = i + \theta$$

(64)

e

$$\alpha' = \alpha - \theta$$

(65)

onde

$$\theta = \arctan C_h$$

(66)

O empuxo “ E_a ” assim calculado deve ainda ser multiplicado por “ A ”, que é dado por:

$$A = \frac{\text{sen}^2 \alpha'}{\text{sen}^2 \alpha \cdot \cos \theta}$$

(67)

O efeito sísmico “ E_{ad} ” será dado então por:

$$A_{ad} = A \cdot E'_a - E_{ae}$$

(68)

onde “ E_{ac} ” é o empuxo ativo estático. A diferença “ E_{ad} ” está aplicada a “ $2H/3$ ” da base do muro.

3.5 Aplicação das teorias a muros de gabiões

Os muros de gabiões são estruturas de gravidade e como tal podem ser dimensionados.

Assim, as teorias clássicas de Rankine e de Coulomb, bem como o método do equilíbrio limite podem ser utilizados na determinação dos empuxos atuantes.

Para os casos mais simples, a teoria de Coulomb é geralmente empregada na determinação do empuxo ativo, pois abrange uma variedade razoável de situações encontradas na prática.

As características do solo arrimado devem ser avaliadas cuidadosamente, pois delas dependem os resultados das análises. Deve-se atentar para o fato de que o maciço é geralmente um reaterro, preferencialmente executado com material não coesivo e assim é normal se considerar como nula a coesão do solo.

Mesmo quando se utiliza solo argiloso no reaterro, a coesão disponível é muito pequena, pois além do amolgamento provocado pela construção, deve-se lembrar que o estado ativo se configura numa situação de descarregamento do maciço; e assim a situação mais crítica é a que corresponde à condição drenada da resistência. Dessa forma a envoltória de resistência ao cisalhamento mais indicada nestes casos é a envoltória efetiva (também chamada envoltória drenada), que normalmente apresenta uma parcela de coesão muito pequena, ou mesmo nula, para solos argilosos.

Para o ângulo de atrito " δ " entre o solo e a estrutura, pode-se adotar o mesmo valor do ângulo de atrito interno " ϕ " do solo, pois a face dos gabiões é bastante rugosa. No caso de haver um filtro geotêxtil entre o solo arrimado e o muro de gabiões o valor de " δ " deve ser diminuído, adotando-se normalmente " $\delta = 0,9$ a $0,95 \cdot \phi$ ".

Caso as condições específicas do problema analisado sejam mais complexas, não permitindo a utilização direta da teoria de Coulomb, recorre-se geralmente ao método do equilíbrio limite. Neste caso, entretanto, o trabalho envolvido na determinação do empuxo atuante é consideravelmente maior. Por isso foram desenvolvidos programas de computador que auxiliam o projetista nessa tarefa. O programa GawacWin[®] distribuído pela Maccaferri, aos projetistas, utiliza o método do equilíbrio limite na determinação do empuxo ativo atuante, o que torna-o capaz de analisar a maioria dos casos que podem surgir.

Para o cálculo do empuxo passivo, que é a resistência ao deslocamento horizontal oferecida pelo terreno à frente do muro, quando este está apoiado numa cota inferior à da sua superfície (figura 3.5.1), a teoria de Rankine é geralmente suficiente. Deve-se, no entanto, ter cautela na consideração desta resistência. Somente deve ser considerada a disponibilidade do empuxo passivo à frente do muro quando for possível garantir que não ocorrerão escavações ou mesmo erosão no solo situado à frente da estrutura de arrimo.

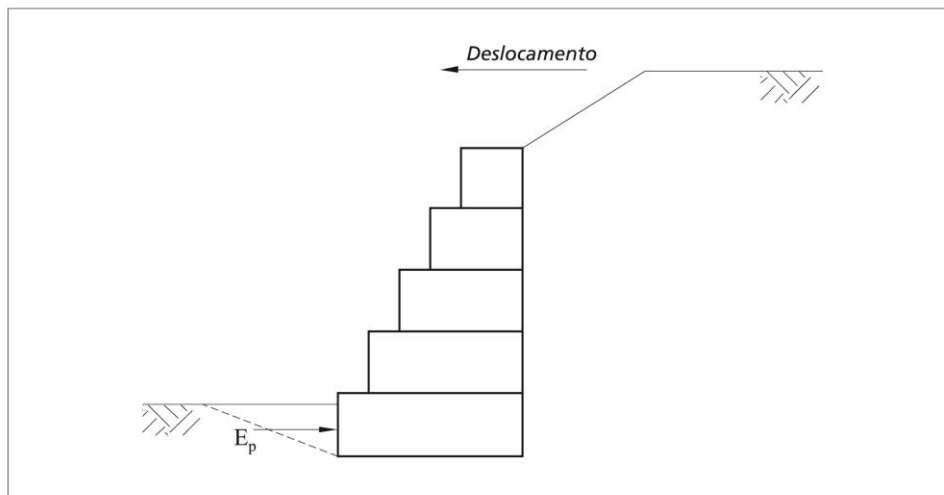


Figura 3.5.1 - Determinação do empuxo passivo

3.5.1 Superfícies de ruptura curvas

Os métodos de Coulomb e do equilíbrio limite adotam a forma da superfície de ruptura como sendo plana, por hipótese. No entanto, nem sempre a forma plana conduz à condição mais crítica para o equilíbrio da cunha de solo formada pela superfície de ruptura. A ocorrência de atrito ao longo da interface solo-estrutura de arrimo faz com que a superfície de ruptura mais crítica seja curva.

Análises mais rigorosas, utilizando superfícies de ruptura com a forma de espirais logarítmicas, foram desenvolvidas. No caso do empuxo ativo, estas análises mostram que o valor calculado com a utilização de superfícies planas difere no máximo em cerca de 10%, ficando em geral esta diferença dentro de 5% do valor calculado com superfícies de ruptura curva [15]. Este fato justifica a utilização das superfícies de ruptura plana para o cálculo do empuxo ativo por serem de análise mais simples e abrangentes.

3.8 Exemplos Resolvidos

3.8.1 Exemplo Teórico 01

3.8.1.1 Dados do problema

Verificar a estabilidade do muro de contenção em gabiões mostrado na figura 3.8.1, sendo dadas as seguintes características:

- **Gabiões:**

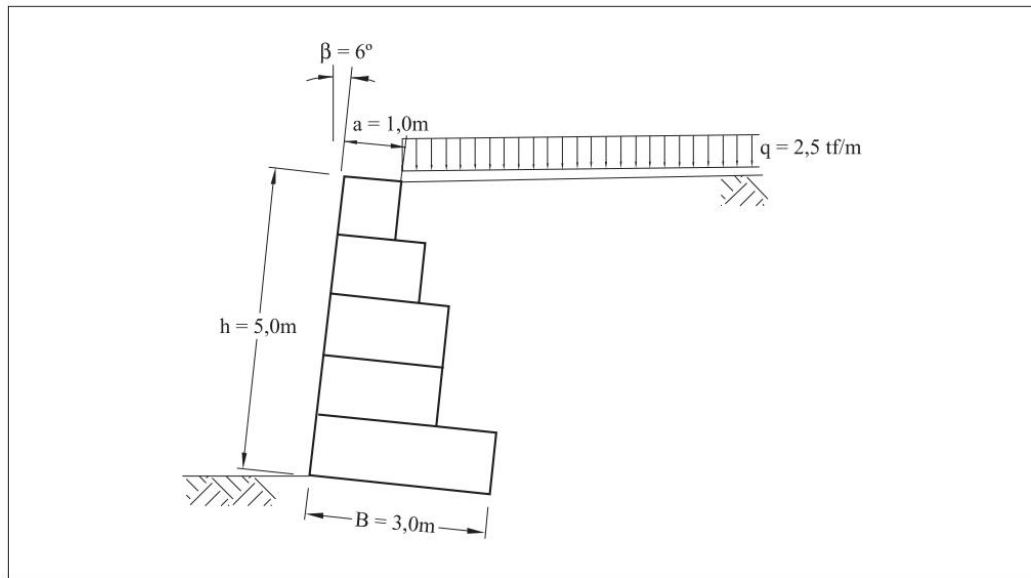


Figura 3.8.1 - Primeiro exemplo

MACCAFERRI

3. Teoria e cálculos de estabilidade

- Peso específico da rocha de enchimento: $\gamma_p = 2,43 \text{ tf/m}^3$.

- Porosidade: $n = 30\%$.

• **Maciço arrimado:**

- Peso específico do solo: $\gamma = 1,8 \text{ tf/m}^3$.

- Ângulo de atrito interno: $\phi = 30^\circ$.

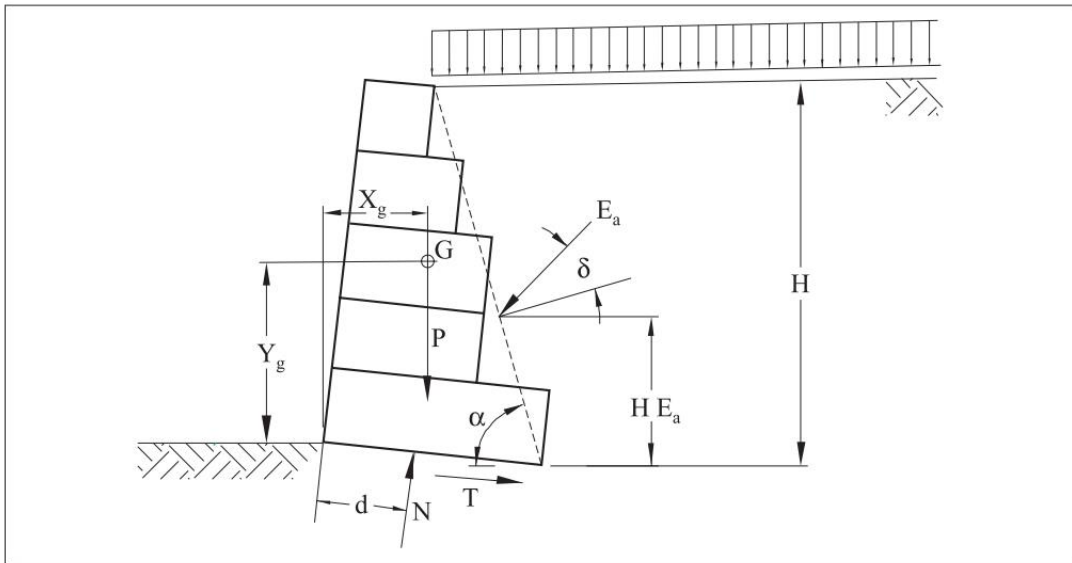


Figura 3.8.2 - Forças que agem sobre o muro

- Coesão: $c = 0$.

$$\alpha = \arctan\left(\frac{h}{B-a}\right) + \beta = 74,2^\circ$$

• **Fundação:**

$$H = \frac{h \cdot \sin \alpha}{\sin (\alpha - \beta)} = 5,18\text{m}$$

- Carga máxima admissível: $q_{adm} = 20,0 \text{ tf/m}^2$.
- Ângulo de atrito interno: $\phi = 27^\circ$.

A superfície superior do maciço arrimado é horizontal "i = 0" e sobre ela está aplicada uma carga uniformemente distribuída "q = 2,5tf/m²".

$$K_a = \frac{\text{sen}^2(\alpha + \phi)}{\text{sen}^2 \alpha \cdot \text{sen}(\alpha + \delta) \cdot \left[1 + \sqrt{\frac{\text{sen}(\phi + \delta) \cdot \text{sen}(\alpha - i)}{\text{sen}(\alpha - \delta) \cdot \text{sen}(\alpha + i)}} \right]^2} = 0,448$$

3.8.1.2 Superfície de aplicação do empuxo ativo

$$E_a = 1 \cdot \gamma \cdot H^2 \cdot K_a + q \cdot H \cdot K_a \cdot \frac{\text{sen} \alpha}{\text{sen}(\alpha + i)} = 16,62 \text{ tf/m}$$

A superfície de aplicação do empuxo ativo é tomada como o plano médio que une as

$$\frac{H_{E_a}}{H_{E_a}} = \frac{\gamma \cdot H_2 + 3 \cdot q \cdot H}{3 \cdot \gamma \cdot H + 6 \cdot q} = 2,03 \text{ m}$$

extremidades inferior e superior das camadas de gabiões da base e do topo do muro, como mostrado na figura 3.8.2 juntamente com as forças que agem sobre a estrutura.

$$\gamma_g = \gamma_p \cdot (1 - n) = 1,70 \text{ tf/m}^3$$

O ângulo “ α ” entre o plano de aplicação do empuxo ativo e a horizontal é:

$$S = h_a + \frac{(B - a) \cdot h}{2} = 10,0\text{m}^2$$

$$P = \gamma_g \cdot S = 17,0\text{tf/m}$$

e a altura total “H” é dada por:

$$x'_G = \frac{\frac{1}{2} \cdot a^2 \cdot h + \frac{1}{6} \cdot h (B^2 + a \cdot B - 2 \cdot a^2)}{S} = 1,08\text{m}$$

$$y'_G = \frac{\frac{1}{2} \cdot a^2 \cdot h + \frac{1}{6} \cdot h^2 (B - a)}{S} = 2,08\text{m}$$

$$x_G = x'_G \cdot \cos \beta + y'_G \cdot \sin \beta = 1,29\text{m}$$

$$y_G = -x'_G \cdot \sin \beta + y'_G \cdot \cos \beta = 1,96\text{m}$$

3.8.1.3 Empuxo ativo

O empuxo ativo “ E_a ” pode ser calculado pela teoria de Coulomb. Tomando-se o valor do

$$N = P \cdot \cos \beta + E_a \cdot \cos (\alpha - \delta - \beta) = 29,97 \text{ tf/m}$$

ângulo de atrito entre o solo e o muro “ $\delta = \phi$ ” e “ $i = 0$ ”, o coeficiente de empuxo ativo “ K_a ”

$$T_d = N \cdot \tan \delta^* = 15,27 \text{ tf/m}$$

é dado por:

$$F_g = \frac{T_d}{E_a \cdot \sin (\alpha - \delta - \beta) - P \cdot \sin \beta} = 1,80 > 1,50$$

O empuxo ativo “ E_a ” será então:

$$x_{E_a} = B \cdot \cos \beta - H_{E_a} \cdot \tan (90^\circ - \alpha) = 2,14 \text{ m}$$

e seu ponto de aplicação é dado por H_{E_a} :

$$y_{E_a} = H_{E_a} - B \cdot \cos \beta = 1,72 \text{ m}$$

3.8.1.4 Peso da estrutura

$$M_{E_{ah}} = E_a \cdot \text{sen}(\alpha - \delta) \cdot y_{E_a} = 19,93 \text{tfm/m}$$

O peso específico dos gabiões “ γ_g ” é dado por:

$$M_p = P_{x_G} = 21,93 \text{tfm/m}$$

e a área “S” da seção transversal do muro é:

$$M_{E_{av}} = E_a \cos(\alpha - \delta) \cdot x_{E_a} = 28,72 \text{tfm/m}$$

O peso total do muro “P” será então:

$$F_1 = \frac{M_p + M_{E_{av}}}{M_{E_{ah}}} = 2,54 > 1,5$$

Para o cálculo da posição do centro de gravidade “G” do muro, determinam-se primeiramente as suas coordenadas para um sistema de eixos “x” e “y” alinhado com a base da estrutura:

$$d = \frac{M_p + M_{E_{av}} + M_{E_{ah}}}{N} = 1,02 \text{m}$$

e

$$e = \frac{B}{2} = 0,48\text{m} < \frac{B}{6} = 0,50\text{m}$$

As coordenadas “ x_G ” e “ y_G ” do centro de gravidade da seção são:

$$q_{\text{máx}} = \frac{N}{B} \cdot \left(1 + 6 \cdot \frac{e}{B} \right) = 19,58\text{tf/m}^2 < q_{\text{adm}} = 20,0\text{tf/m}^2$$

$$q_{\text{mín}} = \frac{N}{B} \cdot \left(1 - 6 \cdot \frac{e}{B} \right) = 0,40\text{tf/m}^2 < q_{\text{adm}} = 20,0\text{tf/m}^2$$

e

3.8.1.5 Segurança contra o escorregamento

A força normal “N” que age na base do muro é dada por:

$\alpha = 82,0^\circ$	$y_{E_a} = 1,43\text{m}$	$M_p = 9,79\text{m}$
$K_\alpha = 0,365$	$P = 10,20\text{tf/m}$	$M_{E_a} = M_{E_{av}} - M_{E_{ah}} = - 0,45\text{tf/m}$
$H = 4,08\text{m}$	$x_G = 0,96\text{m}$	$d = 0,57\text{m}$
$E_a = 9,20\text{tf/m}^2$	$y_G = 1,96\text{m}$	
$x_{E_a} = 1,75\text{m}$	$N = 16,53\text{tf/m}$	

Adotando-se o ângulo de atrito “ δ^* ” entre o solo de fundação e a base do muro “ $\delta^* = \phi = 27^\circ$ ”, a força de resistência disponível “ T_d ” será dada por:

O coeficiente de segurança contra o escorregamento é:

$$\delta^* = 25 \cdot \gamma_g - 10^\circ = 32,50^\circ$$

3.8.1.6 Segurança contra o tombamento

$$c_g = 0,30 \cdot p_u - 0,50 = 2,08 \text{tf/m}^2$$

As coordenadas do ponto de aplicação do empuxo ativo “ E_a ” são:

$$T_{adm} = N \cdot \tan \delta^* + c_g \cdot B = 14,69 \text{tf/m}$$

$$T = -P \cdot \sin \beta + E_a \cdot \sin (\alpha - \delta - \beta) = 5,55 < T_{adm}$$

$$q_{adm} = 50 \cdot \gamma_g - 30 = 55,0 \text{tf/m}^2$$

e

$$q_{\text{máx}} = \frac{N}{2 \cdot d} = 14,63 \text{tf/m}^2 < q_{\text{adm}}$$

O momento de tombamento será dado pelo momento da componente horizontal do empuxo ativo:

Seção	T [tf/1m]	T _{adm} [tf/m]	q _{máx} [tf/m ²]	q _{adm} [tf/m ²]
1	5,55	14,69	14,63	55,00
2	3,63	13,34	8,42	55,00
3	1,88	8,10	5,27	55,00
4	0,56	4,00	2,19	55,00

Tabela 3.8.1 - Resultados das verificações das seções intermediárias

Os momentos resistentes são os momentos do peso próprio da estrutura e o momento da componente vertical do empuxo ativo:

e

O valor do coeficiente de segurança contra o tombamento é:

3.8.1.7 Pressões na fundação

A distância “d” entre o ponto de aplicação de “N” e o fulcro do tombamento é dada por:

e a excentricidade “e” é:

Assim as pressões nas extremidades da base serão:

$$x_0 = -0,499\text{m}$$

$$y_0 = 5,283\text{m}$$

$$R = 6,633\text{m}$$

3.8.1.8 Seções intermediárias

$$F_g = 1,238$$

Para cada seção intermediária entre as camadas de gabiões são determinadas as tensões normais e de cisalhamento atuantes. Para isto são determinados o empuxo ativo e o peso dos gabiões situados acima da seção analisada.

Assim, para a primeira seção intermediária, acima da base, calcula-se, de maneira análoga ao já mostrado:

As distâncias e momentos acima são determinados em relação ao fulcro de tombamento da seção intermediária que se situa na extremidade da seção, à frente do muro.

O ângulo de atrito disponível ao longo da seção intermediária " δ^* " é dado por:

Para gabiões de 1,0m de altura e malha 8x10, o peso da rede metálica " $p_u = 8,6 \text{ kgf/m}^3$ " e, assim, a coesão disponível na seção intermediária " c_g " será:

A máxima força de cisalhamento admissível " T_{adm} ", ao longo da seção será:

e a força de cisalhamento " T ", que atua na seção é:

A máxima tensão normal admissível na seção intermediária " q_{adm} " vale:

e a máxima tensão normal " $q_{máx}$ " que age na seção é:

Repetindo-se o mesmo cálculo para as outras seções intermediárias obtém-se a tabela 3.8.1.

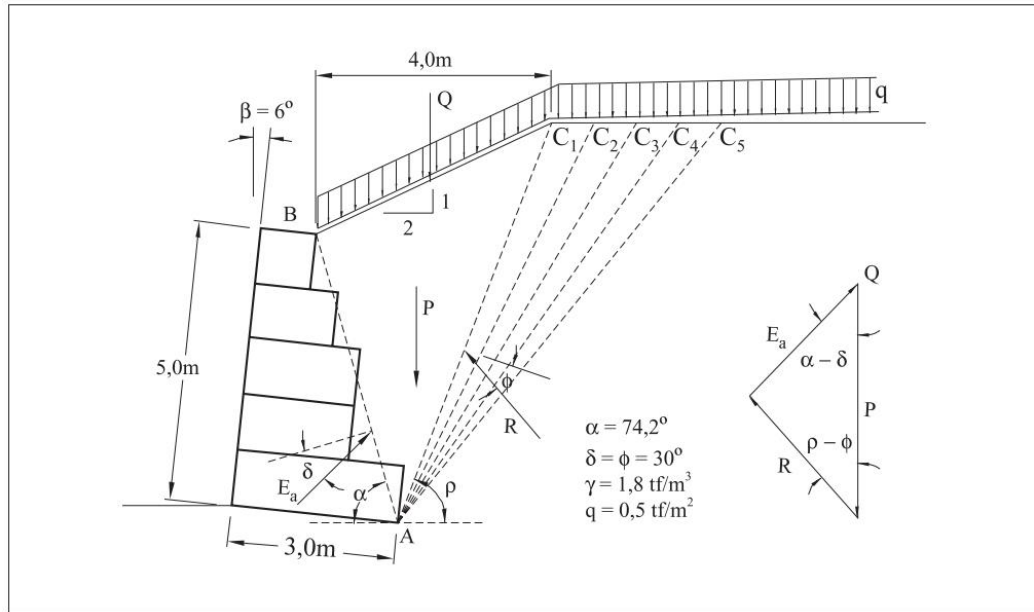


Figura 3.8.3 - Segundo exemplo

3.8.1.9 Estabilidade global

A verificação da estabilidade global do conjunto solo/estrutura de arrimo é geralmente executada pelo método de Bishop, que analisa a ruptura ao longo de superfícies de ruptura cilíndricas que contornam o muro de gabiões.

Para a execução desta análise normalmente são empregados programas de computador, pois a busca da superfície de ruptura mais crítica é bastante trabalhosa.

O programa de análise GawacWin[®] realiza estes cálculos de maneira automática e para este exemplo fornece os seguintes resultados para a superfície cilíndrica mais crítica:

Onde "x₀" e "y₀" são as coordenadas do centro da superfície crítica em relação ao fulcro do

$$\alpha = \arctan \frac{h}{B - a} + \beta = 74,20^\circ$$

tombamento e “R” é o raio.

$$H = \frac{h \cdot \text{sen } \alpha}{\text{sen } (\alpha - \beta)} = 5,18\text{m}$$

O coeficiente de segurança contra a ruptura global “F_g” obtido é:

3.8.2 Exemplo Teórico 02

3.8.2.1 Dados do problema

Neste segundo exemplo, pede-se para analisar a estabilidade de uma estrutura de arrimo de gabiões similar à do exemplo anterior, como mostrado na figura 3.8.3.

$$E_a = (P + Q) \cdot \frac{\text{sen } (\rho - \phi)}{\text{sen } (\alpha + \rho - \phi - \delta)}$$

Os dados dos gabiões, do solo que compõe o maciço arrimado e do solo de fundação são os mesmos do primeiro exemplo:

• **Gabiões:**

- Peso específico da rocha de enchimento: $\gamma_p = 2,43 \text{ tf/m}^3$.

Cunha	P [tf/m]	Q [tf/m]	ρ [graus]	E _a [tf/m ²]
1	22,4	2,71	70,2	15,96
2	28,74	2,71	63,2	17,68
3	35,08	3,21	57,2	18,47
4	41,42	3,71	51,8	18,35
5	47,76	4,21	47,1	17,42

Tabela 3.8.2 - Resultados dos equilíbrios das cunhas

- Porosidade: $n = 30\%$.

• **Maciço arrimado:**

$$\rho_{\text{crit}} = 55,2^\circ$$

- Peso específico do solo: $\gamma = 1,8 \text{ tf/m}^3$.

$$E_a = 18,55 \text{ tf/m}$$

- Ângulo de atrito interno: $\phi = 30^\circ$.

- Coesão: $c = 0$.

$$E_q = Q \cdot \frac{\text{sen}(\rho_{\text{crit}} - \phi)}{\text{sen}(\alpha + \rho_{\text{crit}} - \phi - \delta)}$$

• **Fundação:**

- Carga máxima admissível: $q_{\text{adm}} = 20,0 \text{ tf/m}^2$.

Empuxo	Valor	H_E
E_{as}	17,01 tf/m	1,81 m
E_{q1}	1,01 tf/m	3,80 m
E_{q2}	0,53 tf/m	1,21 m

Tabela 3.8.3 - Empuxos causados pelo solo e pelas duas parcelas da sobrecarga

- Ângulo de atrito interno: $\phi = 27^\circ$.

Neste exemplo, ao contrário do anterior, a superfície superior do terrapleno não é horizontal,

$$H_{E_a} = 1,90 \text{ m}$$

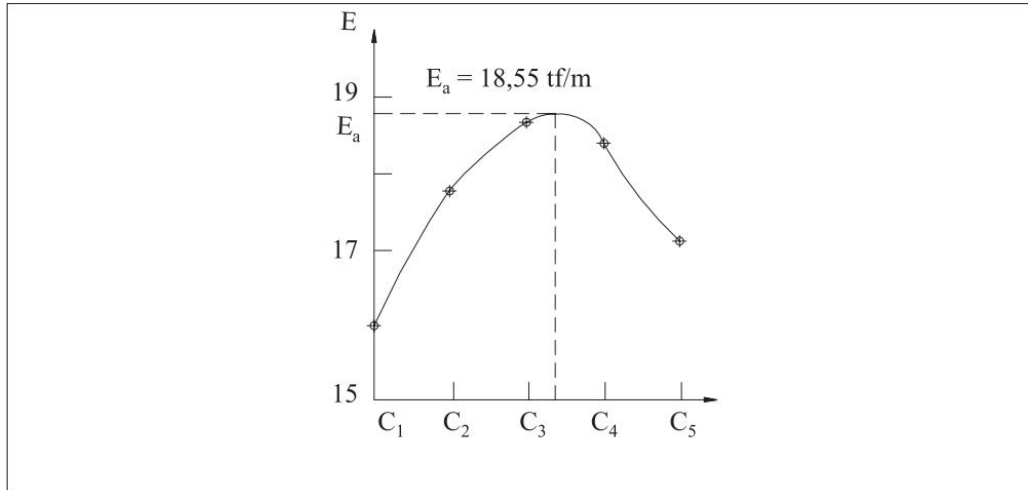


Figura 3.8.4 - Variação do empuxo com a superfície de ruptura

mas apresenta uma inclinação à razão de 1:2 (vertical/horizontal) até uma distância de 4,0m do muro. A partir deste ponto a superfície do terrapleno é horizontal.

$$\gamma_g = \gamma_p \cdot (1 - n) = 1,70 \text{ tf/m}^3$$

Sobre o maciço está aplicada uma carga uniformemente distribuída “ $q = 0,5 \text{ tf/m}^2$ ”.

$$S = h_a + \frac{(B - a)}{2} \cdot h = 10,0 \text{ m}^2$$

3.8.2.2 Superfície de aplicação do empuxo ativo

$$P = \gamma_g \cdot S = 17,0 \text{ tf/m}$$

A superfície de aplicação do empuxo ativo, como no primeiro exemplo, é tomada como o

$$x_G = \frac{\frac{1}{2} \cdot a^2 \cdot h + \frac{1}{6} \cdot h \cdot (B^2 + a \cdot B - 2 \cdot a^2)}{S} = 1,08\text{m}$$

plano médio que une as extremidades inferiores e superiores das camadas de gabiões da

$$y_G = \frac{\frac{1}{2} \cdot a^2 \cdot h + \frac{1}{6} \cdot h^2 \cdot (B - a)}{S} = 2,08\text{m}$$

$$x_G = x_G \cdot \cos \beta + y_G \cdot \sin \beta = 1,29\text{m}$$

base e do topo do muro.

$$y_G = -x_G \cdot \sin \beta + y_G \cdot \cos \beta = 1,96\text{m}$$

O ângulo “ α ” entre o plano de aplicação do empuxo ativo e a horizontal é:

e a altura total “H” é dada por:

3.8.2.3 Empuxo ativo

Neste caso, o empuxo ativo deve ser determinado pelo método do equilíbrio limite, pois a

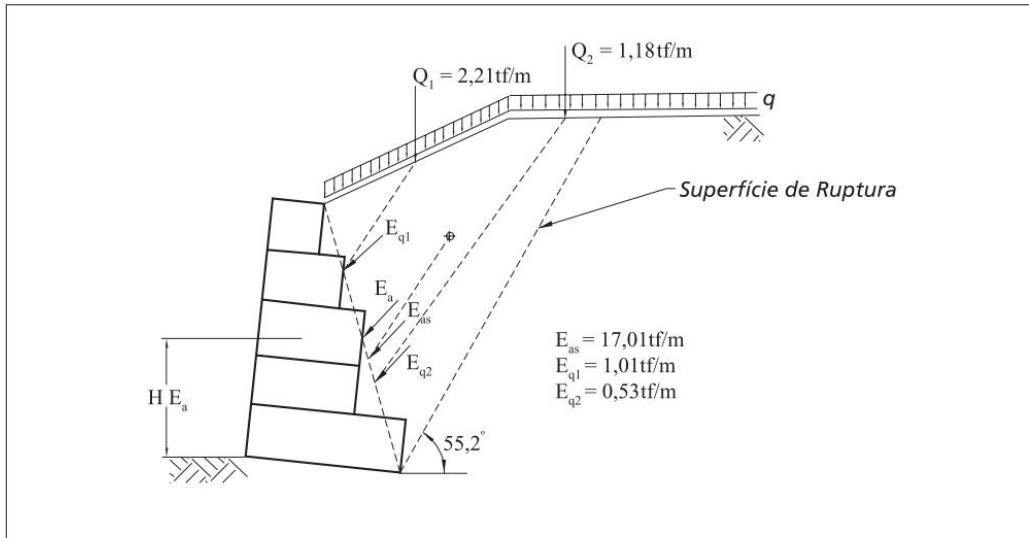


Figura 3.8.5 - Ponto de aplicação do empuxo ativo

superfície superior do maciço arrimado é irregular.

Para esta determinação, traçam-se algumas superfícies de ruptura hipotéticas como

$$N = P \cdot \cos \beta + E_a \cdot \cos (\alpha - \delta - \beta) = 31,48 \text{ tf/m}$$

mostrado na figura 3.8.3. Analisa-se então o equilíbrio das várias cunhas formadas pelas superfícies de ruptura traçadas. O valor do empuxo " E_a " atuante em cada uma delas pode

$$T_d = N \cdot \tan \delta^* = 16,04 \text{ tf/m}$$

ser obtido do equilíbrio de forças dado por:

$$F_d = \frac{T_d}{E_a \cdot \sin (\alpha - \delta - \beta) - P \cdot \sin \beta} = 1,65 < 1,5$$

onde "P" é o peso da cunha e "Q" é a parcela da sobrecarga que se encontra sobre ela.

$$x_{E_a} = B \cdot \cos \beta - H_{E_a} \cdot \tan (90^\circ - \alpha) = 2,45\text{m}$$

$$y_{E_a} = H_{E_a} - B \cdot \sin \beta = 1,59\text{m}$$

Podem-se obter assim os valores do empuxo ativo em função da superfície de ruptura.

$$M_{E_{ah}} = E_a \cdot \sin (\alpha - \delta) \cdot y_{E_a} = 20,56\text{tfm/m}$$

Estes valores estão mostrados na tabela 3.8.2.

$$M_p = P_{x_G} = 21,93\text{tfm/m}$$

$$M_{E_{av}} = E_a \cdot \cos (\alpha - \delta) \cdot x_{E_a} = 32,58\text{tfm/m}$$

Com estes valores construiu-se o gráfico mostrado na figura 3.8.4. Dali pode-se determinar

$$F_t = \frac{M_p + M_{E_{av}}}{M_{E_{av}}} = 2,65 > 1,5$$

a posição da cunha crítica e o valor do empuxo total:

$$d = \frac{M_p + M_{E_{av}} + M_{E_{ah}}}{N} = 1,08\text{m}$$

$$e = \frac{B}{2} = 0,42\text{m} < \frac{B}{6} = 0,5\text{m}$$

e

$$q_{\text{máx}} = \frac{N}{B} \left(1 + 6 \cdot \frac{e}{B} \right) = 19,30\text{tf/m}^2 < q_{\text{adm}} = 20,0\text{tf/m}^2$$

Para a determinação do ponto de aplicação de “E_a“, o efeito da sobrecarga deve ser

$$q_{\text{mín}} = \frac{N}{B} \left(1 - 6 \cdot \frac{e}{B} \right) = 1,68\text{tf/m}^2 < q_{\text{adm}} = 20,0\text{tf/m}^2$$

separado do efeito do solo. A sobrecarga, por sua vez, foi dividida em duas parcelas “Q₁” e “Q₂” e o empuxo causado por elas, determinado por:

Os empuxos causados pelo solo e pelas duas parcelas da sobrecarga, assim como seus pontos de aplicação sobre o muro de arrimo, estão mostrados na figura 3.8.5 e relacionados na tabela 3.8.3 abaixo:

O ponto de aplicação do empuxo total pode ser determinado do centro de gravidade das

$\alpha = 82,0^\circ$	$P = 10,20\text{tf/m}$	$M_p = 9,79\text{m}$
$E_a = 9,20\text{tf/m}^2$	$x_G = 0,96\text{m}$	$M_{E_a} = M_{E_{av}} - M_{E_{ab}} = -0,86\text{tf/m}$
$x_{E_a} = 1,78\text{m}$	$y_G = 1,69\text{m}$	$d = 0,62\text{m}$
$y_{E_a} = 1,28\text{m}$	$N = 17,17\text{tf/m}$	

forças acima. Assim obtém-se:

3.8.2.4 Peso da estrutura

$$\delta^* = 25 \cdot \gamma_g - 10^\circ = 32,5^\circ$$

O peso específico dos gabiões “ γ_g ” é dado por:

$$c_g = 0,30 \cdot p_u - 0,50 = 2,08\text{tf/m}^2$$

e a área “S” da seção transversal do muro é:

$$T_{adm} = N \cdot \tan \delta^* + c_g \cdot B = 15,10 \text{ tf/m}$$

O peso total do muro “P” será então:

$$T = -P \cdot \sin \beta + E_a \cdot \sin (\alpha - \delta - \beta) = 6,19 \text{ tf/m} < T_{adm}$$

Para o cálculo da posição do centro de gravidade “G” do muro, determinam-se primeiramente as

$$q_{adm} = 50 \cdot \gamma_g - 30 = 55,0 \text{ tf/m}^2$$

suas coordenadas para um sistema de eixos “x” e “y” alinhado com a base da estrutura:

$$q_{m\acute{a}x} = N = 13,84 \text{ tf/m}^2 < q_{adm}$$

e

Seção	T [tf/m]	T _{adm} [tf/m]	q _{máx} [tf/m ²]	q _{adm} [tf/m ²]
1	6,19	15,10	13,84	55,00
2	3,96	13,56	8,02	55,00
3	1,88	8,11	4,87	55,00
4	0,41	3,94	1,98	55,00

Tabela 3.8.4 - Resultados das verificações das seções intermediárias

As coordenadas “ x_G ” e “ y_G ” do centro de gravidade da seção são:

e

$$x_0 = -0,477\text{m}$$

$$y_0 = 6,988\text{m}$$

$$R = 8,120\text{m}$$

$$F_g = 1,210$$

3.8.2.5 Segurança contra o escorregamento

A força normal “ N ” que age na base do muro é dada por:

Adotando-se o ângulo de atrito “ δ^* ” entre o solo de fundação e a base do muro “ $\delta^* = \phi = 27^\circ$ ”, a força de resistência disponível “ T_d ” será dada por:

O coeficiente de segurança contra o escorregamento é:

3.8.2.6 Segurança contra o tombamento

As coordenadas do ponto de aplicação do empuxo ativo “ E_a ” são:

e

O momento de tombamento será dado pelo momento da componente horizontal do empuxo ativo:

Os momentos resistentes são os momentos do peso próprio da estrutura e o momento da componente vertical do empuxo ativo:

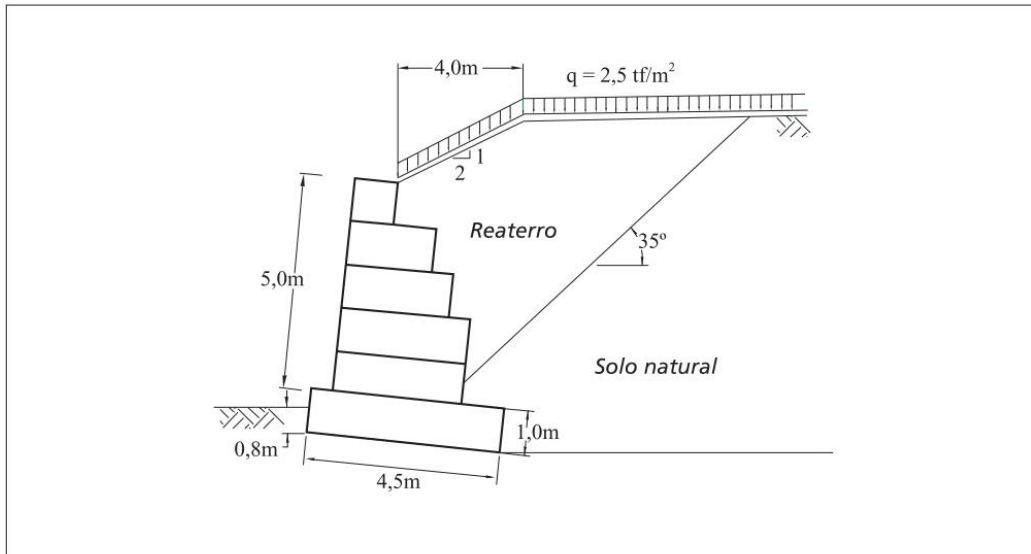


Figura 3.8.6 - Terceiro exemplo

e

O valor do coeficiente de segurança contra o tombamento é:

3.8.2.7 Pressões na fundação

A distância "d" entre o ponto de aplicação de "N" e o fulcro do tombamento é dada por:

e a excentricidade "e" é:

RELATÓRIO GAWACWIN®

GawacWin 1.0

Página 1

Programa licenciado para: Maccaferri do Brasil Ltda.

Projeto: exemplo teórico

Arquivo: exemplo

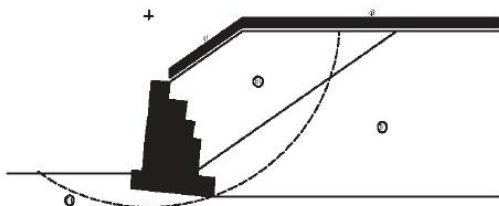
Data: 21/1/2005

DADOS DE ENTRADA

Dados sobre o muro

Inclinação do muro : 6,00 graus
 Peso específico da pedra : 24,00 kN/m³
 Porosidade dos gabiões : 30,00 %
 Geotêxtil no terrapleno : Sim
 Redução do atrito : 5,00 %
 Geotêxtil sob a base : Não
 Redução do atrito : %
 Malha e diâm. do arame: 8x10, ø 2.7 mm CD

Camada	Compr. m	Altura m	Início m
1	4,50	1,00	-
2	3,00	1,00	0,50
3	3,00	1,00	0,50
4	2,50	1,00	0,50
5	2,00	1,00	0,50
6	1,00	1,00	0,50



Dados sobre o terrapleno

Inclinação do 1º trecho : 35,00 graus
 Comprimento do 1º trecho : 4,00 m
 Inclinação do 2º trecho : 0,00 graus
 Peso específico do solo : 18,00 kN/m³
 Ângulo de atrito do solo : 30,00 graus
 Coesão do solo : 0,00 kN/m²

Camadas Adicionais no Terrapleno

Camada	Altura inicial m	Inclinação graus	Peso específico kN/m ³	Coesão kN/m ²	Ângulo de atrito graus
1	1,00	35,00	18,50	10,00	35,00

GawacWin 1.0**Página 2**

Programa licenciado para: Maccaferri do Brasil Ltda.

Projeto: exemplo teórico

Arquivo: exemplo

Data: 21/1/2005

Dados sobre a fundação

Altura da sup. superior	:	0,85 m
Comprimento inicial	:	m
Inclinação	:	0,00 graus
Peso específico do solo	:	18,50 kN/m ³
Ângulo de atrito do solo	:	35,00 graus
Coesão do solo	:	10,00 kN/m ²
Pressão adm. na fundação	:	kN/m ²
Altura do nível d'água	:	m

Camadas Adicionais na Fundação

Camada	Prof. m	Peso específico kN/m ³	Coesão kN/m ²	Ângulo de atrito graus
--------	------------	--------------------------------------	-----------------------------	---------------------------

Dados sobre a superfície freática

Altura inicial	:	m
Inclinação do 1º trecho	:	graus
Comprimento do 1º trecho	:	m
Inclinação do 2º trecho	:	graus
Comprimento do 2º trecho	:	m

Dados sobre as cargas

Cargas distribuídas sobre o terrapleno	Primeiro trecho	:	25,00 kN/m ²		
	Segundo trecho	:	25,00 kN/m ²		
Cargas distribuídas sobre o muro	Carga	:	kN/m ²		
Linhas de carga sobre o terrapleno					
Carga 1	:	kN/m	Dist. ao topo do muro	:	m
Carga 2	:	kN/m	Dist. ao topo do muro	:	m
Carga 3	:	kN/m	Dist. ao topo do muro	:	m
Linha de carga sobre o muro					
Carga	:	kN/m	Dist. ao topo do muro	:	m

Dados sobre as ações sísmicas

Coefficiente horizontal	:	Coefficiente vertical	:
-------------------------	---	-----------------------	---

RELATÓRIO GAWACWIN®

GawacWin 1.0

Página 3

Programa licenciado para: Maccaferri do Brasil Ltda.

Projeto: exemplo teórico

Arquivo: exemplo

Data: 21/1/2005

RESULTADOS DAS ANÁLISES

Empuxos Ativo e Passivo

Empuxo Ativo	:	364,21 kN/m
Ponto de apl. ref. ao eixo X	:	3,40 m
Ponto de apl. ref. ao eixo Y	:	2,39 m
Direção do empuxo ref. ao eixo X	:	49,07 graus
Empuxo Passivo	:	57,32 kN/m
Ponto de apl. ref. ao eixo X	:	0,04 m
Ponto de apl. ref. ao eixo Y	:	0,36 m
Direção do empuxo ref. ao eixo X	:	0,00 graus

DESLIZAMENTO

Força normal sob a base	:	551,56 kN/m
Ponto de apl. ref. ao eixo X	:	1,65 m
Ponto de apl. ref. ao eixo Y	:	-0,17 m
Força tangente sob a base	:	124,34 kN/m
Força de resistência sob a base	:	474,10 kN/m

Coef. de Segurança contra o Deslizamento : 2,61

TOMBAMENTO

Momento Atuante	:	570,01 kN/m x m
Momento Resistente	:	1499,02 kN/m x m

Coef. de Segurança contra o Tombamento : 2,63

Tensões na Fundação

Excentricidade	:	0,59 m
Tensão normal na borda externa	:	225,67 kN/m ²
Tensão normal na borda interna	:	24,80 kN/m ²
Tensão máx. admissível na fundação	:	717,70 kN/m ²

Não assumimos nenhuma responsabilidade pelos cálculos e desenhos aqui apresentados, visto que eles se constituem apenas em sugestões para a melhor utilização dos produtos MACCAFERRI.

GawacWin 1.0**Página 4**

Programa licenciado para: Maccaferri do Brasil Ltda.

Projeto: exemplo teórico

Arquivo: exemplo

Data: 21/1/2005

Estabilidade Global

Distância inicial à esquerda	:	m
Distância inicial à direita	:	m
Distância inicial abaixo da base	:	m
Máxima profundidade permitida no cálculo	:	m
Centro do arco ref. ao eixo X	:	0,98 m
Centro do arco ref. ao eixo Y	:	9,44 m
Raio do arco	:	10,51 m
Número de superfícies pesquisadas	:	65

Coef. de Segurança contra a Rup. Global : 2,03**Estabilidade Interna**

Camada	H m	N kN/m	T kN/m	M kN/m x m	$\tau_{M\acute{a}x}$ kN/m ²	$\tau_{Adm.}$ kN/m ²	$\sigma_{M\acute{a}x}$ kN/m ²	$\sigma_{Adm.}$ kN/m ²
1	5,18	380,24	159,40	305,26	53,13	101,58	236,83	
2	4,19	334,29	126,09	377,78	42,03	91,70	147,91	545,79
3	3,14	228,39	89,04	238,43	35,62	78,74	109,38	
4	2,09	139,66	57,27	137,32	28,64	64,86	71,02	
5	0,99	33,27	28,74	11,48	28,74	41,27	48,22	

Não assumimos nenhuma responsabilidade pelos cálculos e desenhos aqui apresentados, visto que eles se constituem apenas em sugestões para a melhor utilização dos produtos MACCAFERRI.

RELATÓRIO GAWACWIN®

GawacWin 1.0

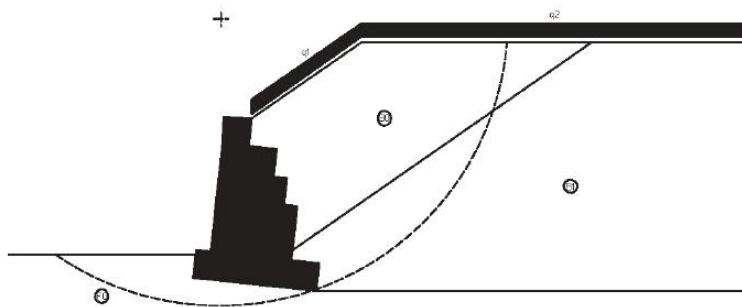
Página 5

Programa licenciado para: Maccaferri do Brasil Ltda.

Projeto: exemplo teórico

Arquivo: exemplo

Data: 21/1/2005



DADOS SOBRE O SOLO

Solo	γ kN/m ³	c kN/m ²	ϕ graus	Solo	γ kN/m ³	c kN/m ²	ϕ graus
B0	18,00	0,00	30,00	F0	18,50	10,00	35,00
B1	18,50	10,00	35,00				

CARGAS

Carga	Valor kN/m ²	Carga	Valor kN/m
q1	25,00		
q2	25,00		

VERIFICAÇÕES DE ESTABILIDADE

Coef. de Seg. Deslizamento	2,61	Tensão na base (esquerda)	225,67kN/m ²
Coef. de Seg. Tombamento	2,63	Tensão na base (direita)	24,80kN/m ²
Coef. de Seg. Rup. Global	2,03	Máxima tensão admissível	717,70kN/m ²

Não assumimos nenhuma responsabilidade pelos cálculos e desenhos aqui apresentados, visto que eles se constituem apenas em sugestões para a melhor utilização dos produtos MACCAFERRI.